CECIL AND IDA GREEN INSTITUTE OF GEOPHYSICS AND PLANETARY PHYSICS

2020 ANNUAL REPORT

SCRIPPS INSTITUTION OF OCEANOGRAPHY | UNIVERSITY OF CALIFORNIA, SAN DIEGO

IGPP 2020

DIRECTOR'S WELCOME

During a year of unprecedented disruption in the world and at IGPP, the stories in this report tell a tale of resiliency and hope. We have learned new and innovative ways to teach, to run seminars, to do research, and to go to sea and into the field. Our ranks are swelling with new investigators—many of whom have contributed to this report—and our student cohort is expanding to match. We can now even look at a map of Antarctica and see geography (the Fricker Ice Piedmont) named after one of our own.

While our work has continued, certain members of our community have born a disproportionate share of the burden. Every engineer who went to sea this past year endured weeks of confinement in pre-cruise quarantine, and many have quarantined multiple times. Those with children at home have been working two jobs in parallel, tending to the needs of their home and away teams. We are looking expectantly to the year ahead—to meeting each other on campus, to impromptu conversations, to the joy of returning to our private spaces—and none deserve it more than those who have given the most.

I look forward to seeing everyone again and anew in the halls of Munk and Revelle.

Adrian Borsa, Director, IGPP

Matt Dzieciuch aboard K/V *Svalbard*.
Photo courtesy of the Norwegian Coast Guard

CONTENTS

** Individual report not available this year*

GREEN FOUNDATION

The Cecil H. and Ida M. Green Foundation for Earth Sciences supports visiting scholars and resident scientists at IGPP. Established with a gift from the late Cecil Green in 1971, the Green Foundation holds an endowment managed by the UC San Diego-IGPP Director and overseen by an independent Board of Directors. A selection committee comprised of IGPP faculty screens nominees and applicants for both the Green Scholar and the Miles Fellowship.

The Green Foundation is currently supporting:

Green Scholar: *James Badro, IPGP, France*

Green Scholar: *Catherine Johnson, UBC, Canada*

Green Scholar: *Pieter-Ewald Share, postdoc*

Green Scholar: *Brook Tozer, postdoc*

Green Scholar: *Shunguo Wang, postdoc*

Miles Fellow: *Ignacio Sepulveda, postdoc*

UC San Diego membership in Southern California Earthquake Center *www.scec.org*

GRADUATE PROGRAM

More than the Oceans..

Our multidisciplinary program offers graduate students a unique hands-on, collaborative learning environment. In addition to our core academic curriculum, we emphasize observational techniques and the collection of novel datasets.

Graduate Students who successfully defended in 2020

Drake Singleton, Ph.D.*(JPD*): Neotectonics in San Diego, California: Paleoseismology, Slip Rate, and Offshore Structure of the Rose Canyon Fault*

Yuval Levy, Ph.D. *(JPD*): Structural architecture of the Western and Central Transverse Ranges, California, USA*

Joshua Kelly, *Ph.D. (JPD*): Climate-driven coastal morphodynamics along Southeast Queensland, Australia"*

Hannah Peterson, MS *(S. Constable): Combining Land and Lake Bottom Magnetotelluric Measurements to Study Volcanic Systems in Mono Basin, California*

**JPD = Joint Doctoral Program with San Diego State University*

SCIENCE AT SEA

PRECAUTIONS AND PRE-CRUISE QUARANTINES FOR SCIENCE

In 2019, Peter Worcester and Matt Dzieciuch went to sea with their American and Norwegian Coast Guard colleagues to repeat an experiment conducted 25 years ago to determine the spread of warm and salty Atlantic water through the middle of the Arctic ocean water column. Peter Worcester, aboard K/V *Svalbard* in the Eastern Arctic, and Matt Dzieciuch aboard USCGC *Healy* in the Western Arctic, each participated in the their groups' respective deployment of 3 deep-ocean moorings with low-frequency (35 Hz) sound sources and receivers—with the intent to recover the moorings one year later. The global pandemic has made mince of most 2020 plans—research cruises were not unaffected.

There were supposed to be two cruises in 2020. One on the *Svalbard* that would recover the Norwegian moorings and one on the *Healy* that would recover the moorings near Alaska. After Dzieciuch his colleagues quarantined for two weeks in Anchorage, USCGC *Healy* suffered a motor fire which kept her in port for the summer.

The Norwegian moorings were recovered successfully, but COVID-precautions prevented Worcester from participating. In order to rescue the data from the Alaska moorings, the groups schedules a second cruise aboard *Svalbard* which left Norway and went across the Arctic to the Beaufort to get the Alaska moorings. A round trip of more than 6500nm thru the Russian EEZ.

Dziechiuch was on the *Healy* for the fire and on the second cruise on the KV *Svalbard*. The moorings were successfully recovered with all the data intact.

COVID WORK ENVIRONMENT

Class by Zoom, home school lesson breaks, and fear of the short nap were among the challenges IGPPers navigated in 2020. We look forward to the time when collaboration occurs in person, social distance is a personal choice rather than a CDC guideline, and our kids study Common Core in the classroom.

Mia Morzfeld (2, pictured) attended her first colloquium, when her father Matti presented his work at UC Berkeley's department of Earth and Planetary Science, "She did not explain reversals of Earth's magnetic field all so well, but she definitely caught the attention of everybody in attendance."

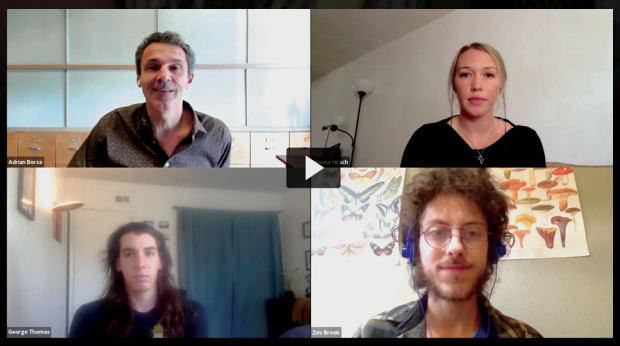

FRICKER ICE PIEDMONT

"MODERN EXPLORER" HONORED WITH ANTARCTIC A PLACE NAMING

IGPP glaciologist and Scripps Polar Center founder and co-leader Helen Fricker whose satellite altimetry contributions to Antarctic study have been recognized by the government of the British Antarctic Treaty (BAT) with the newly named ***Fricker Ice Piedmont***. To mark the 200th anniversary of the discovery of Antarctica, BAT conferred place name honors to 28 British scientists and support staff, or "Modern Explorers," for their contributions to advance the understanding of polar regions.

The ***Fricker Ice Piedmont*** is about 12 km wide and 6 km deep on the eastern side of Adelaide Island, bounded to the west by Mount Reeves and Mount Bouvier, and forms the coastline of Adelaide Island along Barlas Channel.

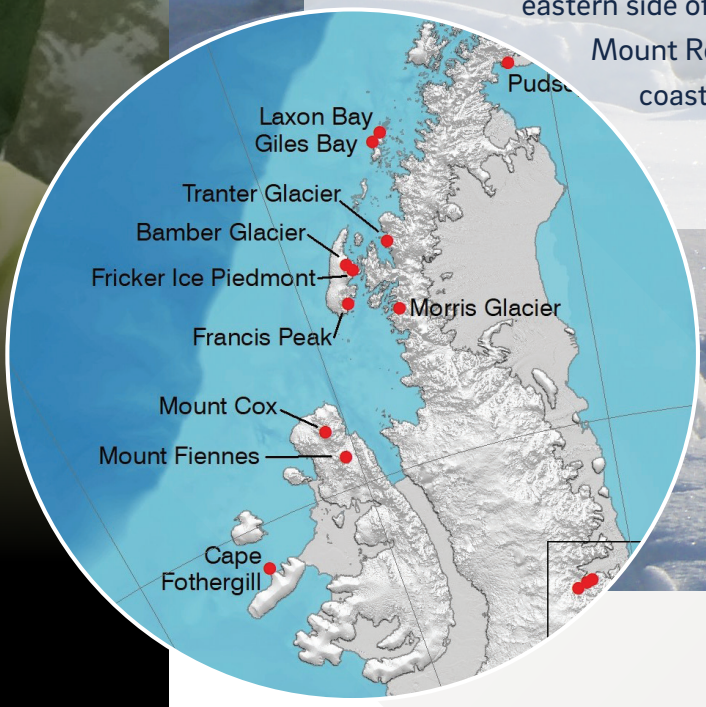

GETTING A BIT SHIFTY

SALTON SEA SWARM OBSERVATIONS

The laser strainmeter at Durmid Hill, which records seismic activity at, and adjacent to, the Salton Sea has provided IGPP geophysicists with a boon of seismic data for decades. Debi Kilb, Frank Wyatt, Don Elliott and Billy Hatfield used the strainmeter collection to monitor swarm activity leading up to, and coinciding with, the August 10 Mw4.6 Salton Sea tremor. Kilb's illustration of the 2020 swarm (map, in red) shows that the swarm's spatial extent is unique from prior years. This raised the question: Are they all part of the same fault? According to Kilb, "Yes! They are part of a complicated system of cross-faults trending primarily perpendicular to the San Andreas Fault."

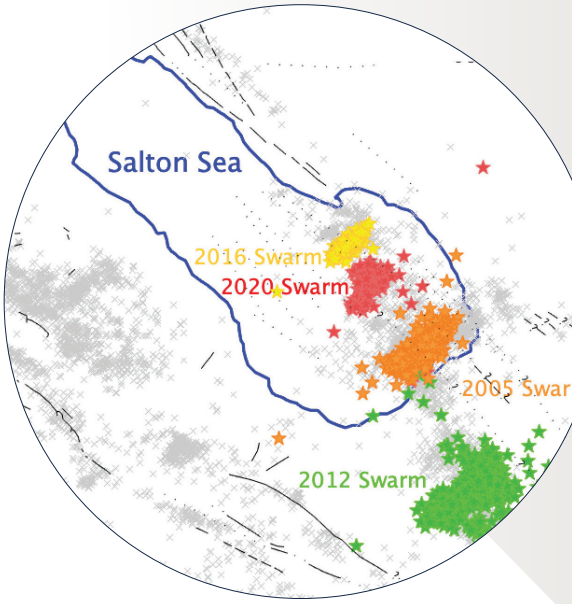

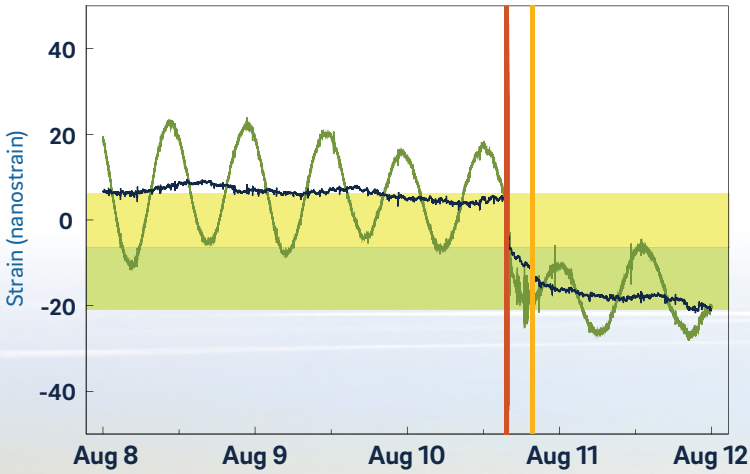

Data that includes the sinusoidal behavior from the Earth Tides
Data with the signature of the Earth Tides removed
Time of magnitude 4.6 earthquake
Time of magnitude 4.0 earthquake
Strain change from magnitude 4.6 earthquake
Continued strain change following magnitude 4.6 earthquake

Strain change immediately following the earthquake (yellow vertical extent) is similar to the strain change in the following day (green vertical extent). Simplistically, this indicates the mainshock size doubled and is continuing to grow.

The graph, above, created by Wyatt, shows the time leading up to, and just after, the August 10 Mw4.6 event. Of interest, is the post-seismic deformation (earth strain) that is similar in extent as the coseismic component. This may reflect a doubling of the main-shock rupture area, which is still growing—slowly.

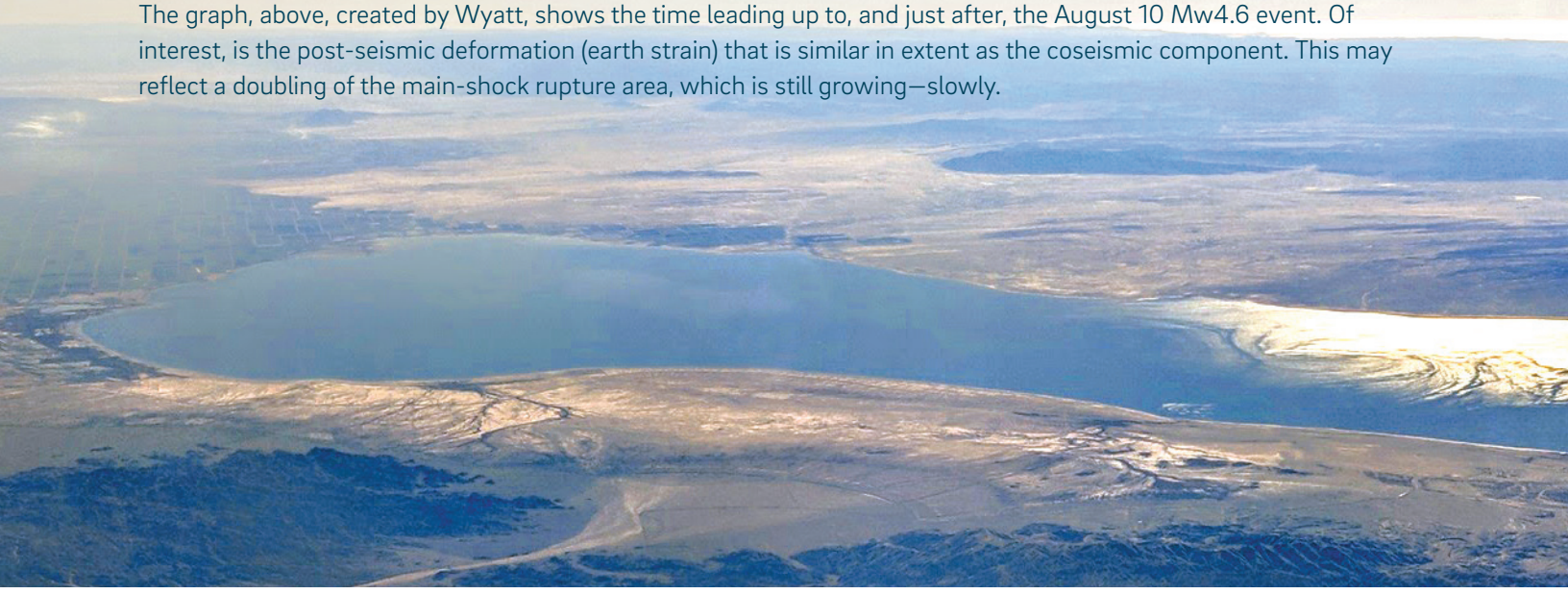

APPLY YOURSELF...

Students in the IGPP graduate program study Earth and other planets to advance our fundamental understanding their origin, composition, and evolution, and explore the implications for life, for the environment, and for society. The graduate program provides a broad education in the fundamentals of geophysics, alongside research and coursework spanning multiple specializations.

Our multidisciplinary program offers graduate students a unique hands-on, collaborative learning environment. In addition to our core academic curriculum, we emphasize linking observational techniques and the collection of novel datasets for testing new theoretical and computational approaches. GP students participate extensively in field experiments, instrument development, laboratory investigations, and shipboard expeditions. Graduates go on to careers in research, education, industry, and public policy. Scripps has strong working relationships with the NSF, NASA, NOAA, the USGS, and the Office of Naval Research, and can provide graduates with long-term networking and professional support.

Is this graduate program for you? Read about some ongoing research in the following pages and learn more about the program online: igpp.ucsd.edu/program-study.

DUNCAN CARR AGNEW

Professor

dagnew@ucsd.edu, 858-534-2590

Crustal deformation measurement and interpretation, Earth tides, Southern California seismicity, history of science.

In January through March 2020 I was on sabbatical at the Geophysical Laboratory of the Carnegie Institution of Washington, to begin the study of an early example of combined scientific research, industrial production, and military application. Such joint programs are usually associated with World War II, but there were precursors in World War I, in this case for the production of optical glass. This glass, all imported from Germany, was a crucial part of battlefield equipment: binoculars, periscopes, and rangefinders. But all the formulas for making it were secret, and no US glass maker had the chemical knowledge needed to develop their own. The Geophysical Lab, already engaged in the study of rock melting and formation, could apply its expertise to a different class of high-temperature silicates. Teams of GL scientists, through systematic study in cooperation with three glass makers, had by 1918 created US optical-glass production facilities that met military needs.

The archives of the Geophysical Lab contain the reports and letters of the scientists involved, notably A. L. Day and F. W. Wright; my main activity was evaluating, transcribing, and scanning these. Other sources examined and scanned included the papers of the Optical Glass Committee of the National Academy, and the records of the Navy Bureau of Ordnance, the Army Ordnance Department, the War Industries Board, and the National Bureau of Standards. Though cut short by the pandemic, enough material was collected for a basic narrative.

Continuing with papers combining horology and geophysics, I re-examined historic data and analyses of rate changes in pendulum clocks caused by gravity tides; the first measurements of tidal variations in gravity were in fact made this way, in 1929. The best data, from the clocks developed by F. M. Fedchenko in the 1950's and 1960's, were comparable to early tidal gravimeter data—which could easily be re-analyzed because in 1963 Walter Munk included it in the "Geotapes" data set, preserved to the present thanks to IGPP staff Flicki Dormer and David Horwitt.

As a byproduct of my work as a journal editor, I examined why some earthquakes have many more papers written about them than others, using the Event Bibliography of the International Seismological Centre.

The result (see figure) shows some correlation with magnitude, but also that some earthquakes become "seismological celebrities" for reasons not always clear.

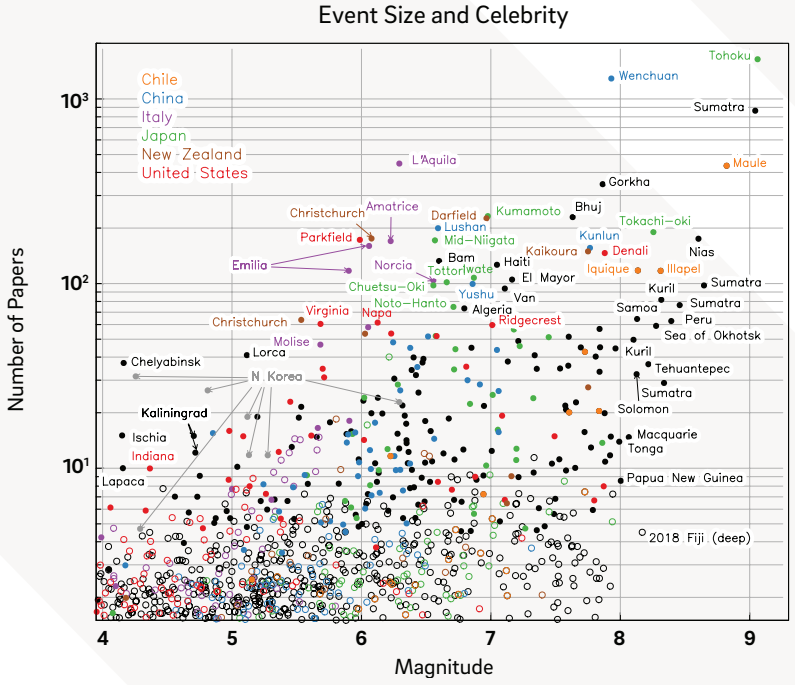

Figure 1. Earthquakes with magnitude from 2000 through 2019 with more than one paper listed in the ISC Event Bibliography. Filled circles are for events given names in the Bibliography. Names are for the 62 events with 60 or more publications or magnitude above 8.0.

RECENT PUBLICATIONS

Agnew, D. C. (2020.) Time and tide: Pendulum clocks and gravity tides, *Hist. Geo. Space Sci.*, ***11***, 215-224, htpp//dx.doi.org/10.5194/hgss-11-215-2020

Agnew, D. C. (2020.) Celebrity earthquakes, *Seismol. Res. Lett.*, ***91,*** in press.

Ruins after Tohoku earthquake and tsunami, March 2011. Image courtesy of Douglas Sprott, Creative Commons

JONATHAN BERGER

Emeritus Researcher, RTAD

jberger@ucsd.edu, 858-534-2889

Global seismological observations, marine seismo-acoustics, geophysical instrumentation, deep ocean observing platforms, ocean robotics, global communications systems

This year my colleagues and I, while struggling under Covid-19 restrictions, managed to complete the upgrade of the facilities at Pinyon Flat Observatory (PFO) which we began last year. These included a number of 100-m deep GSN-style boreholes, fully cased and cemented, and installations of several new seismometers. We tested the boreholes with temporary installations of STS6 broadband seismometers in the boreholes and chose the one with the best performance (SDG) to become the new official PFO GSN sensor replacing the previous STS-1 units.

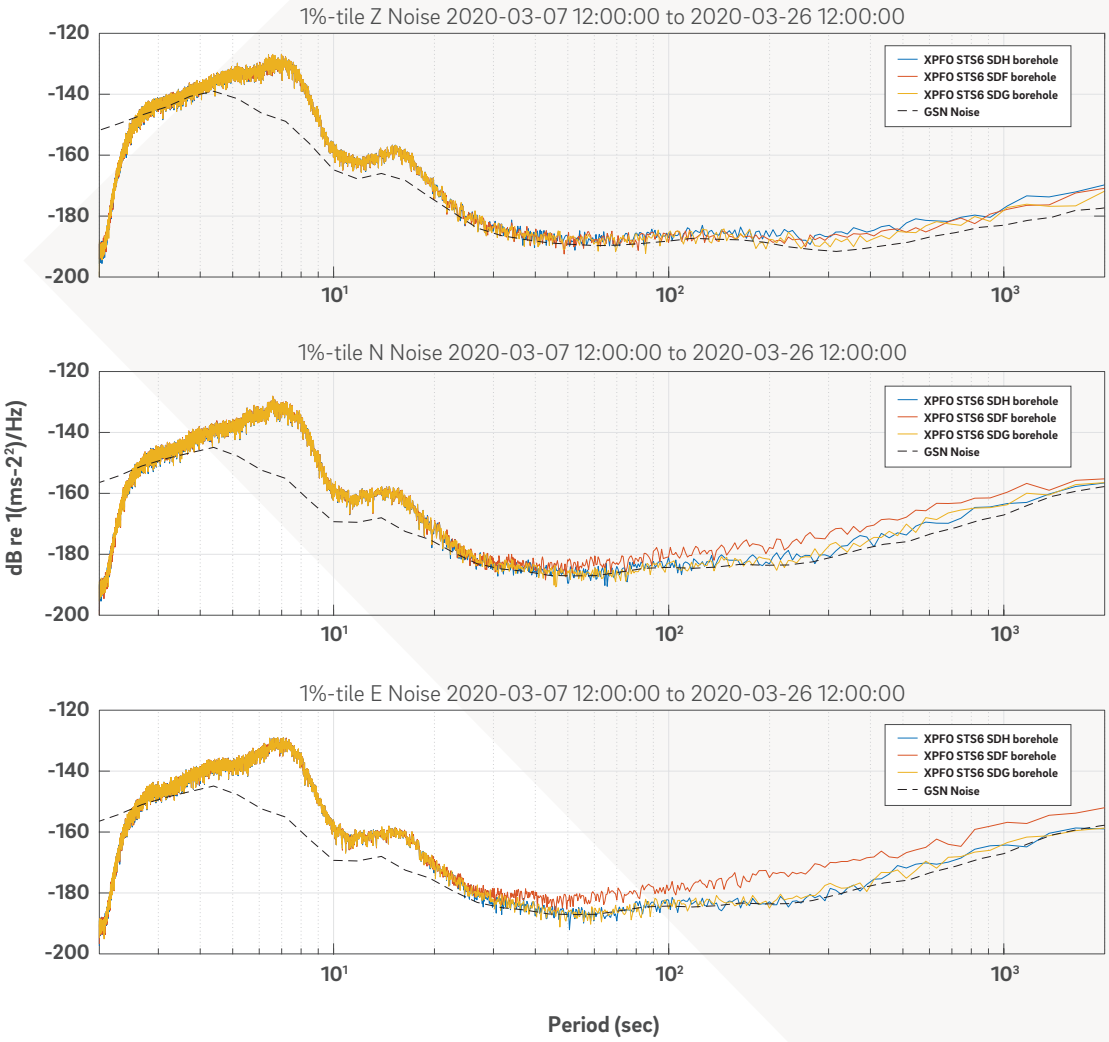

Figure 2. Long period noise levels observed on the STS6 seismometers installed in the PFO borehole.

Additionally, we installed 4 new Nanometrics T360 3-component seismometers in the PFO underground facility all on a common granite slab. The recent results show that while the long period vertical components are comparable, horizontal long-period components are significantly more noisy in the underground facility in comparison to the borehole unit. We attribute this to site effects rather than seismometer noise.

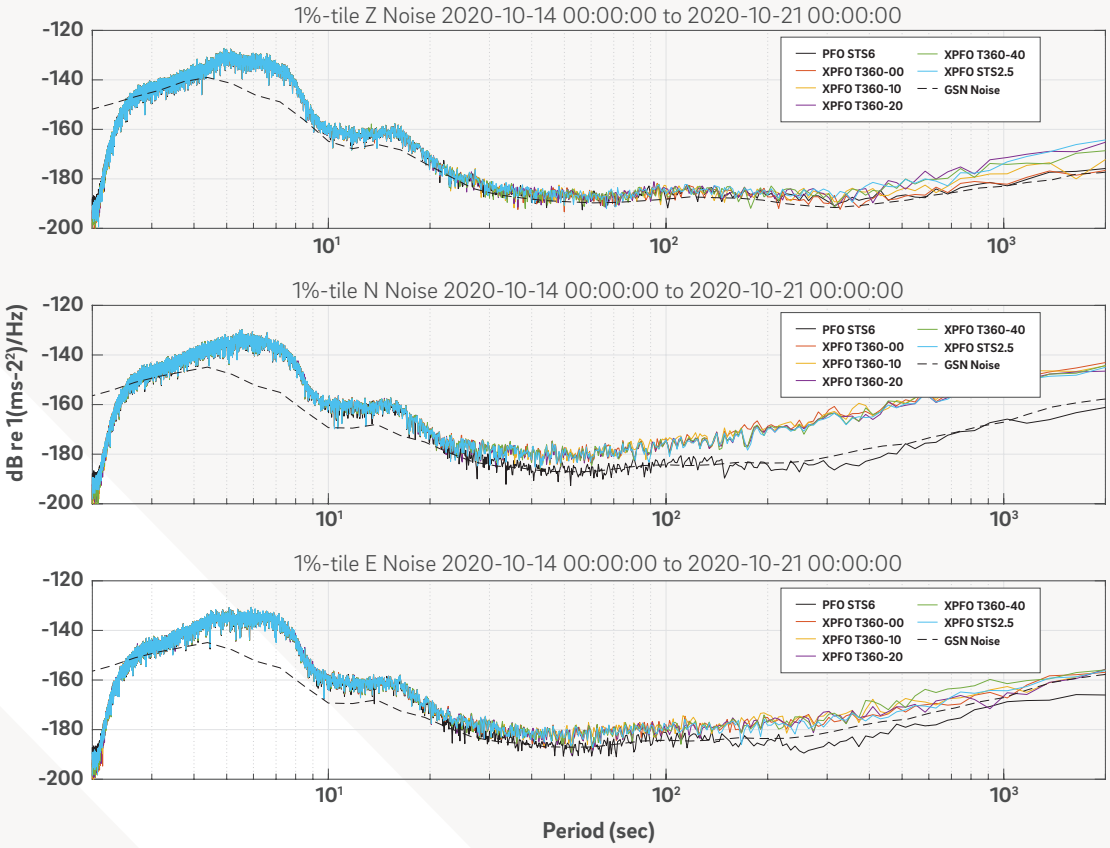

Figure 3. Long period noise levels observed on the Nanometrics T360 seismometers installed in the PFO underground facility compared with the PFO STS6 borehole .

RECENT PUBLICATIONS

Orcutt,J., Berger,J. (2020) " Building and Maintaining a global seismic network in the ocean." AGU Fall Meeting

Monica D. Kohler, Katrin Hafner, Jeffrey Park, Jessica C. E. Irving, Jackie Caplan-Auerbach, John Collins, Jonathan Berger, Anne M. Tréhu, Barbara Romanowicz, Robert L. Woodward; A Plan for a Long-Term, Automated, Broadband Seismic Monitoring Network on the Global Seafloor. *Seismological Research Letters;* ***91*** (3): 1343–1355. doi: https://doi.org/10.1785/0220190123

Berger, J., G. Laske, J. Babcock, and J. Orcutt (2016). An ocean bottom seismic observatory with near real-time telemetry, *Earth Space Sci.* ***3***, 68-77, doi: 10.1002/2015EA000137.

YEHUDA BOCK

Distinguished Researcher and Senior Lecturer; Director, Scripps Orbit and Permanent Array Center (SOPAC); Director, California Spatial Reference Center (CSRC)

ybock@ucsd.edu, 858-534-5292
sopac-csrc.ucsd.edu/index.php/sopac

GPS/GNSS, crustal deformation and transients, geodetic reference frames, early warning systems for earthquakes and tsunamis, seismogeodesy, GPS meteorology, structural health monitoring, data science, MEMS sensors

The SOPAC group's current focus includes the combined use of seismic and geodetic methods to support natural hazard mitigation for communities affected by earthquakes, tsunamis, volcanoes, and severe weather. The research is aided by in-house instrument design, field deployment of sensor packages, real-time data collection and analysis and development of rapid hazard characterization methods. Using close to 30 years of geodetic displacement time series, we also study tectonic signals of interest, including interseismic, coseismic and postseismic deformation, and transients such as fault creep, subsidence and episodic tremor and slip (ETS). We also archive and analyze GNSS data for the International GNSS Service and the California Spatial Reference Center. Over the last year, the SOPAC group included Peng Fang, Katherine Guns, Dorian Golriz, Anne Sullivan, Songnian Jiang, Allen Nance, Maria Turingan and Wang Hu, with laboratory and field assistance by Matt Norenberg, Glen Offield and Jennifer Mathews (design of our new Web pages).

EARLY POSTSEISMIC DEFORMATION

The crustal deformation cycle is traditionally divided into coseismic, postseismic, and interseismic phases on which may be superimposed transient motions from various sources. It is important to distinguish between coseismic and postseismic slip to improve our understanding of the physics of earthquakes and crustal deformation processes. Strict reliance on displacements to bracket the coseismic phase is somewhat arbitrary and depends on the choice of an appropriate pre- and post-earthquake data span. Instead, we use seismic velocities; the start time is based on P-wave arrivals and the end time by the total energy of the signal integrated from seismic velocities, which is equivalent to summing the spectral power across frequency. When geodetic and seismic instruments are not collocated, the coseismic time window can be transferred to the GNSS stations observing at high-rate (e.g., 1 Hz). In addition to a delay in time for farther stations, the coseismic

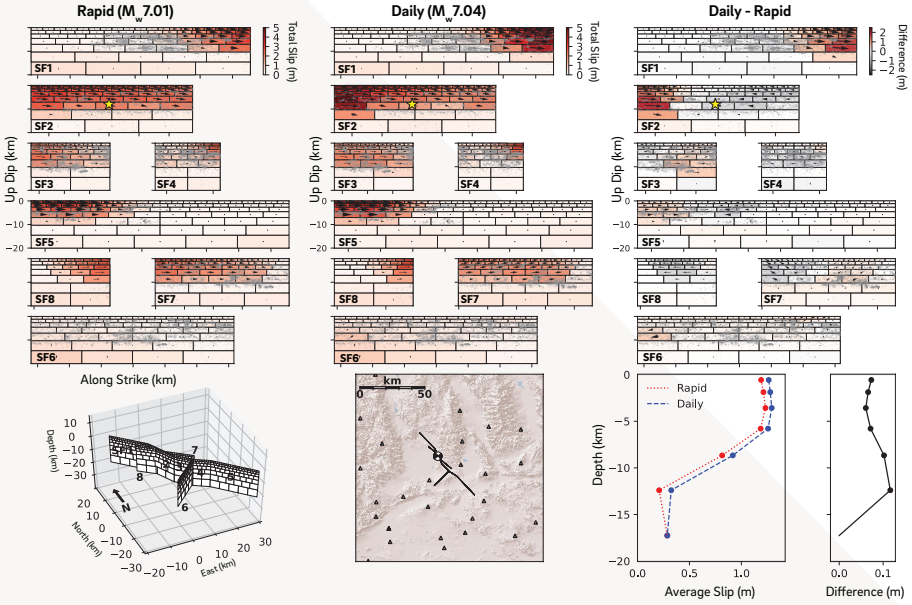

Figure 4. Fault slip models for the 2019 Mw7.1 Ridgecrest earthquake using seismogeodetic (rapid) (left) and daily (middle) offsets as input. Right panels show the difference between the two models. Hypocenter (USGS) is shown as a yellow star, grey dots show 24-hours aftershocks within 5 km of the model fault plane. Bottom panels show the fault model geometry (left), study area map with GNSS stations and event epicenter (middle) and averaged slip with depth for each model together with their differences. Source: Golriz et al. (2021).

window gets extended, depending on fault geometry, rupture directivity and site properties such as soil conditions. In Figure 4, we compare a fault slip model of the 2019 Mw7.1 Ridgecrest earthquake based on the seismogeodetic (rapid) estimate of the time span of the coseismic window vs. one day. We find that in both models most of the slip occur on two main segments: northern segment that includes subfaults 1-3, with the adjacent subfaults 7-8, and southern segment that includes subfaults 4-5. We find up to 3 meters of total slip in the rapid model, and more than 4 meters in the daily model. We attribute the difference to early postseismic deformation taking place during the first few hours. Most of these differences (up to 1.5 meters) appear to be in the shallow part of the northern segment in agreement with models relying on InSAR observations (e.g., Wang and Burgmann, 2020, Seismological Research Letters). Our method, using 1 Hz seismogeodetic velocities and displacements and tested for other earthquakes of a range of fault mechanisms and magnitudes, allows for a more physics-based approach to estimate the transition of coseismic to early postseismic deformation and an improved understanding of earthquake processes.

RECENT PUBLICATIONS

Bock, Y. and S. Wdowinski (2020), The Role of GPS Geodesy in Geophysics, Natural Hazards, Climate and the Environment, in Position, Navigation, and Timing Technologies in the 21st Century: Integrated Satellite Navigation, *Sensor Systems, and Civil Applications*, **Vol. 1**, Y. T. J. Morton et al., eds., Wiley.

Goldberg, D. E., D. Melgar, Y. Bock (2019), Seismogeodetic P-wave amplitude: No evidence for strong determinism. *Geophys. Res. Lett.*, **46**, 11118–11126, https://doi.org/10.1029/2019GL083624

Golriz, Bock & Xu (2021), Distinguishing the Coseismic Phase of the Earthquake Cycle with Seismogeodesy, in review, *J. Geophys. Res*

Klein, K., Y. Bock, X. Xu, D. Sandwell, D. Golriz, P. Fang, L. Su (2019), Transient deformation in California from two decades of GPS displacements: Implications for a three-dimensional kinematic reference frame, *J. Geophys. Res.,* DOI:10.1029/2018JB017201.

Murray, J. R. et al. (2019), Regional Global Navigation Satellite System Networks for Crustal Deformation Monitoring, *Seismo. Res. Lett.* https://doi.org/10.1785/0220190113

Wang M., J. Wang, Y. Bock, H. Liang, D. Dong, P. Fang (2019), Dynamic Mapping of the Movement of Landfalling Atmospheric Rivers over Southern California with GPS Data, *Geophys. Res. Lett,* **46**. https://doi.org/10.1029/2018GL081318.

Xu, X., D. T. Sandwell, L. Ward, C, Milliner, B. Smith-Konter, P. Fang, and Y. Bock (2020) Surface deformation associated with fractures near the 2019 Ridgecrest earthquake sequence, *Science,* **370**(6516), 605-608.

ADRIAN BORSA

Associate Professor, Director IGPP

aborsa@ucsd.edu; 858-534-6845

Remote hydrology from joint analysis of GPS/GNSS, GRACE and InSAR. Transient surface deformation from natural and anthropogenic sources using InSAR and GNSS. Noise sources in geodetic remote sensing, calibration/validation of geodetic observations, and optimal combinations of geodetic information. Differential lidar techniques applied to problems in geomorphology and tectonic geodesy. Dry lake geomorphology. Socioeconomic responses to water scarcity and implications for public policy.

Much of my current research involves the characterization of the hydrological cycle using observations of Earth surface deformation and mass distribution. Specifically, I am interested in observing and analyzing changes in terrestrial water storage (the total water in glaciers, snowpack, lakes, soil, and groundwater) which are critical to closing Earth's water budget but which have been poorly observed until recently. My group combines satellite gravity measurements of water mass change (from the GRACE mission) with GNSS (Global Navigation Satellite System) observations of crustal deformation associated with these water mass changes to recover the evolution of water storage across the continental USA and beyond (e.g. Figure 5). While seasonal signals from hydrology have been extensively studied, changes over both shorter and longer periods have not been broadly documented. We use a variety of techniques to investigate spatiotemporal patterns of water storage in watersheds across the United States, the extent and duration of droughts, and watershed flooding/recovery from storms such as Hurricane Harvey.

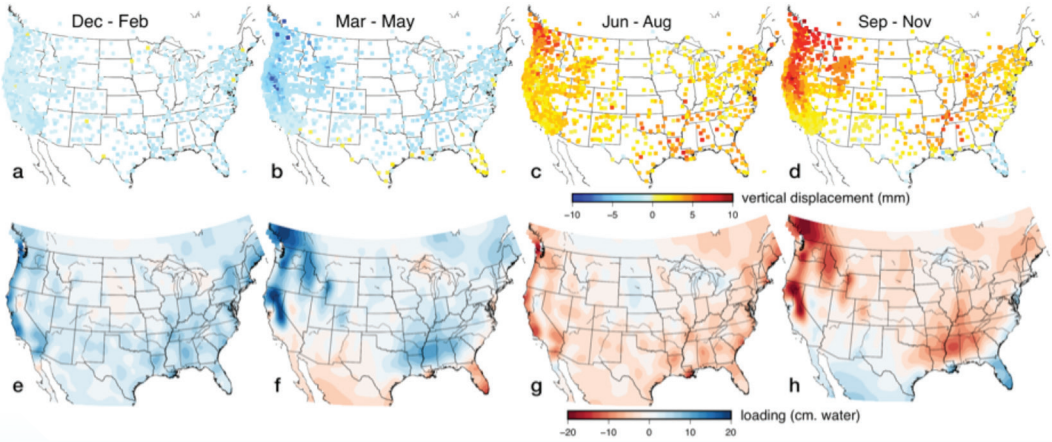

Figure 5. (a-d) Seasonal vertical displacements from GPS across the continental United States (CONUS), showing overall subsidence (cool colors) in the winter and spring, and uplift (warm colors) in the summer and fall. (e-h) Estimated terrestrial water storage anomalies (TWSA) corresponding to panels a-d, from joint analysis of GPS and GRACE data. TWSA typically peaks in winter-spring and is smallest in summer-fall, except on the southern/southeastern CONUS boundary (e.g. Florida and the Gulf and Atlantic coasts), where the seasonal phase is advanced by 3 months.

We are also investigating linkages between water and the solid earth, including possible triggering of seismicity (the L'Aquila, South Napa and El Mayor–Cucapah earthquakes) and volcanism (Long Valley Caldera) by water-related crustal stresses. These studies often incorporate InSAR (Interferometric Synthetic Aperture Radar) observations of subsidence from groundwater extraction, which provide high spatial resolution and broad coverage of impacted areas. Additionally, we are using our InSAR time series over California's Central Valley in a collaboration with colleagues at UCSD's School of Global Policy and Strategy to study crop selection and planting decisions in response to changes in rainfall, surface water deliveries, and groundwater availability.

Our group has also been working to improve interpretations of GNSS-observed vertical crustal motion for North America. These collaborative efforts (with The University of Texas at Austin and the Jet Propulsion Laboratory) have focused on estimating and removing the contribution of elastic displacements from long-term changes in terrestrial water storage, which can obscure signals from tectonics and mantle dynamics (e.g. Figure 6). Most recently, we have begun to investigate differences between Glacial Isostatic Adjustment models for North America and the possibility that these models have missed long-wavelength GIA-related crustal motion that is apparent in GNSS-derived velocity fields.

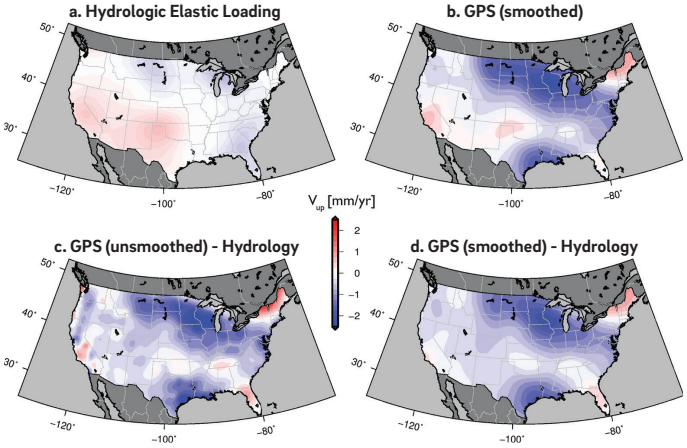

Figure 6. (a) Vertical rates due to elastic hydrologic loading, modeled using GRACE-derived terrestrial water storage estimates as input loads. (b) 300 km Gaussian smoothed GNSS vertical velocity field. (c) Residual velocities after removing hydrologic loading rates from unsmoothed GNSS vertical velocities. (d) Residual velocities after removing hydrologic loading rates from the smoothed GNSS velocity field.

RECENT PUBLICATIONS

Adusumilli, S., A.A. Borsa, M.A. Fish, H.K. McMillan, and F. Silverii (2019). "A Decade of Water Storage Changes Across the Contiguous United States from GPS and satellite gravity." *Geophysical Research Letters,* **46**(22)

Borsa, A., H.A. Fricker, K. Brunt (2019). "A terrestrial validation of ICESat elevation measurements." *IEEE Transactions on Geoscience and Remote Sensing,* **57**(9)

Enzminger, T.L., E. E. Small, A.A. Borsa. "Subsurface water dominates Sierra Nevada seasonal hydrologic storage." *Geophysical Research Letters,* **46**(21)

Kraner, M., W. Holt, A. Borsa, (2018). "Seasonal non-tectonic loading inferred from cGPS as a potential trigger for the M6. 0 South Napa Earthquake." *Journal of Geophysical Research: Solid Earth,* **123**(6), 5300-5322

Lau, N, A. A. Borsa, and T.W. Becker. "Present-Day Crustal Vertical Velocity Field for the Contiguous United States." *Journal of Geophysical Research: Solid Earth* **125**, no. 10 (2020)

Levy, M. C., Neely, W. R., Borsa, A. A., & Burney, J. A. (2020). Fine-scale spatiotemporal variation in subsidence across California's San Joaquin Valley explained by groundwater demand. *Environmental Research Letters*.

Neely, W.R., A.A. Borsa, F. Silverii (2019). "GInSAR: A cGPS correction for enhanced InSAR time series." *IEEE Transactions on Geoscience and Remote Sensing,* **58**(1)

Silverii, F., Montgomery-Brown, E. K., Borsa, A. A., & Barbour, A. J. (2020). Hydrologically induced deformation in Long Valley Caldera and adjacent Sierra Nevada. *Journal of Geophysical Research-Solid Earth,* 125(5)

CATHERINE CONSTABLE

Distinguished Professor of Geophysics

cconstable@ucsd.edu, 858-534-3183

Earth's magnetic field and electromagnetic environment; Paleo and geomagnetic secular variation; Linking paleomagnetic observations to geodynamo simulations; Paleomagnetic databases; Electrical conductivity of Earth's mantle; Inverse problems; Statistical techniques.

The natural spectrum of geomagnetic variations at Earth's surface extends across an enormous frequency range and is dominated by low frequency changes, associated with the predominantly dipolar internal field produced by the geodynamo in Earth's liquid outer core. Fluid flow and diffusive processes in the electrically conductive core produce secular variation in the magnetic field. The dipole part of the field exhibits the largest changes, associated with geomagnetic excursions and reversals which require the axial dipole part of the field to vanish as it changes sign. Finite electrical conductivity of the mantle eectively filters variations in the core field on time scales much less than a year. Satellite observations and ground based observatory data can be used to study geomagnetic variations on the timescales of the solar cycle, and are used for studies of deep mantle electrical conductivity. Paleomagnetic data from volcanics, archeomagnetic artifacts, and sediments provide information on longer time periods ranging from hundreds to millions of years.

Major results from my recent research have been improved understanding the evolution of the geomagnetic field over 0–100 ka, a time interval which is long enough to represent paleosecular variation and several geomagnetic excursions, during which the geomagnetic dipole strength drops and global or regional field direction show large departures from their more usual stable polarity configurations. Syntheses of paleomagnetic data were used to produce the time varying field model GGF100k, and over the past year there been a focus on analyzing what can be learned from studying this model. The Laschamp excursion appears to be the only magnetic event with a strong global signature during the past 100 kyr. In work together with Sanja Panovska and Monika Korte (of GeoForschungs Zentrum, Helmholtz Center, Potsdam), we have conducted a study of field structure during the Laschamp excursion which occurred around 40 ka and of other regional excursional events (see Figure 7 and Panovska et al., 2019, 2020 for more details and animations).

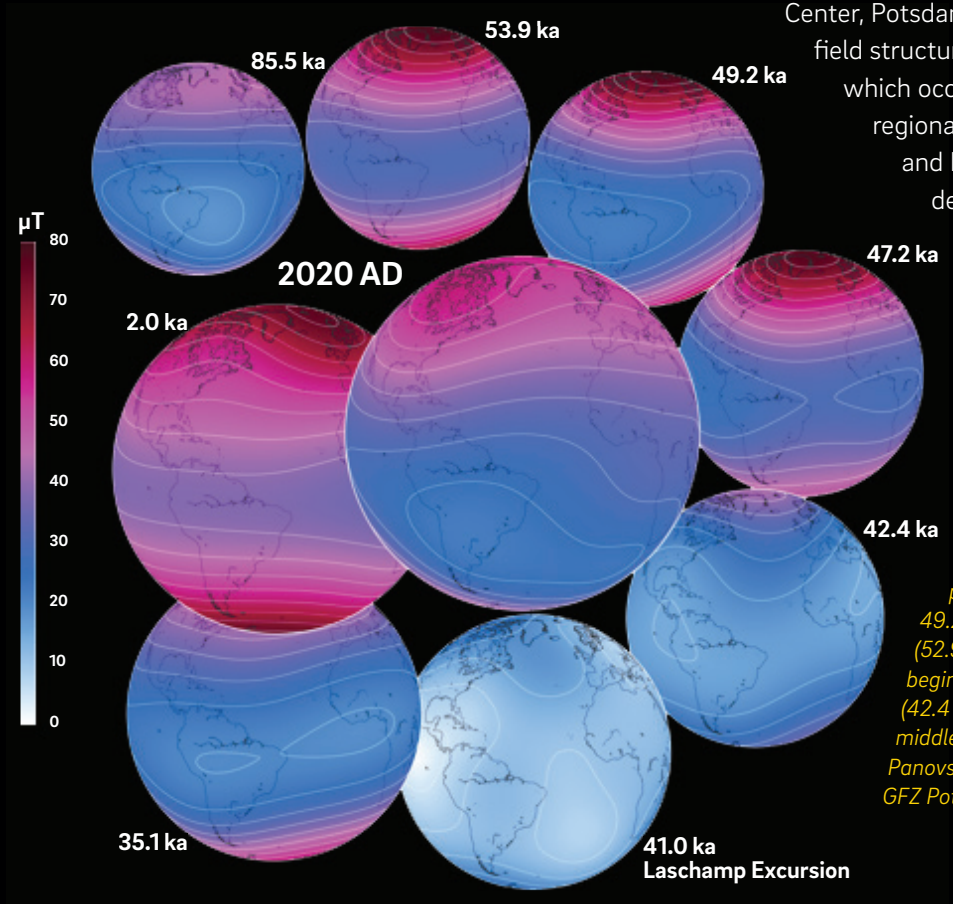

Figure 7. Time slices of geomagnetic field strength (in T) at Earth's surface from the global GGF100k model over the past 100 ka. There are structures resembling the present day (2020 AD) field (see 85.5 ka, 49.2 ka), intervals of stronger dipole dominance (52.9 ka, 47.2 ka, 2.0 ka), weaker field at the beginning and following the Laschamp excursion (42.4 ka, 35.1 ka) and the very weak field in the middle of the Laschamp excursion (41.0 ka). (From Panovska et al, 2020, Credit: Alexander Jordan, GFZ Potsdam.)

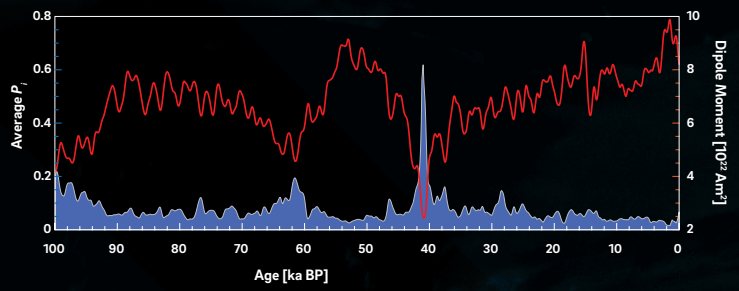

Figure 8. Axial dipole moment and the globally averaged PSV index of the GGF100k model for 0-100 ka.

Work with Christopher Davies (Leeds University, U.K.) has been continued on linking numerical geodynamo simulations with paleomagnetic results, especially in the analysis of rapid changes in the magnetic field. Broad similarities between behavior in the paleofield and numerical simulations allow us to link potential physical processes in the simulations with actual field behavior that is not easily resolvable from paleomagnetic data and models. We have identified remarkably rapid changes in magnetic field directions in both GGF100k and numerical dynamo simulations reaching as high as 10/year, almost 100 times faster than current rates of change in the geomagnetic field. Detailed analyses and a simple analog model have been used to link these changes (which mainly occur at low latitudes) to movement of reversed flux patches across the surface of Earth's core. In a new project in collaboration Professor Matthias Morzfeld of SIO, I have begun an investigation of the extent to which it might be possible to predict geomagnetic excursions or reversals from variations in dipole strength and direction. These are currently focused on our recently developed paleosecular variation (PSV) index (see, e.g. Figure 8) which provides a means for evaluating the level of departure from a stable dipolar field configuration.

RECENT PUBLICATIONS

Panovska, S., C.G. Constable, & M. Korte, 2019. One hundred thousand years of geomagnetic field evolution, *Reviews of Geophysics*, **57**, doi:10.1029/2019RG000656.

Brandt, D., C. Constable, M. Ernesto, 2020. Giant Gaussian process models of geomagnetic paleosecular variation: a directional outlook, *Geophysical Journal International*, **222**, 1526-1541, doi:10.1093/gji/ggaa258.

Davies, C., & C.G. Constable, 2020. Rapid geomagnetic changes inferred from Earth observations and numerical simulations, *Nature Communications*, **11**, 3371, doi:10.1038/s41467-020-16888-0.

Panovska, S.,M. Korte, and C. G. Constable, 2020.The global geomagnetic field of the past hundred thousand years, *Eos*, **101**, doi:10.1029/2020EO146890.

Kamchatka Peninsula volcanoes, courtesy of NASA

STEVEN CONSTABLE

Distinguished Professor

sconstable@ucsd.edu, marineemlab.ucsd.edu, 858-534-2409

Marine EM methods

Steven Constable heads the SIO Marine EM (Electromagnetic) Laboratory at IGPP. EM methods can be used to probe the geology of the seafloor, and we have used them to study plate boundaries, marine gas hydrate, offshore geothermal prospects, permafrost, hydrothermal venting and associated massive sulfides, groundwater, and conventional oil and gas reservoirs.

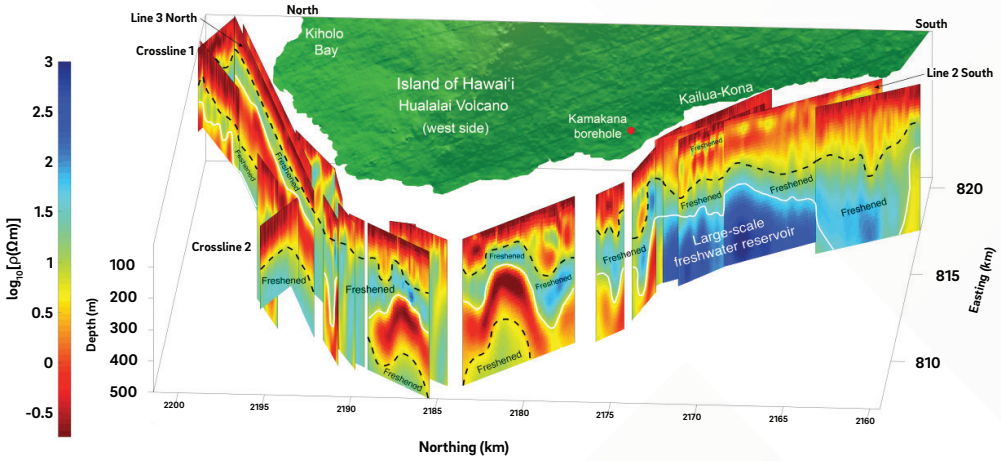

Figure 9. Electrical conductivity models from surface-towed EM data collected o the west coast of Hawai'i. Blue (resistive) regions are offshore freshwater deposits. The broken lines represent impermeable confining layers. From Attias et al., Science Advances, in press.

We had two cruises this year, one to study the deep oceanic lithosphere o San Diego using the R/V *Sally Ride*, and one off New Zealand to study gas hydrate on the R/V *Tangaroa*. Both were delayed due to COVID-19: the lithosphere cruise sailed in early August, and the gas hydrate cruise is about to sail out of Wellington, after a 2-week quarantine period for the US science party. In other work PhD student Roslynn King collected more surface-towed EM data off San Diego to look for offshore fresh groundwater, and tested a new high resolution bottom-towed system designed for archaeological studies.

The surface-towed shallow-water EM system was also used last year by Eric Attias to study offshore groundwater off Hawai'i, and his work has produced some remarkable results. The EM models show extensive layers of offshore fresh water trapped under impermeable layers of ash and soil (Figure 9). The fresh water migrates from the recharge region

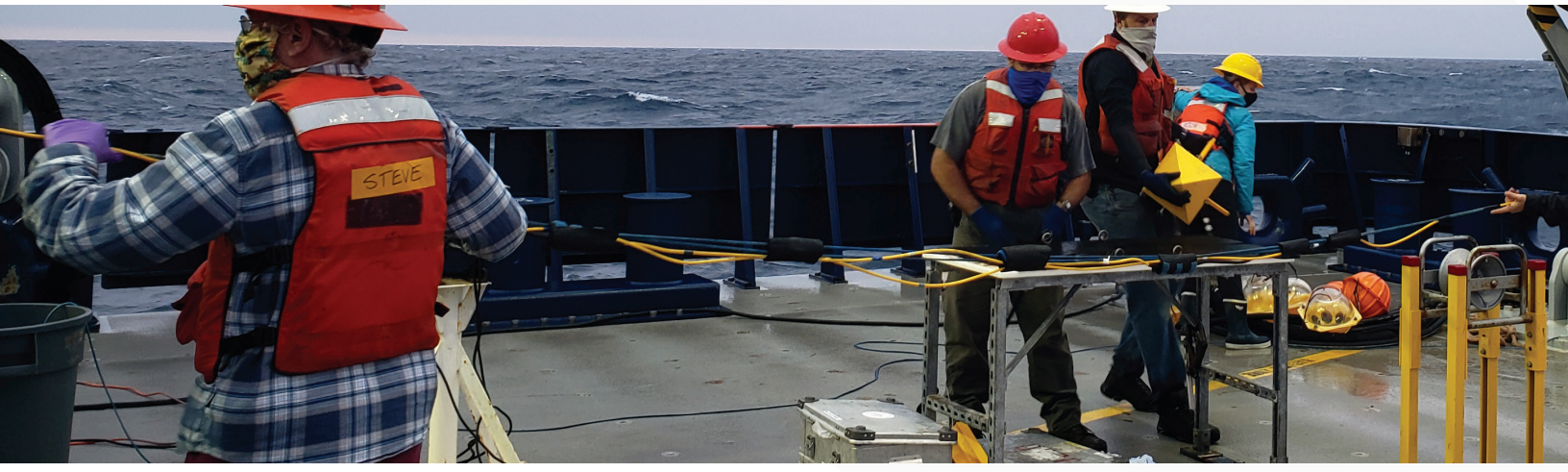

in the volcanic highlands and migrates through fractured basalt down to the ocean, where it floats on denser seawater but is prevented from escaping by the confining layer. We think that this newly discovered transport mechanism of fresh groundwater may be the governing mechanism in other volcanic islands. In such a scenario, volcanic islands worldwide can utilize these renewable offshore reservoirs as new water resources, which are considered more resilient to climate change-driven droughts. Further, extraction of groundwater offshore would avoid impacts to the coastal freshwater springs that are important in Hawai'ian culture.

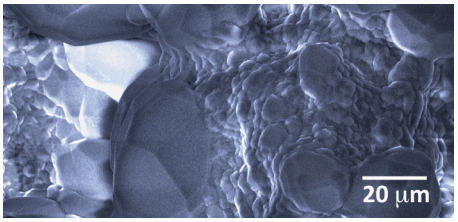

Figure 10. Cryogenic scanning electron microscopy image of a methane hydrate (image courtesy Laura Stern, USGS). For several years we have been measuring the electrical conductivity of methane hydrate synthesized in the laboratory in order to better understand borehole resistivity logs and our marine EM data collected over hydrate deposits in the seafloor. Cryo-SEM images such as this help us to understand what factors contribute to the conduction of electricity in this material.

RECENT PUBLICATIONS

Rychert, C.A., N. Harmon, S. Constable, and S. Wang (2020): The nature of the lithosphere-asthenosphere boundary. *J. of Geophy. Res.: Solid Earth*, **125**, e2018JB016463. 10.1029/2018JB016463

Wang, S., S. Constable, C.A. Rychert, and N. Harmon (2020): A lithosphere-asthenosphere boundary and partial melt resolved using marine magnetotelluric data. *Geochem. Geophy. Geosys.*, **21**, 10.1029/2020GC009177

Esquivel, T.A., C. Flores, V. Reyes-Ortega, S. Constable, E. Gómez-Treviño, and A. González-Fernández (2020): Magnetotelluric exploration of the Wagner Basin, Gulf of California, Mexico: Evidence for an axial magma chamber and hydrothermal circulation. *J. of South American Earth Sciences*, **99**, 10.1016/j.jsames.2020.102501

Constable, S., R. Lu, L.A. Stern, W.L. Du Frane, and J.J. Roberts (2020): Laboratory electrical conductivity of marine gas hydrate. *Geophys. Res. Lett.*, **47**, e2020GL087645. 10.1029/2020GL087645

Constable, S. (2020): Perspectives on marine electromagnetic methods. *Perspectives of Earth and Space Scientists*, **2**, e2019CN000123. 10.1029/2019CN000123

Kannberg, P.K., S. Constable (2020): Characterization and quantification of gas hydrates in the California Borderlands. *Geophys. Res. Lett.*, **47**, e2019GL084703, 10.1029/2019GL084703

Montiel-Alvarez, A.M., J.M. Romo, S. Constable, and E. Gómez-Treviño (2019): Invariant TE and TM impedances in marine magnetotelluric method. *Geophy. J. Int.*, **221**, 163–177, 0.1093/gji/ggz571

Avilés-Esquivel, T., C. Flores, V. Reyes-Ortega, S. Constable, E. Gómez-Treviño, and A. González- Fernández (2020): Magnetotelluric exploration of the Wagner Basin, Gulf of California, Mexico: Evidence for an axial magma chamber and hydrothermal circulation. *J. of South American Earth Sciences*, **99**, 10.1016/j.jsames.2020.102501

Chesley, C., K. Key, S. Constable, J. Behrens, and L. MacGregor (2019): Crustal cracks and frozen flow in oceanic lithosphere inferred from electrical anisotropy. *Geochem. Geophy. Geosystems*, **20**, 5979–5999 10.1029/2019gc008628

Lu, R., L.A. Stern, W.L. Du Frane, J.C. Pinkston, J.J. Roberts, and S. Constable (2019): The eect of brine on the electrical properties of methane hydrate. *J. of Geophy. Res.: Solid Earth*, **124**, 10, 877–10,892 10.1029/2019JB018364

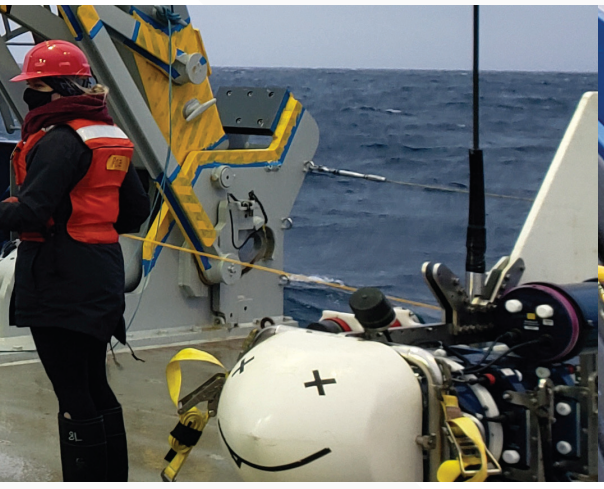

J. PETER DAVIS
Specialist

pdavis@ucsd.edu, 858-534-2839

Seismology, time series analysis, geophysical data acquisition

My research responsibilities at IGPP center upon managing the scientific performance of Project IDA's portion of the IRIS/USGS Global Seismographic Network (GSN), a collection of 41 seismographic and geophysical data collection stations distributed among 29 countries worldwide. NSF recently renewed funding for an additional five years of GSN network operations via the IRIS Consortium.

Figure 11. IDA's Chris Sites and Don Elliott prepare to lower the new STS6A seismometer into the 100m deep borehole at Pinyon Flat Observatory. Sensors from deep boreholes like this one are particularly effective for recording horizontal earth motions. Photo courtesy J. Conley.

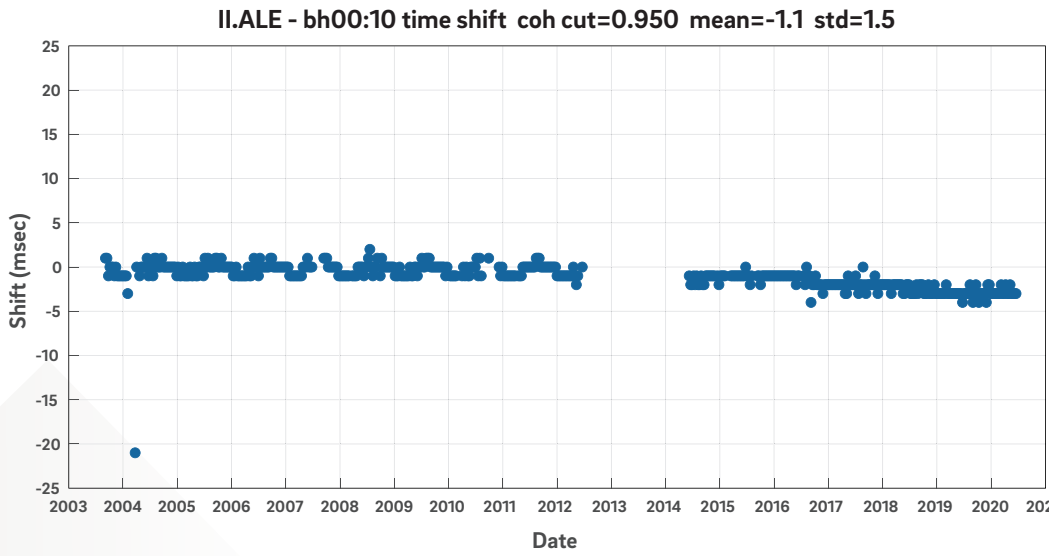

Figure 12. Apparent time shift between the primary and secondary seismometers at II.ALE measured from the cross spectrum of 10min-long segments drawn daily. The low values and small scatter over this long time period provides evidence to support the highly accurate timing of these data. Accurate timing is essential for many studies of deep Earth seismic structure.

GSN network maintenance has proven to be a particular challenge during the COVID pandemic. Normally IDA technicians would be traveling around the world to repair malfunctioning equipment or install new instruments to keep the network in optimal operating condition. Prior to the lockdown, IDA technicians installed new borehole instruments at two sites in Kazakhstan and one in Uganda. Figure 1 shows one of these sensors being lowered into a 100m deep borehole at Pinyon Flat Observatory, our local station and the only field trip we have conducted during the pandemic lockdown. Placing this seismometer in a borehole is a way to insure the quietest possible setting for recording distant earthquakes.

IDA staff members are constantly working to ensure the finest quality data are collected from each instrument including fine-tuning our models of each station's instrument responses and checking data timing to enable scientists to extract the most accurate information possible from the data collected. One method for accomplishing this task is by examining key phenomena such as Earth tides and normal modes that should register the same on these important geophysical sensors. To the extent that measurements made with multiple instruments that have been calibrated in very different fashions match, we may have greater confidence that the instrument response information IDA distributes with GSN waveform data is accurate. Investigators use this information to compensate for the frequency-dependent sensitivity of sensors so that they may study true ground motion and its underlying physical causes.

Figure 2 shows the results of one data quality test we performed at many stations this year. We exploited the fact that almost every station had more than one broadband seismometer deployed there to test the accuracy of the timing. Short data segments from co-located pairs of sensors were compared to see if, within a common frequency band, the time series were synchronized properly. The results for station II.ALE shown in this figure indicate that the apparent time shift between the sensors was less than 5 milliseconds, an acceptable result and about as accurate as can be obtained with this method. This encourages confidence that these recordings may be used in studies of deep mantle and core structure that require accurate measurements of time shifts of this order.

RECENT PUBLICATIONS

http://dx.doi.org/doi:10.7914/SN/II

http://dx.doi.org/doi:10.1785/0220170280

CATHERINE DE GROOT-HEDLIN

Research Scientist

chedlin@ucsd.edu; 858-534-2313

Acoustic propagation modeling with application to infrasound (sound at frequencies lower than human hearing); application of infrasound and seismic data to nuclear test-ban verification and hazard monitoring; use of seismic and infrasound networks to detect small-scale signals. Here, I outline two projects that I have worked on in the past several years.

An automated event detector and locator: Ihave developed a 'Big Data' approach to detect and locate events in two-dimensional space and time using large volumes of data. This approach is called AELUMA (Automated Dectection and Location of Events Using a Mesh of Arrays). AELUMA is used to create a catalog of infrasound sources in the eastern United States and southeastern Canada using infrasonic and seismic data recorded by large-scale networks. There are two main reasons to develop this catalog. First, the catalog provides a list of sources that can be used for basic infrasound research, either for remote study of the events themselves or to study of properties of the atmosphere. Second, we need to understand and document the noise field or other sources that may hamper the performance of International Monitoring System infrasound arrays in monitoring the Comprehensive Nuclear Test Ban Treaty.

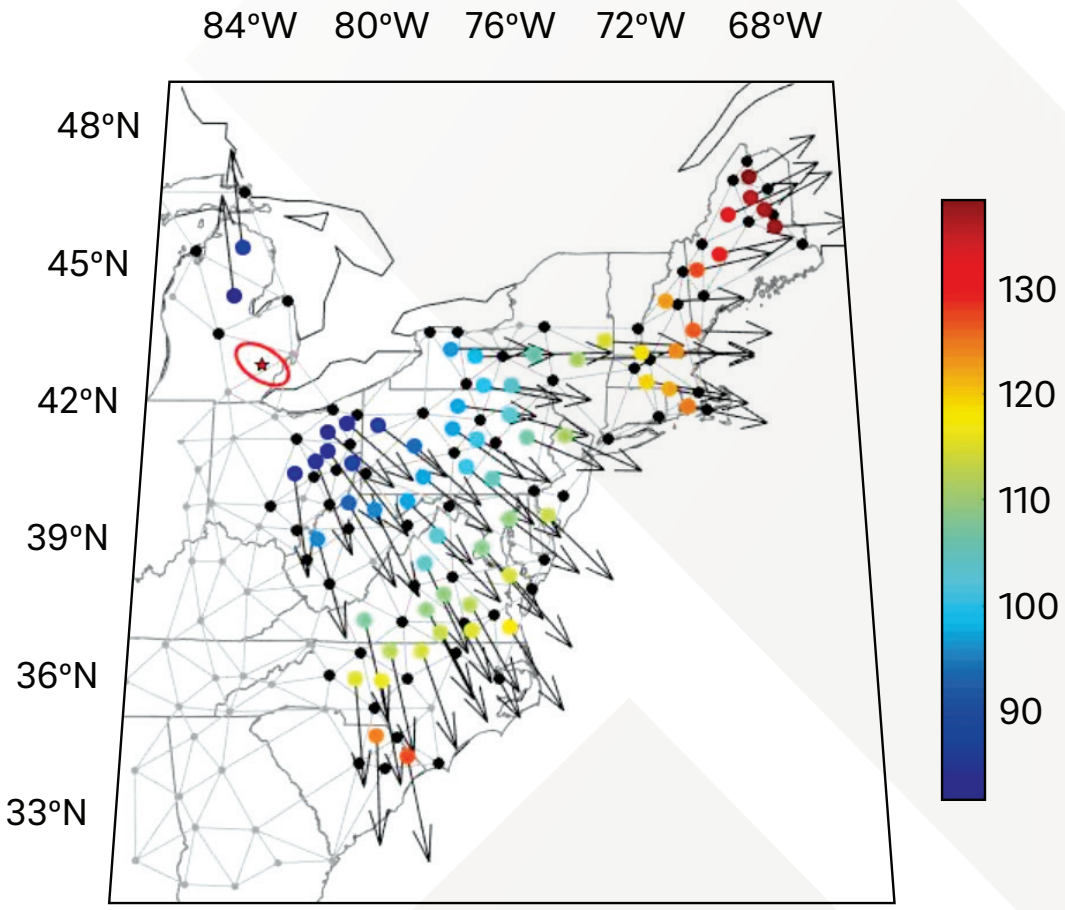

Figure 13. Grey lines show groups of 3 stations (triads) used to estimate a bolide source location. Gray dots indicate infrasound stations where coherent signals were not detected; black dots mark where they were detected. Color-coding, at triads where coherent signals were detected show the signal arrival time in minutes after the start of 17 January 2018 (UTC). The arrows show the signal azimuth at each triad. The star marks the optimal source location in southwest Michigan. The error ellipse shows the range of acceptable locations.

Since its initial introduction to gravity data and infrasound data, the method has been expanded to include its application to seismic data, including both seismic surface waves and seismic body waves. The method has proven successful at finding small-scale signals in continental scale data sets, comprising several hundreds of seismic and infrasound stations. The detected signals include gravity waves caused by solar terminator waves observed in in surface pressure, as well as gravity waves caused by convective storms. AELUMA has also been used to detect small seismic events caused by fracking in Oklahoma detected by high frequency seismic data, and a bolide terminal burst over southeast Michigan, detected in infrasound data. Low frequency seismic surface wave data have been used to detect ice-quakes in Greenland, and most recently, stormquakes resulting from atmosphere-ocean-earth interaction during hurricanes or winter storms. A current project involves expanding the methodology to global data.

Numerical modeling: A basic research goal in infrasound is to understand the transmission of infrasound through variable atmospheric conditions. To this end, I developed a computationally efficient numerical method to synthesize the propagation of nonlinear acoustic waves through the atmosphere. Nonlinearity, or shock wave propagation, arises when pressure perturbations associated with acoustic waves are a significant fraction of the ambient atmospheric pressure. Shock waves are associated with meteoroid explosions in the upper atmosphere, volcanic eruptions, or nuclear and chemical explosions. Work on this code has progressed to allow for the incorporation of realistic atmospheric effects, such as spatially varying sound speeds and wind speeds, topography, and atmospheric attenuation. This code has been used to compute the penetration of sound into areas typically thought of as being in a "shadow zone", where sound refracts upwards, away from the Earth's surface due to the decrease in sound speed with altitude, much as light bends as it travels between air and water.

This code is now publicly available and has been used in several volcanology studies, including propagation of sound waves from volcanoes in Japan and Vanuatu.

RECENT PUBLICATIONS

de Groot-Hedlin, C., 2017, Infrasound propagation in tropospheric ducts and acoustic shadow zones, *J. Acoust. Soc. America*, ***142***, 1816-1827.

de Groot-Hedlin, C., Hedlin, M., L. Hoffmann M.J. Alexander, C. Stephan, 2017, Relationships between Gravity Waves Observed at Earth's Surface and in the Stratosphere over the Continental United States, *J. Geop. Res. – Atmos.*, doi.org /10.1002/2017JD027159.

de Groot-Hedlin, C.D., Hedlin, M.A.H. 2018, A New Automated Approach to Detecting and Locating Seismic Events Using Data from a Large Network. *Bull. Seis. Soc. Am.,* ***108:*** 2032–2045. doi: https://doi.org/10.1785/0120180072

de Groot-Hedlin, C.D., Hedlin, M.A.H. 2019, Detection of infrasound signals and sources using a dense seismic network, chapter in "Infrasound Monitoring for Atmospheric Studies," pp. 669-700.

Fan, W. JJ McGuire, CD. de Groot-Hedlin,, MAH. Hedlin, S. Coats, J. Fiedler. 2019, Stormquakes, *Geop. Res. Lett,* https://doi.org/ 10.1029/2019GL084217

Fan, W. C.D. de Groot-Hedlin,, M.A.H. Hedlin, Z. Ma. 2018, Using surface waves recorded by a large mesh of three-element arrays to detect and locate disparate seismic sources, *Geop. J. Int.,* https://doi.org/10.1093/gji/ggy316

Hedlin, M.A.H., J. Ritsema, C.D. de Groot-Hedlin, E.A. Hetland, 2018, A Multidisciplinary Study of the 17 January 2018 Bolide Terminal Burst over Southeast Michigan. *Seis. Res. Lett.* doi: https://doi.org/10.1785/0220180157

Hedlin, M.A.H., C.D. de Groot-Hedlin, J.M. Forbes, D.P. Drob, Solar Terminator Waves in Surface Pressure Observations, *Geop. Res. Lett,* https://doi.org/10.1029/2018GL078528

MATTHEW DZIECIUCH

Research Geophysicist

mdzieciuch@ucsd.edu; 858-534-7986

Acoustical Oceanography, Ocean Acoustic Tomography, Signal Processing

My research focuses on the remote sensing of the ocean with long-range acoustic transmissions. This offers a unique capability for measuring ocean interior properties, such as horizontally averaged temperatures and currents. The travel-time of sound waves propagating through the depths is affected by both small-scale and large-scale ocean processes. Acoustical oceanography seeks to use sound propagation in the ocean to understand some of the dynamic processes that are present. Some of the processes that can be studied include climate change, ocean circulation, internal waves, and tides.

This past year, along with Peter Worcester, we have deployed moorings for a new experimental program in the Arctic that will measure the heat content along a trans-Arctic path extending from near Svalbard to near the North Slope of Alaska. A map of the 2019 deployment is shown in Figure 1. The extreme environment of the Arctic is perhaps the most vulnerable to anthropogenic climate change. Part of the experimental motivation is to repeat a measurement done 25 years ago by Mikhalevsky et al. in order to see how much the acoustic propagation (and by inference, the heat content) has changed.

The sound source operates near 35 Hz in order to avoid the rough ice-cover scattering losses associated with higher frequencies. The stratification of the Arctic is complicated and has been changing rapidly in past few years. Above the deep Arctic water, there is the warm, salty Atlantic layer, the less salty but cold Pacific winter water, then the warmer Pacific summer water, while on top is fresher but cold water either from the melting ice or from the large amount of river inflows. The composition and thicknesses of these layers have been greatly affected by climate change and thus acoustic propagation through these layers has also been affected. The experiment has been designed to learn the most possible from the acoustic travel-time, transmission loss, and scattering as the sound interacts with the stratification and with the rough ice-cover. Another important goal is to examine the feasibility of underwater acoustic navigation of autonomous instruments which are expected to be increasingly deployed in the under-sampled ice-covered Arctic ocean.

The field program collected data for one year and was meant to be recovered in the late summer of 2020. During this extraordinary year, it has been more difficult than expected to organize an expedition to the always challenging Arctic. The logistics of loading people and gear onto an icebreaker while keeping them COVID free has

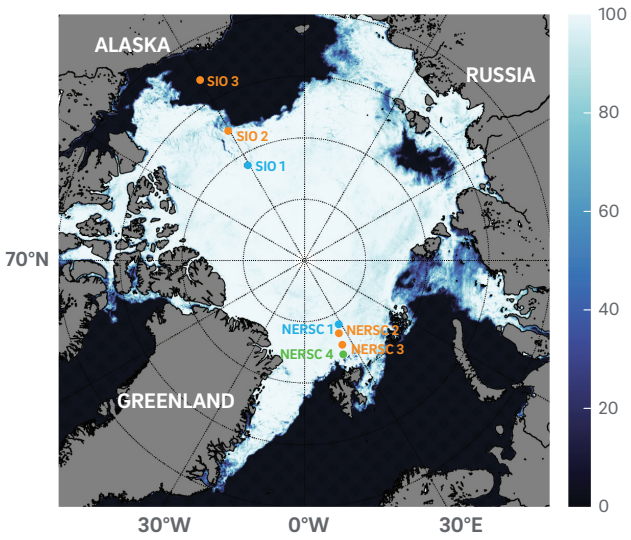

Figure 14. Deployed experimental layout of the CAATEX field program. The blue dots designate acoustic transceivers (sources and vertical line arrays.) While the orange dots designate acoustic receivers only.

been a time-consuming task. We were further hampered by a main propulsion motor failure on the one capable USGC vessel. Fortunately, we were able to reorganize with the help of our Norwegian partners, Hanne Sagen at the Nansen Environmental and Remote Sensing Center and the Norwegian Coast Guard vessel KV Svalbard. As of the time of this report, late October 2020, we are on the eve of leaving Longyearbyen to retrieve the three moorings in the Beaufort Sea.

RECENT PUBLICATIONS

Dzieciuch, M.A., "Signal processing and tracking of arrivals in ocean acoustic tomography," *J. Acoust. Soc. Am.*, **136**, 2512–2522. (2014)

Sagen, H., Geyer, F., Sandven, S., Babiker, M., Dushaw, B., Worcester, P., Dzieciuch, M., and Cornuelle, B., "Resolution, identification, and stability of broadband acoustic arrivals in Fram Strait," *J. Acoust. Soc. Am.*, **141**, 2055–2068. (2017)

Colosi, J. A., Cornuelle, B. D., Dzieciuch, M. A., Worcester, P. F., and Chandrayadula, T. K., "Observations of phase and intensity fluctuations for low-frequency, long-range transmissions in the Philippine Sea and comparisons to path-integral theory," *J. Acoust. Soc. Am.*, 146, 567–585. (2018)

Mikhalevsky, P. N., Sperry, B. J., Woolfe, K. F., Dzieciuch, M. A., and Worcester, P. F., "Deep ocean long range underwater navigation," J. Acoust. Soc. Am., 147, 2365-2382. (2020)

WENYUAN FAN

Assistant Professor

wenyuanfan@ucsd.edu; 858-246-4585

My research focuses on understanding seismic source processes, including both earthquakes and environmental seismic sources. Understanding the seismic source processes is critical for hazard assessment and mitigation, and it can also serve as a probe to investigate understand large-scale lithospheric tectonic processes. In addition to tectonic earthquakes, a variety of seismic sources have been discovered in the past few decades, including slow earthquakes, which are deficient in high-frequency seismic radiation, and various surface processes such as landslides, rivers, and glaciers. My research seeks to unmask earthquake propagation, earthquake triggering processes, and the mechanisms of abnormal slip events by developing new imaging techniques, using dense seismic arrays, and acquiring onshore and offshore geophysical observations.

I led an effort of discovering abundant submarine landslides in the Gulf of Mexico. By analyzing eight years of continuous data from seismic stations across the United States and applying a novel detection method, we identify and locate 85 previously unknown submarine landslides in the Gulf of Mexico from 2008 to 2015. Out of the 85 landslides, ten occurred spontaneously without preceding earthquakes (e.g., Figure 15), while the remaining 75 occurred nearly instantaneously after the passage of surface waves from distant earthquakes, and hence were likely dynamically triggered by the earthquakes. The triggering earthquakes can have magnitudes as small as M_w ~5. The observed landslides suggest a possible tsunami hazard for coastal communities along the Gulf of Mexico and that seabed infrastructure in the Gulf of Mexico, including oil platforms and pipelines, is also at risk from the landslides. Our study is the first to demonstrate directly from seismic records that abundant submarine landslides occur in the Gulf of Mexico and is one of only a few studies that provide robust seismological evidence of submarine landslides dynamically triggered by distant earthquakes.

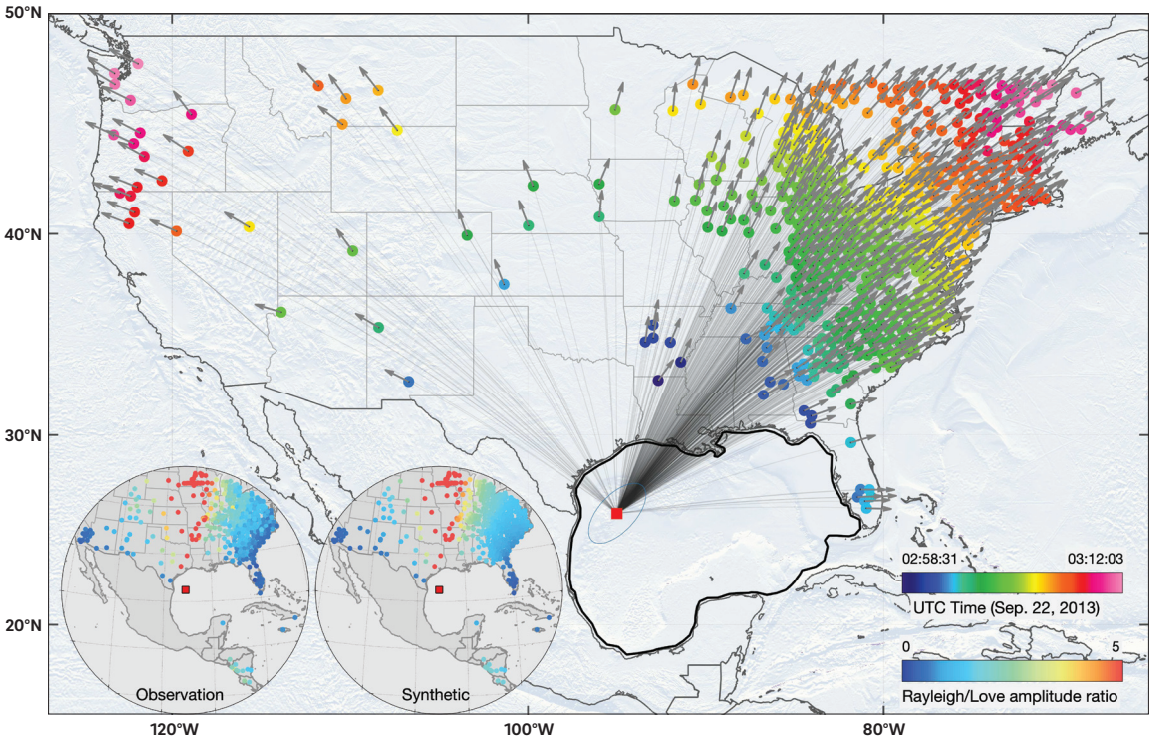

Figure 15. Shaded topographic map showing a spontaneous submarine landslide on 22 September 2013 (red square). The ellipse shows the estimated location uncertainty of the landslide. The Rayleigh-wave arrival times and propagation directions at each subarray (triad) are shown as the colored dots and arrows. The thin line between the detected submarine landslide and each triad shows the great circle path. The inserts show the observed and synthetic Rayleigh-to-Love amplitude ratios.

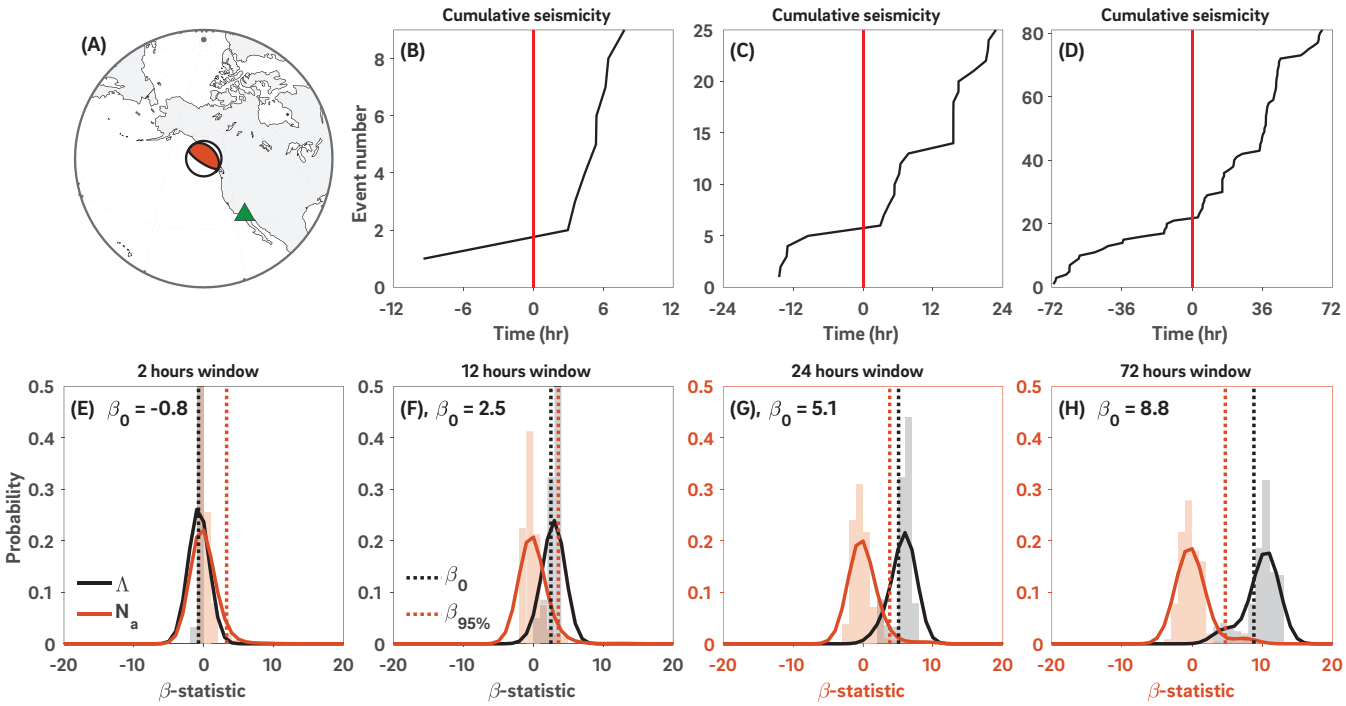

Figure 16. The 2012 M_w7.8 Haida Gwaii earthquake and the dynamic triggering responses in the SJFZ-I region during the 2-, 12-, 24-, and 72-hour time-windows. (A), location and the focal mechanism of the 2012 Haida Gwaii earthquake. The green triangle shows the study region. (B)-(D), cumulative seismicity. The P-wave arrival time is denoted at time 0, showing as the red line. (E)-(H), β-statistic distributions. Distribution-N_a (red histogram and red curve) is obtained from randomly sampling 10,000 times of the seismicity in a δ_a window (e.g., two hours) with uniformly distributed random starting time of the δ_a within 30 days before and after the P-wave arrival of the mainshock. Distribution-Λ (gray histogram and black curve) is obtained from randomly sampling 10,000 times of the seismicity in 60 days δ_b with uniformly distributed random starting time within half a year of the mainshock P-wave arrival (183 days before and after). In each panel, the black dashed line indicates the β_0 value, and the red dashed line shows the triggering threshold $\beta_{95\%}$. The identified triggering windows are outlined in red box panels (G, H). In such cases, distribution-N_a and distribution-Λ are clearly distinct from each other.

I investigated the characteristics of the dynamic triggering of microearthquakes in Southern California with a focus on the San Jacinto Fault Zone and the Salton Sea Geothermal Field from 2008 to 2017. Using a new high-resolution earthquake Catalog, we develop a new statistical approach to identify triggered cases, finding that approximately 1 out of every 5 global M_w6 earthquakes dynamically trigger microearthquakes in Southern California (e.g., Figure 16). The triggering responses include both instantaneous and delayed triggering, showing a highly heterogeneous pattern and indicating possible evolving triggering thresholds. We do not observe a clear peak ground velocity triggering threshold that can differentiate triggering earthquakes from non-triggering events, but there are subtle differences in the frequency content that may possibly differentiate the earthquakes. In contrast to the depth distribution of background seismicity, the identified triggered earthquakes tend to concentrate at the edges of the seismogenic zones. Although instantaneously triggered earthquakes are likely a result of dynamic Coulomb stress changes, the cases of delayed dynamic triggering are best explained by nonlinear triggering processes, including cyclic material fatigue, accelerated transient creep, and stochastic frictional heterogeneities.

RECENT PUBLICATIONS

Fan, W., McGuire, J., \& Shearer, P. M. (2020). Abundant spontaneous and dynamically triggered submarine landslides in the Gulf of Mexico. *Geophysical Research Letters*, **47**, e2020GL087213, doi.org/10.1029/2020GL087213, DOI

Fan, W., Barbour, A. J., Cochran, E. S., \& Lin, G. (2020). Characteristics of frequent dynamic triggering of microearthquakes in Southern California. *JGR-Solid Earth*, in revision

YURI FIALKO

Professor

yfialko@ucsd.edu; 858-822-5028

Earthquake physics, crustal deformation, space geodesy, volcanology

Professor Fialko's research is focused on understanding the mechanics of seismogenic faults and magma migration in the Earth's crust, through application of principles of continuum and fracture mechanics to earthquakes and volcanic phenomena. Prof. Fialko is using observations from space-borne radar satellites and the Global Positioning System (GPS) to investigate how the Earth's crust responds to seismic and magmatic loading.

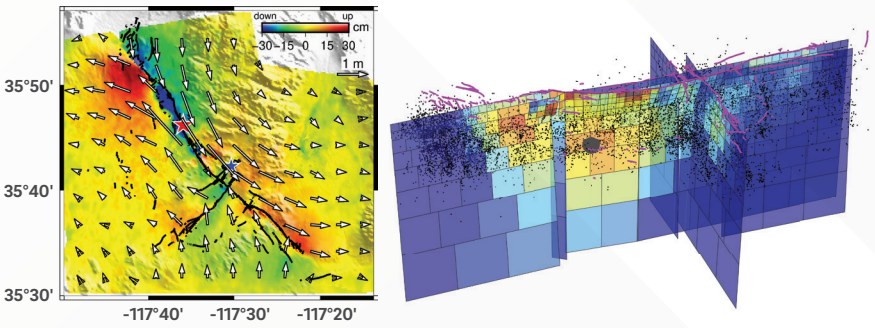

Figure 17: (Left) Co-seismic displacements due to M6.4 and M7.1 Ridgecrest earthquakes derived from Sentinel-1, ALOS-2 and Cosmo-Skymed Synthetic Aperture Radar data. Colors denote the amplitude of vertical displacements (in cm), and arrows are the horizontal displacements sub-sampled on a sparser grid. Black wavy lines denote the surface rupture mapped by field surveys. Blue and red stars indicate epicenters of the M6.4 foreshock and the M7.1 mainshock, respectively. (Right) A slip model of the Ridgecrest earthquakes derived from inversions of geodetic data and precisely located seismicity. From Jin and Fialko (2020).

One of the long-term research interests of Prof. Fialko is deformation due to active faults in Southern California. In July of 2019, a remarkable sequence of strong earthquakes occurred near the town of Ridgecrest (Figure 17). The 2019 M7.1 Ridgecrest earthquake was the third major earthquake to occur in the Eastern California Shear Zone since the advent of satellite space geodesy in the 1970's and 1980's. All three events exemplify how high quality geodetic data can provide new insights into earthquake processes. The 1992 M7.3 Landers earthquake famously showed for the first time how Interferometric Synthetic Aperture Radar (InSAR) can image surface displacements in high resolution, enabling the mapping of fault slip in unprecedented detail. Through improved InSAR data processing and coverage, the surface displacement field of the 1999 M7.1 Hector Mine earthquake was the first to be mapped in 3D at high resolution, revealing not only the complexities of subsurface fault geometry, but also variations in mechanical properties of the fault zones themselves. Global Navigation Satellite Systems (GNSS) measurements during and after both earthquakes recorded ongoing postseismic deformation at ever improving density and precision, providing a window into the constitutive properties of the crust and the mantle beneath. Even compared to their lofty predecessors, the 2019 Ridgecrest earthquakes (the July 5th M7.1 mainshock and its M6.4 foreshock on July 4th) set new standards for the amount and quality of observations of surface deformation due to large earthquakes. The Ridgecrest earthquakes were imaged by multiple radar satellite missions, including Sentinel-1A/B, ALOS-2, and COSMO-SkyMed. Short revisit times (e.g., 6 days for Sentinel-1 satellites) and systematic acquisitions from both the ascending and descending satellite tracks (providing different lines of sight), combined with nearly ideal surface conditions for radar interferometry, made the 2019 Ridgecrest earthquake sequence one of the best geodetically-recorded seismic events to date. Figure 1 shows the horizontal and vertical coseismic displacements for the pair of the Mw6.4 foreshock-M7.1 mainshock, derived from a combination of Sentinel-1, ALOS-2, and Cosmo-Skymed data. The data reveal an expected pattern of uplift and subsidence in the compressional and extensional quadrants, respectively, of a strike-slip rupture, and \rotating" horizontal displacements that are predominantly anti-symmetric with respect to the M7.1 rupture. Deviations from anti-symmetry are manifested in larger amplitude of displacements on the western/eastern sides of the fault to the north/south of the mainshock epicenter, and can be attributed to along-strike variations in fault dip. In the south-west quadrant, the displacement pattern is further complicated due to a contribution of the M6.4 foreshock. The data also reveal a mini-graben to the north of the epicenter formed by antithetic normal faults representing shallow splays of the M7.1 rupture.

Robust seismic activity, combined with large volumes of high-quality observations, makes the Ridgecrest sequence an excellent target for investigations aimed at improving our understanding of the mechanisms of spatio-temporal earthquake clustering, stress-mediated earthquake interaction, and triggering. We used a rich combination of space geodetic, geologic, and seismic observations to derive finite slip models of the 2019 foreshock-mainshock sequence, and subsequently applied these models to investigate the role of static and dynamic stress changes and stress heterogeneity in the earthquake triggering. Static stress changes near the hypocenter resolved on a mean trend of the M7.1 rupture were less favorable for failure compared to stress changes resolved on a more northerly striking fault plane indicated by the first motion data. This suggests that the M7.1 mainshock may have been triggered by the M6.4 foreshock on a slip patch that was optimally oriented for failure with respect to the local stress field, and subsequently triggered unstable slip on a less favorably oriented pre-existing right-lateral fault system. Dynamic stress changes from the nearby earthquakes failed to trigger the mainshock, despite the fact that they were much larger than any static stress change that might have advanced the nucleation of unstable slip. Subsequent studies of postseismic deformation will show if the inferred amount of the co-seismic slip deficit can be accommodated by means of creep in the uppermost crust.

Other currently active projects include a joint seismic-geodetic study of the sub-surface structure of the Southern San Andreas fault, and postseismic transients due to large earthquakes on the edges of the Tibetan Plateau.

RECENT PUBLICATIONS

Jin, Z. and Y. Fialko, Finite slip models of the 2019 Ridgecrest earthquake sequence constrained by space geodetic data and aftershock locations, *Bull. Seismol. Soc. Am.*, **110**, 1660-1679, 2020.

Floyd, M., G. Funning, Y. Fialko, R. Terry, and T. Herring (2020). Survey and Continuous GNSS in the vicinity of the July 2019 Ridgecrest earthquakes, *Seismol. Res. Lett.*, **91,** 2047-2054, 2020.

Erickson, B. et al., The Community Code Verification Exercise for Simulating Sequences of Earthquakes and Aseismic Slip (SEAS), *Seismol. Res. Lett.*, **91**, 874-890, 2020.

Tymofyeyeva, E., Y. Fialko, et al., Slow slip event on the southern San Andreas fault triggered by the 2017 Mw8.2 Chiapas (Mexico) earthquake, *J. Geophys. Res.*, **124**, 9956-9975, 2019.

HELEN AMANDA FRICKER

Professor, co-lead Scripps Polar Center

hafricker@ucsd.edu; 858-534-6145, polar.ucsd.edu

Cryosphere, Antarctic ice sheet, subglacial lakes, ice shelves, satellite remote sensing

We are located in MESOM with OA Prof Fiamma Straneo, forming the core of the Scripps Polar Center. I am a member of NASA's ICESat-2 Science Team. I became an AGU Fellow in December 2017 and gave the John F. Nye Lecture at AGU in 2019. I am an Honorary Professor at University of Swansea (1 February 2020 to present).

My research focuses on understanding the processes driving changes on the Antarctic ice sheet. One of the main unknowns is Antarctica's current contribution to global sea level rise, & predicting how that will change in the future. Because Antarctica is so large, & the time scales on which it changes are so long (decades to centuries), the only viable way to monitor it is with satellites. The main technique we use is **satellite altimetry** (radar altimetry from ESA's ERS-1/ERS-2/ Envisat (1994-2012) or laser altimetry from NASA's Ice, Cloud & land Elevation Satellite (ICESat 2003-2009) & ICESat-2 (launched 15 Sept 2018)); these multiple missions have provided ice sheet height data for ~25 years. Using the long, continuous altimeter records we can learn about the processes that are leading to accelerated mass loss. **We focus mainly on two key dynamic components of the Antarctic ice-sheet system: (i) floating ice shelves & (ii) active subglacial lakes.**

Ice shelves: Antarctica's ice shelves are where most of the mass loss takes place. Since ice shelves are floating, their melting does not contribute directly to sea level. However, ice shelves provide mechanical support to 'buttress' seaward flow of grounded ice, so that ice-shelf thinning and retreat result in enhanced ice discharge across the grounding line (GL) to the ocean. Our group specializes in monitoring Antarctic ice shelves from satellite altimetry (radar and laser). We also perform fieldwork on ice shelves.

Satellite laser altimetry (ICESat and ICESat-2): ICESat-2 was launched in September 2018 and I also led the writing of the first paper that came out on ICESat-2 over the ice sheets, comparing with the previous NASA laser altimetry mission (ICESat) to make an estimate of mass loss of all the ice sheets from 2003 to 2019, including the ice shelves; his allowed us to make direct comparisons between loss of floating ice and subsequent loss of grounded ice (through loss of buttressing).

ICESat-2 brings a new capability to surface melt detection on ice sheets: the 532 nm photons penetrate through standing water and are reflected from both the water and the underlying ice; the difference between the two (corrected for refractive index) provides a depth estimate.

Surface melting has been difficult to quantify because depth estimates are challenging. We led a pilot project with several investigators who contributed depth estimates for four Amery melt features with depths ranging to 6 m, using seven different ICESat-2 algorithms and compared them with estimates from coincident Landsat MSS and Sentinel-2 images. This showed ICESat-2 water depth estimates can be used to tune image-based depth algorithms, enabling improved ice-sheet wide estimates of melt volumes across Antarctica and Greenland; 3rd year student Philipp Arndt just received a NASA FINESST award to continue the surface melt work.

Field-based studies: I was PI on an NSF project ROSETTA-Ice which investigated the Ross Ice Shelf using airborne geophysics (gravity, laser and radar) conducted over four Antarctic field seasons. GP student Maya Becker participated in the 2016/2017 and 2017/2018 field seasons. We also worked with GP postdoc Emilie Klein who used GPS data from Ross Ice Shelf (from an NSF project led by SIO's Peter Bromirski) to identify a seasonal cycle in ice velocities. Ice-sheet modeling by GP postdoc Cyrille Mosbeux demonstrated that the seasonal cycle in velocity was consistent with the seasonality of near-ice-front basal melting, and that this seasonality extended onto the surrounding grounded ice; i.e., short-term changes in basal melting had a significant effect on the ice shelf's buttressing of the grounded catchments. Cyrille Mosbeux also worked on modelling the Ross ice front, working with GP student Maya Becker.

Subglacial water system: In 2006, I discovered active subglacial water systems under the fast-flowing ice streams of Antarctica in repeat-track ICESat data. Height changes on the order of several meters corresponded to draining and filling of active subglacial lakes. We continue to monitor active lakes and have found 124 in total throughout Antarctica. I was PI on two large NSF projects that culminated in drilling of two subglacial lakes (Whillans in 2013 and Mercer in Jan 2018). Matt Siegfried (former GP student) led the geophysics team, which also included former IGPP Prof. Kerry Key and GSR Chloe Gustafson (for EM measurements) in 2018, and 3rd year student Philipp Arndt in 2019.

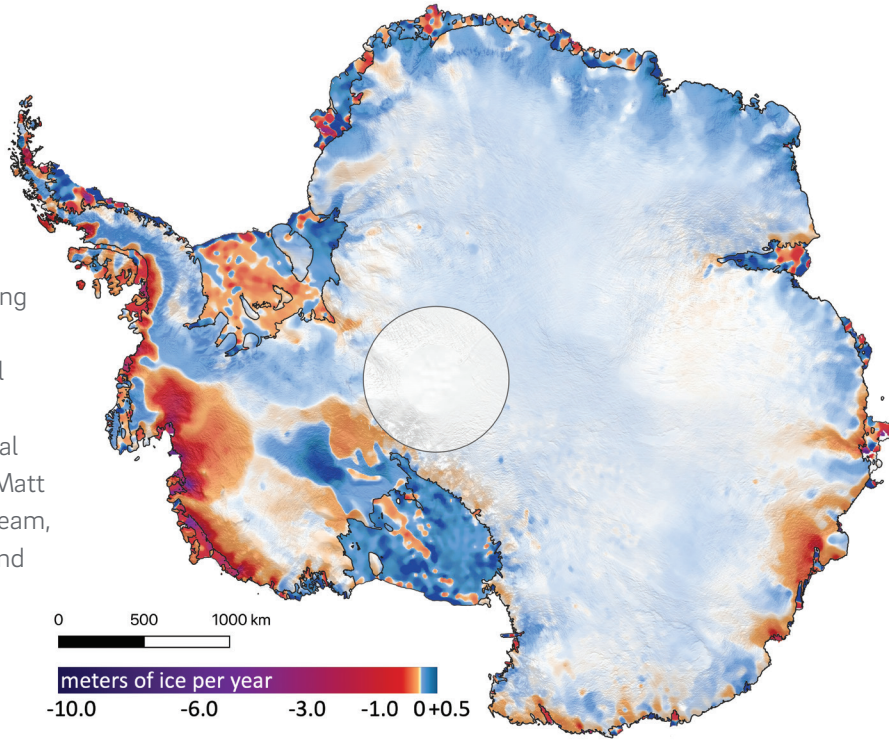

Figure 18: Ice thickness change for the Antarctic Ice Sheet from 2003 to 2019 from ICESat & ICESat-2. Reproduced from the New York Times.

RECENT PUBLICATIONS

Venturelli, R. A., M. R. Siegfried, K. A. Roush, W. Li, J. Burnett, R. Zook, H. A. Fricker, J. C. Priscu, A. Leventer, B. E. Rosenheim (2020) Mid-Holocene Grounding Line Retreat and Readvance at Whillans Ice Stream, West Antarctica. *Geophysical Research Letters*, **47**(15), doi: e2020GL088476.

Khalsa, S. J. S., A. Borsa, V. Nandigam, M. Phan, K. Lin, C. Crosby, H. Fricker, C. Baru, And L. Lopez (2020) OpenAltimetry-rapid analysis and visualization of Spaceborne altimeter data. *Earth Science Informatics* (2020): 1-10.

Fair, Z., M. Flanner, K. M., Brunt, H. A., Fricker, A. S., Gardner (2020) Using ICESat-2 and Operation IceBridge altimetry for supraglacial lake depth retrievals, *The Cryosphere Discuss.*, https://doi.org/10.5194/tc-2020-136.

Klein, E*. C. Mosbeux*, P. D. Bromirski, L. Padman, Y. Bock, S. R. Springer, H. A. Fricker (2020) Annual cycle in flow of Ross Ice Shelf, Antarctica: Contribution of variable basal melting, *Journal of Glaciology,* 1–15. https:// doi.org/10.1017/jog.2020.61.

Mosbeux, C., T. J. Wagner, M. K. Becker, H. A. Fricker (2019) Viscous and elastic buoyancy stresses as drivers of ice-shelf calving. *Journal of Glaciology*, 1-15, doi.org/10.1017/jog.2020.35

Adusumilli, S., H. A. Fricker, B. Medley, L. Padman, M. R. Siegfried (2020) Interannual variations in meltwater input to the Southern Ocean from Antarctic ice shelves, *Nature Geoscience*, https://doi.org/10.1038/s41561-020-0616-z.

Smith, B., H. A. Fricker, A. S. Gardner, B. Medley, J. Nilsson, F. S. Paolo, N. Holschuh, S. Adusumilli, K. Brunt, B. Csatho, K. Harbeck, T. Markus, T. Neumann, M. R. Siegfried, H. J. Zwally (2020) Pervasive ice sheet mass loss driven by competing ocean and atmosphere processes, *Science*, **368**(6496), 1239-1242.

Begeman, C. B., S. Tulaczyk, L. Padman, M. King, M. R. Siegfried, T. O. Hodson, H. A. Fricker (2020). Tidal pressurization of the ocean cavity near an Antarctic ice shelf grounding line. *Journal of Geophysical Research: Oceans*, **125**(4), e2019JC015562.

Das, I., L. Padman, R. E. Bell, H. A. Fricker, K. J. Tinto, C. L. Hulbe, C. S. Siddoway, T. Dhakal, N.p. Frearson, C. Mosbeux, S. I. Cordero, M. R. Siegfried (2020) Multi-decadal basal melt rates and structure of the Ross Ice Shelf, Antarctica from airborne ice penetrating radar, *Journal of Geophysical Research,* **125(**3), e2019JF005241.

JAMIN S. GREENBAUM

Assistant Research Geophysicist

jsgreenbaum@ucsd.edu

Cryosphere, Ice-ocean interactions, Ice shelves, Airborne remote sensing

My work is guided by a desire to understand the causes and impacts of ongoing and future sea level change. Recently I have been focused understanding the processes controlling ice shelf melt and grounding line retreat in Antarctica, emphasizing the acquisition and analysis of airborne remote sensing data over ice shelf cavities and other under-observed areas along the Antarctic continental shelf. Beyond data analyses and interpretation, I also seek to develop novel techniques to access and observe difficult to reach environments. I am additionally dedicated to inclusive global collaborative science and maintain close collaborations with scientists, pilots, and other experts from around the world.

Ice-ocean interactions: We use a variety of observations to constrain boundary conditions and identify processes related to Antarctic coastal ice sheet stability. Recently, this work has included analyses of radar data to detect subglacial water systems and grounding lines and to infer surface and basal melting of ice shelves (Fig. 19). We also use gravity and magnetics data to infer the geology and geothermal heat flux beneath the Antarctic Ice Sheet, and the shape of the seafloor beneath sea ice and ice shelves where icebreakers struggle to sail. We are particularly interested in understanding the impact of discharged subglacial meltwater on ice shelf basal melt.

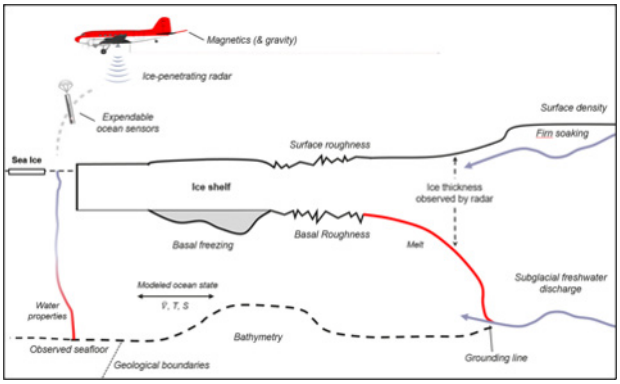

Figure 19. Conceptual profile of an ice shelf from upstream of the grounding line (right) to the adjacent ocean and sea ice (left). Ice-penetrating radar data are useful for inferring atmo-sphere- and ocean-driven melt processes, gravity and magnetics are useful for constraining the depth and shape of the seafloor; expendable ocean probes may be deployed from the aircraft into small sea ice leads impossible or impractical for conventional platforms to access.

Airborne remote sensing for ice-ocean interactions: Airborne platforms can effectively and repeatedly access areas impossible or impractical for surface-based platforms (Fig.19). We use ice-penetrating radar data to characterize boundary conditions useful for numerical ice sheet and ocean circulation models (e.g. basal morphology and small scale roughness); we apply gravity and magnetics data to infer the depth and shape of the seafloor beneath floating ice; and we use airborne-deployed ocean sensors to sample the ocean state along glacier calving fronts where no prior data have been acquired.

RECENT PUBLICATIONS

Indrigo, C., C. Dow, J.S. Greenbaum, M. Morlighem (accepted), Drygalski Ice Tongue stability influenced by rift formation and ice morphology, Journal of Glaciology.

Roberts, J.L., L.M. Jong, F.S. McCormack, M.A. Curran, A.D. Moy, D. Etheridge, J.S. Greenbaum, D.A. Young, S.J. Phipps, W. Xue, T.D. van Ommen, D.D. Blankenship, M.J. Siegert (2020), Integral correlation for uneven and differently sampled data: Application to the Law Dome Antarctic climate record, Nature Scientific Reports.

Aitken, A, L. Ramos, J.L. Roberts, J.S. Greenbaum, D.A. Young, D.D. Blankenship (2020), A magnetic data correction workflow for sparse, four dimensional data, Journal of Geophysical Earth – Solid Earth.

Cui, X., Jeofry, H., Greenbaum, J.S., Guo, J., Li, L., Lindzey, L.E., Habbal, F.A., Wei, W., Young, D.A., Ross, N. and Morlighem, M., (2020). Bed topography of Princess Elizabeth Land in East Antarctica. Earth System Science Data Discussions, pp.1-25.

Cui, X., J.S. Greenbaum, S. Lang, X. Zhao, L. Li, J. Guo, Scientific Operations of "Snow Eagle 601" in Antarctica in the Past Five Austral Seasons" (in review), Remote Sensing.

Guo, J., W. Yang, Y. Dou, X. Tang, J.S. Greenbaum, R. Dou, Y. Pan, Y. Zhang, M. Ding, S. Jiang, G. Shi, X. Cui, B. Sun (2020), Historical surface mass balance from a frequency-modulated continuous-wave (FMCW) radar survey from Zhongshan Station to Dome A, Journal of Glaciology.

Wei, Wei, D.D. Blankenship, J.S. Greenbaum, N. Gourmelen, C. Dow, T.G. Richter, C.A. Greene, D.A. Young, S.H. Lee, T.W. Kim, W.S. Lee, A. Wåhlin, K. Assmann, (2020), Getz Ice Shelf melt enhanced by freshwater discharge from beneath the West Antarctic Ice Sheet, The Cryosphere.

Dow, C., F.F. McCormack, D.A. Young, J.S. Greenbaum, J.L. Roberts, D.D. Blankenship (2020), Totten Glacier subglacial hydrology determined from geophysics and modeling, Earth and Planetary Science Letters.

JENNIFER S. HAASE

Research Geophysicist

jhaase@ucsd.edu; 858-534-8771; https://jhaase.scrippsprofiles.ucsd.edu

I work in two broad research areas: 1) Earthquakes, seismic hazard, and tsunami hazard and 2) hazards from severe weather using GPS signals as a remote sensing technique from aircraft and stratospheric balloons.

AIRCRAFT OBSERVATIONS OF MOISTURE IN ATMOSPHERIC RIVERS

Atmospheric rivers (ARs) are long narrow filaments of high moisture transport over the ocean usually associated with extreme and long duration rainfall when they impact the western coast of the US. The moisture distribution within atmospheric rivers when they arrive at the coastline is a major factor in determining the spatial distribution and intensity of precipitation. Aircraft reconnaissance missions with targeted dropsondes have been operationalized recently to provide high resolution observations and improve forecast model initial conditions of winds, moisture, and temperature in the region of extensive cloud cover and rain that is difficult to measure from satellites. We seek to increase the amount of data available from the reconnaissance missions with airborne GNSS (Global Navigation Satellite System) radio occultation (ARO) profiles that are collected continuously during flight without additional expendable costs. We derive the first refractivity profiles from the European Galileo system, and combine them with Global Positioning System profiles to demonstrate accuracy comparable to dropsonde observations. The combined dataset enhances the coverage at a scale relevant for mesoscale weather modeling. The refractivity anomaly from the mesoscale model reveals key features of the atmospheric river including the low-level jet and tropopause fold that illustrate the potential strength of the ARO method to directly measure AR characteristics.

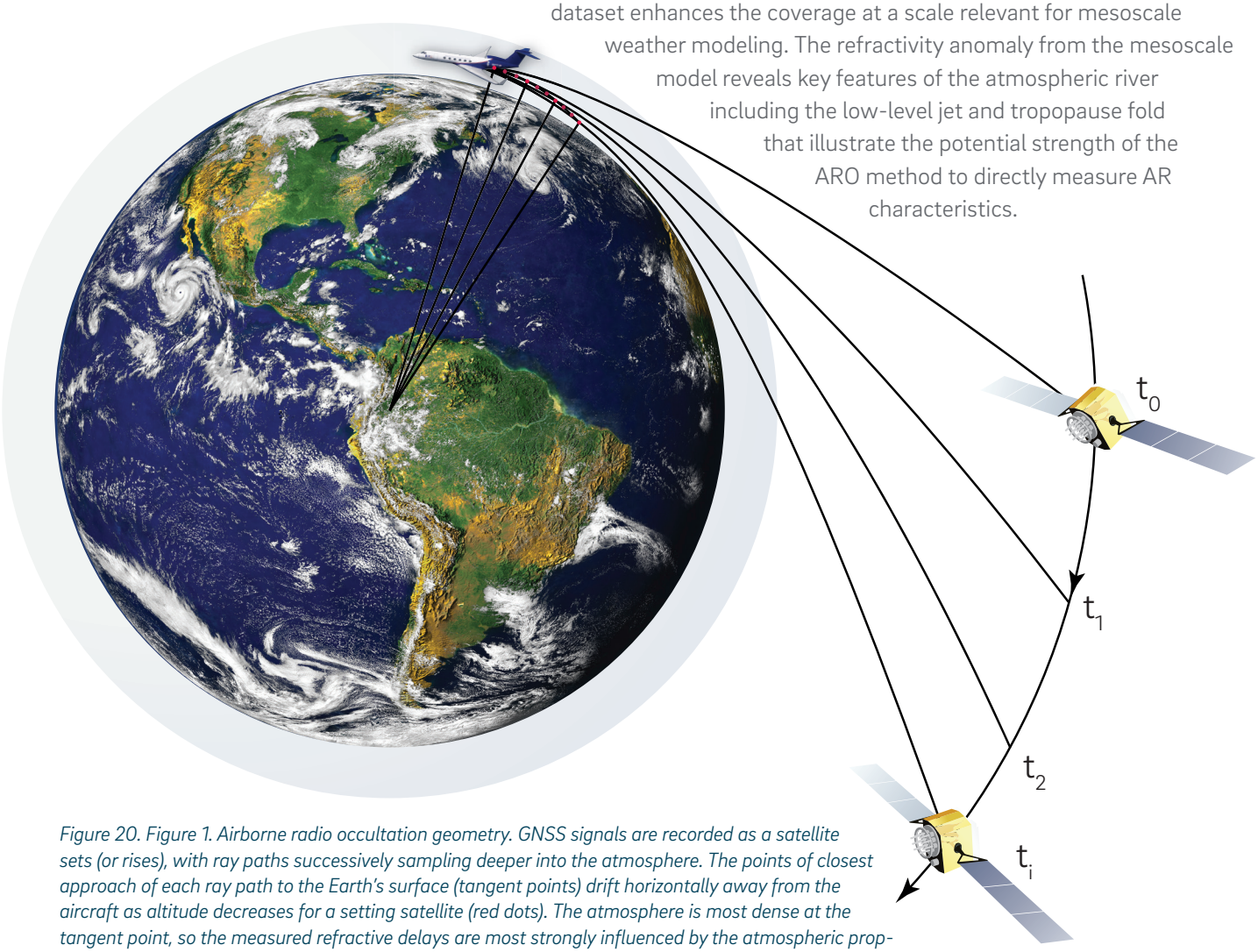

Figure 20. Figure 1. Airborne radio occultation geometry. GNSS signals are recorded as a satellite sets (or rises), with ray paths successively sampling deeper into the atmosphere. The points of closest approach of each ray path to the Earth's surface (tangent points) drift horizontally away from the aircraft as altitude decreases for a setting satellite (red dots). The atmosphere is most dense at the tangent point, so the measured refractive delays are most strongly influenced by the atmospheric properties at this location. Retrievals of atmospheric refractivity, moisture, and temperature are represented as values along these slanted tangent point profiles.

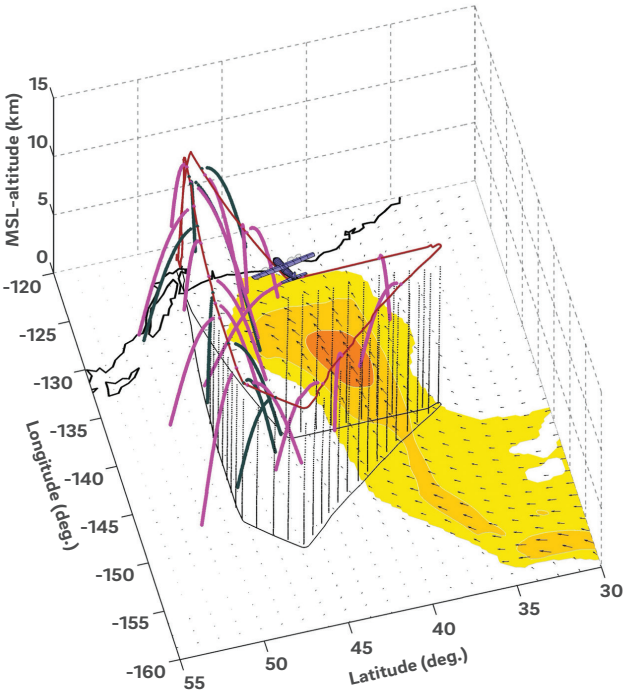

Figure 21. Three-dimensional view of sampling by airborne radio occultation drifting tangent points and dropsondes. Dark grey and magenta curves are Galileo and GPS occultations, vertical black lines are dropsondes released from the aircraft, whose trajectory is denoted by the brown line. Integrated water vapor transport is shown in color contours on the lower surface.

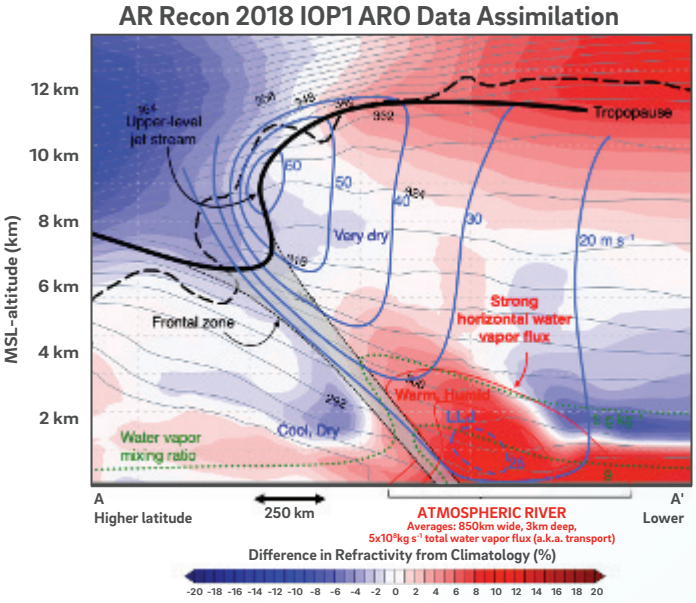

Figure 22. Refractivity anomaly cross-section through the mesoscale weather model that incorporated the aircraft observations, perpendicular to the atmospheric river transport direction. Refractivity anomaly (%) is the difference from a climatological model. The 2 PVU contour is represented by the thick black dashed line. Potential temperature contours are shown in gray. The schematic representation of the vertical structure of the AR [Ralph et al., 2017] is superimposed on the refractivity anomaly, with no adjustments to the horizontal or vertical scale to illustrate how refractivity anomaly captures the key features of the atmospheric river structure and in particular the area at the top of the moist low level jet where convection occurs.

RECENT PUBLICATIONS

Haase, J. S., J. Michael J. Murphy, B. Cao, F. M. Ralph, M. Zheng, and L. D. Monache (2020), Accuracy of multi-GNSS airborne radio occultation observations in an atmospheric river as a complement to dropsondes, *Geophysical Research Letters*, to be submitted.

Sepulveda, I., J. S. Haase, M. Carvajal, X. Xu, and P. L.-F. Liu (2020), Modeling the sources of the 2018 Palu, Indonesia, tsunami using videos from social media, *Journal of Geophysical Research-Solid Earth*, **125**.

Carvajal, M., C. Araya-Cornejo, I. Sepúlveda, D. Melnick, and J. S. Haase (2019), Nearly instantaneous tsunamis following the Mw 7.5 2018 Palu earthquake, *Geophysical Research Letters*, **46**, 5117-5126.

Cao, B., J. S. Haase, J. Michael J. Murphy, M. J. Alexander, and M. Bramberger (2020), Tropical waves observed by balloon-borne GPS Radio Occultation measurements of Strateole-2 campaign over the equatorial area, paper presented at American Geophysical Union Annual Meeting, San Francisco, CA, USA.

Haase, J. S., B. J. Murphy, P. Muradyan, F. Nievinski, K. M. Larson, J. L. Garrison, and K.-N. Wang (2014), First Results from an Airborne GPS Radio Occultation System for Atmospheric Profiling, *Geophysical Research Letters*, **40**.

Haase, J. S., J. Maldonado-Vargas, F. Rabier, P. Cocquerez, M. Minois, V. Guidard, P. Wyss, and A. V. Johnson (2012), A proof-of-concept balloon-borne Global Positioning System radio occultation profiling instrument for polar studies, *Geophysical Research Letters*, **39**.

MICHAEL A.H. HEDLIN

Research Geophysicist

hedlin@ucsd.edu; 858-534-8773

Study of large atmospheric phenomena, study of long-range propagation of subaudible sound in the atmosphere, seismo-acoustics

INFRASOUND: The study of subaudible sound, or infrasound, has emerged as a new frontier in geophysics and acoustics. We have known of infrasound since 1883 with the eruption of Krakatoa, as signals from that event registered on barometers around the globe. Initially a scientific curiosity, the field briefly rose to prominence during the 1950's and 1960's during the age of atmospheric nuclear testing. With the recent Comprehensive Test-Ban Treaty, which bans nuclear tests of all yields in all environments, we have seen renewed interest in infrasound. A worldwide network of infrasound arrays, being constructed for nuclear monitoring, is fueling basic research into man-made and natural sources of infrasound, how sound propagates through our dynamic atmosphere and how best to detect infrasonic signals amid noise due to atmospheric circulation. This network has been supplemented with deployments, such as the 400-station seismo-acoustic USArray Transportable Array (TA), for basic research and enhanced monitoring of regions of great interest.

RESEARCH AT L2A: The Laboratory for Atmospheric Acoustics (L2A) is the home of research in this field at IGPP. Several faculty, post-docs and PhD students work full or part time in L2A, supported by engineers and technicians in the lab and the field. More information about this lab can be found at l2a.ucsd.edu. Presently we study a broad suite of problems related to both natural and man-made sources.

DENSE NETWORK STUDIES: The global infrasound network is unprecedented in scale however it is still very sparse, with ~ 100 stations operating worldwide. To increase the density of sampling of the infrasonic wavefield we have used acoustic–to-seismic coupled signals recorded by dense networks, such as the 400-station USArray Transportable Array (TA) and various PASSCAL deployments. We have used the original (seismic-only) TA network to create a catalog of atmospheric events in the western United States similar to commonly used seismic event catalogs. The acoustic

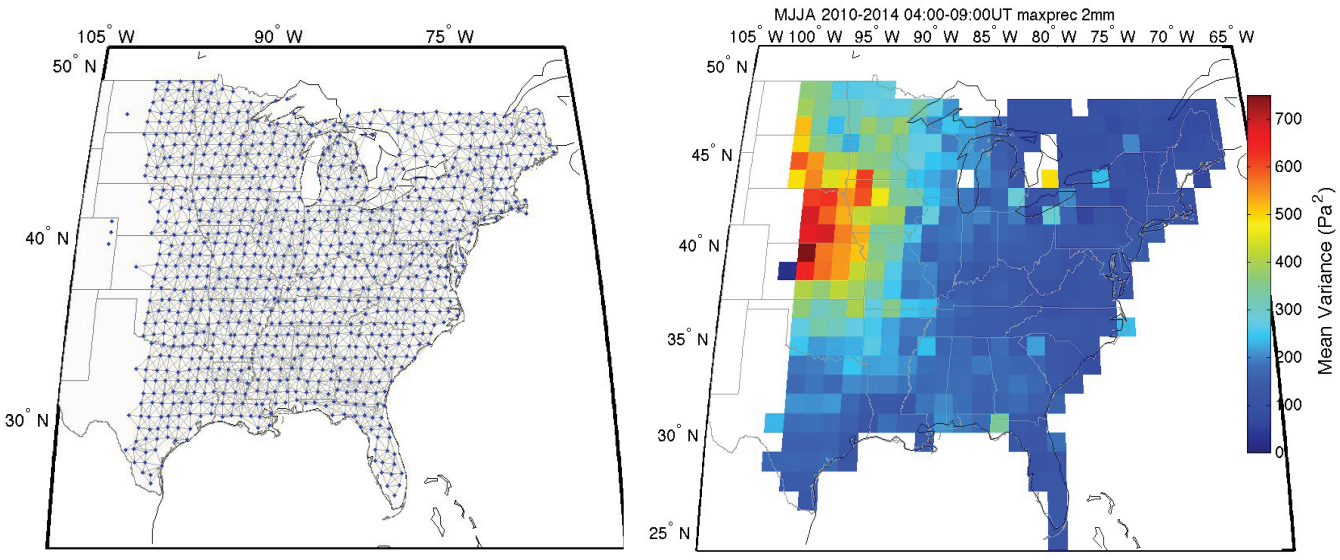

Figure20: (left) sites occupied by stations in the TA from January 1, 2010 through Sept 30, 2014. These stations have been grouped into 3-element arrays (triads) for the study of long-period atmospheric gravity waves. The panel on the right shows the variance of atmospheric pressure in the 2-6 hr passband during the thunderstorm seasons from 2010 through 2014. The high variance near the Great Lakes is due to gravity waves excited by convective storms.

catalog is used in part to find sources of interest for further study and to use the recorded signals to study long-range infrasound propagation. Recorded signals from instantaneous sources are commonly dispersed in time to several 10's of seconds. Modeling indicates that this is due to interaction of the sound waves with fine-scale structure in the atmosphere due to gravity waves. We are currently using infrasound to constrain the statistics of this time-varying structure.

The National Science Foundation funded our group to upgrade the entire TA with infrasound microphones and barometers. Our sensor package is sensitive to air pressure variations from D.C. to 20 Hz, at the lower end of the audible range. The upgrade converted the TA into the first-ever semi-continental-scale seismo-acoustic network. The network has moved east across the US as stations are redeployed. Figure 20 (left panel) shows station locations from January 1, 2010 through the end of September, 2014. We have divided this collection of stations into 3,600 elemental arrays (triads) to study atmospheric gravity waves. An early result is shown in the right panel of Figure 18. This map shows the variance of atmospheric pressure in the 2-6 hour pass-band at local night. Elevated variance of atmospheric pressure is due to the presence of atmospheric gravity waves. As expected, large gravity waves are common to the west of the Great Lakes and are from convective activity.

FIELD OPERATIONS: Our group has built infrasound arrays for nuclear monitoring in the US and Africa. We operate research arrays located near San Diego.

RECENT PUBLICATIONS

Brown, P., Assink, J., Astiz, L.,Blaauw, R., Boslough, M., Borovicka, J., Brachet, N., Brown, D., Campbell-Brown, M., Ceranna, L., Cooke, W., de Groot-Hedlin, C., Drob, D., Edwards, W. Evers, L., Garces, M., Gill, J., Hedlin, M.A.H., Kingery, A., Laske, G., Le Pichon, A., Mialle, P., Moser, D., Saffer, A., Silber, E., Smets, P., Spalding, R., Spurny, P., Tagliaferri, E., Uren, D., Weryk, R., Whitaker, R., Krzeminski, Z., 2013, The Chelyabinsk airburst: Implications for the Impact Hazard, *Nature*, DOI: 10.1038/nature12741.

de Groot-Hedlin, C.D., Hedlin, M.A.H., Hoffmann, L., Alexander, M.J. and Stephan, C., 2017, Relationships between Gravity Waves Observed at the Surface and in the Stratosphere over the Continental United States, *JGR Atmospheres,* DOI: 10.1002/2017JD027159.

Fan, W., de Groot-Hedlin, C.D., Hedlin, M.A.H. and Ma, Z., 2018, Using surface waves recorded by a large mesh of three-element arrays to detect and locate disparate seismic sources, *Geophysical Journal International,* ***215,*** p942-958, https://doi.org/10.1093/gji/ggy316

Fan, W., McGuire, J.J., de Groot-Hedlin, C.D., Hedlin, M.A.H., Coats, S. and Fiedler, J.W. 2019, Stormquakes, *Geophysical Research Letters,* doi: 10.1029/2019GL084217

Hedlin, M.A.H. and Drob, D.P., 2014, Statistical characterization of atmospheric gravity waves by seismoacoustic observations, *J. Geophys. Res. Atmos.,* doi: 10.1002/2013JD021304.

Hedlin, M.A.H., de Groot-Hedlin, C.D., Forbes, J. and Drob, D., 2018, Solar Terminator Waves in Surface Pressure Observations, *Geophysical Research Letters,* ***45,*** DOI:10.1029/2018GL078528.

Hedlin, M.A.H., de Groot-Hedlin, C.D., Ritsema, J., Hetland, E., 2018, A multidisciplinary study of the January 17, 2018 bolide terminal burst over southeast Michigan, *Seismological Research Letters,* ***89*** (6): 2183-2192, https://doi.org/10.1785/0220180157.

GLENN IERLEY

Professor Emeritus

grierley@ucsd.edu

Rank-based distribution-free characterization of noise as a universal basis for signal detection and extraction. Detection and localization of marine mammal species.

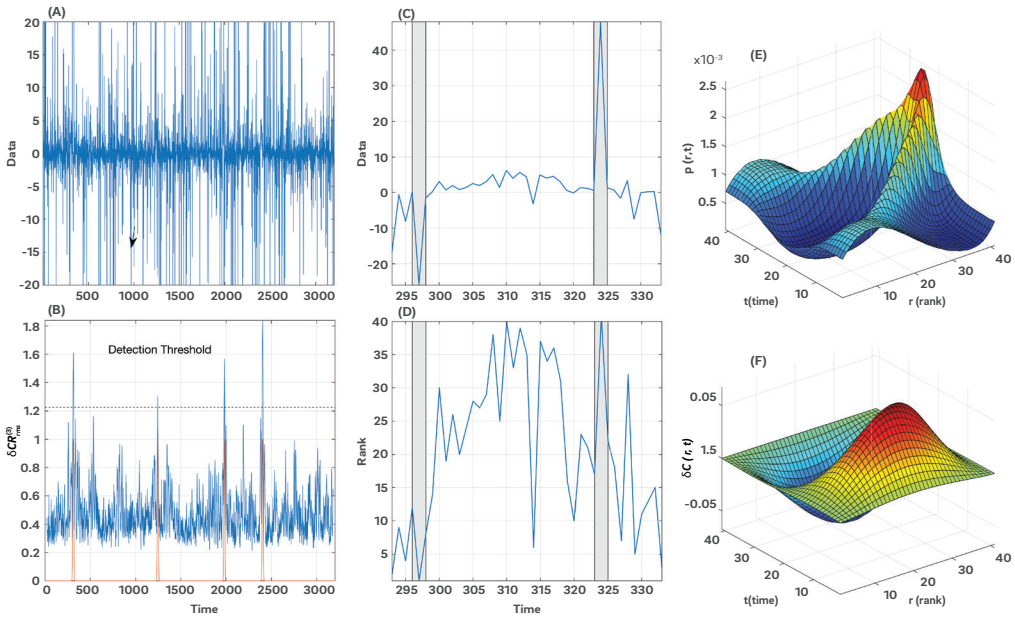

Figure 21. Detection of Gaussian pulses embedded in Cauchy noise. (a): Time series of Cauchy noise with four (unknown) Gaussian pulses to detect. Vertical scale is clipped to show detail. (b): The detection metric, with the four spikes lining up with the true pulse locations (red). (c): raw data for the sliding window of N = 41 centered about the rst detected pulse, plotted full scale. (d): The raw data of (b) converted to rank from 1 to 41. Ratio of variance or signal-to-noise power ratio (SNR), is technically zero for Cauchy noise but the nominal, sample-based value is ≈4 x 10^{-4}. (e): Ensemble limit of the rank-order probability mass function (pmf), p(r; t), of signal plus noise (10^6 trials), with the Gaussian "ridge" seen in the maximum of p vs. t. (f): Ensemble limit of the deviation cumulative distribution function δC of signal plus noise.

RECENT PUBLICATIONS

Ierley, G. A. Kostinski (2020) Detection of unknown signals in arbitrary noise, *Phys. Rev. E*, 102:3 032221, DOI

Kestner, D., G. Ierley, A. Kostinski (2020) A fast algorithm for computing a matrix transform used to detect trends in noisy data, *Comput. Phys. Commun.*, **254**, 107382, DOI

Durbach, I. N., S. W. Martin, C. Martin, T. A. Helble, E. Henderson, G. Ierley, C. M. Harris, L. Thomas (2020) Changes in the movement and calling behaviour of minke whales (Balaenoptera acutorostrata) in response to navy training, In preparation.

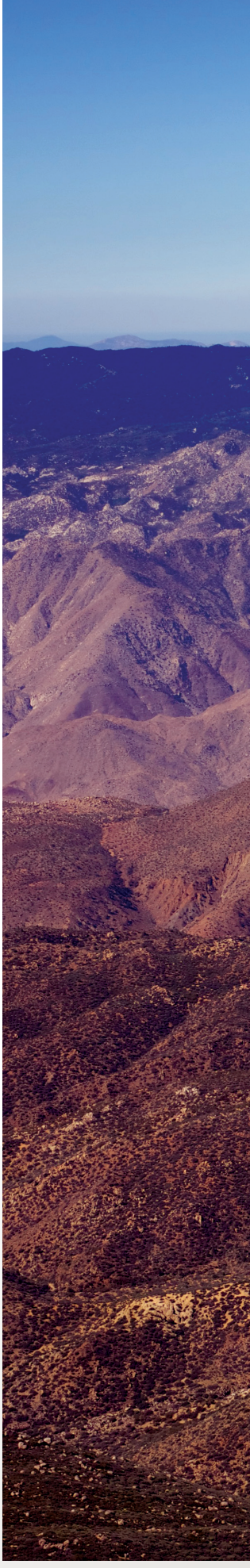

DEBORAH LYMAN KILB

Project Scientist

dkilb@ucsd.edu; 858-822-4607

Research Interests: Crustal seismology, earthquake early warning and earthquake triggering. Diversity Interests: Improving how science is communicated to students and the public. Promoting jobs requiring skills within the intersection of science and art. Cultivating diversity within our communities.

DYNAMIC EARTHQUAKE TRIGGERING [PANKOW & KILB, 2020]. Remote earthquake triggering is a well-established phenomenon. Triggering is commonly identified from statistically significant increases in earthquake rate coincident with the passage of seismic energy. In establishing rate changes, short duration earthquake catalogs are commonly used, and triggered sequences are not typically analyzed within the context of background seismic activity. Using 500 mainshocks and four western USA 33-yearlong earthquake catalogs (Figure 22), we compare the ability of three different statistical methods to identify remote earthquake triggering. Counter to many prior studies, we find remote dynamic triggering is rare (conservatively, <2% of the time). For the mainshocks associated with remote rate increases, the spatial and temporal signatures of triggering differ. We find that a rate increase coincident in time with mainshock energy alone is insufficient to conclude that dynamic triggering occurred. To classify dynamically triggered sequences, we suggest moving away from strict statistical measurements and instead use a compatibility assessment that includes multiple factors, like spatial and temporal indicators.

EXTRAPOLATING GROUND MOTIONS [JOHNSON ET AL., 2020]. There are an infinite number of locations where seismic waves interact with Earth's surface, yet seismologists can only record a finite set of ground motions. This requires assumptions about how known measurements or predictions can be extrapolated to nearby locations. We test to what extent extrapolation is viable using an array of 1,108 geophones installed 10–20 meters apart within a 0.36 square-km study area for 1 month atop the San

Jacinto Fault in Southern California. Measuring ground motions from 38 small local earthquakes, we observe peak ground velocity (PGV) variations up to 22% across the array. We find the basin structure consistently traps energy, amplifying the seismic velocities, and that the damaged region within the fault reduces the PGVs. Comparing surface and borehole measurements (148 meters deep), we find PGVs recorded at the surface are 3–10 times greater than the measurements at depth. We attribute these differences to amplification from soft sediments within the basin. We show that by leveraging information from >1,000 measurements per earthquake the ground motion velocities can be tightly constrained. These results suggest the spatial extrapolation of PGVs in regions of known faults and basins, even across a small area, should be done with caution.

OPTIMALLY ORIENTED REMOTE EARTHQUAKE TRIGGERING [ALFARO-DIAZ ET AL., 2020]. Using 13 years of earthquake data (2004–2016) from the EarthScope USArray Transportable Array and the Southern California Seismic Network, we search for remotely triggered earthquakes in an extended region encompassing the Coso Geothermal Field, California. Analyzing 211 M ≥ 7 global earthquakes, we identify 41 earthquakes consistent with remote triggering in the Coso Geothermal Field. Of these 41 triggering mainshocks, the back azimuths primarily range between ~70–100° (35, West Pacific) and ~240–300° (6, South America). Earthquakes from these two locations (Figure 23) will produce seismic waves across our study region that geometrically align with the local stress field in a way that is most conducive to local earthquake triggering. We conclude that the fault geometry and local stress orientations in the Coso Geothermal Field region are uniquely positioned to host remotely triggered earthquakes following large earthquakes originating from the West Pacific and South America.

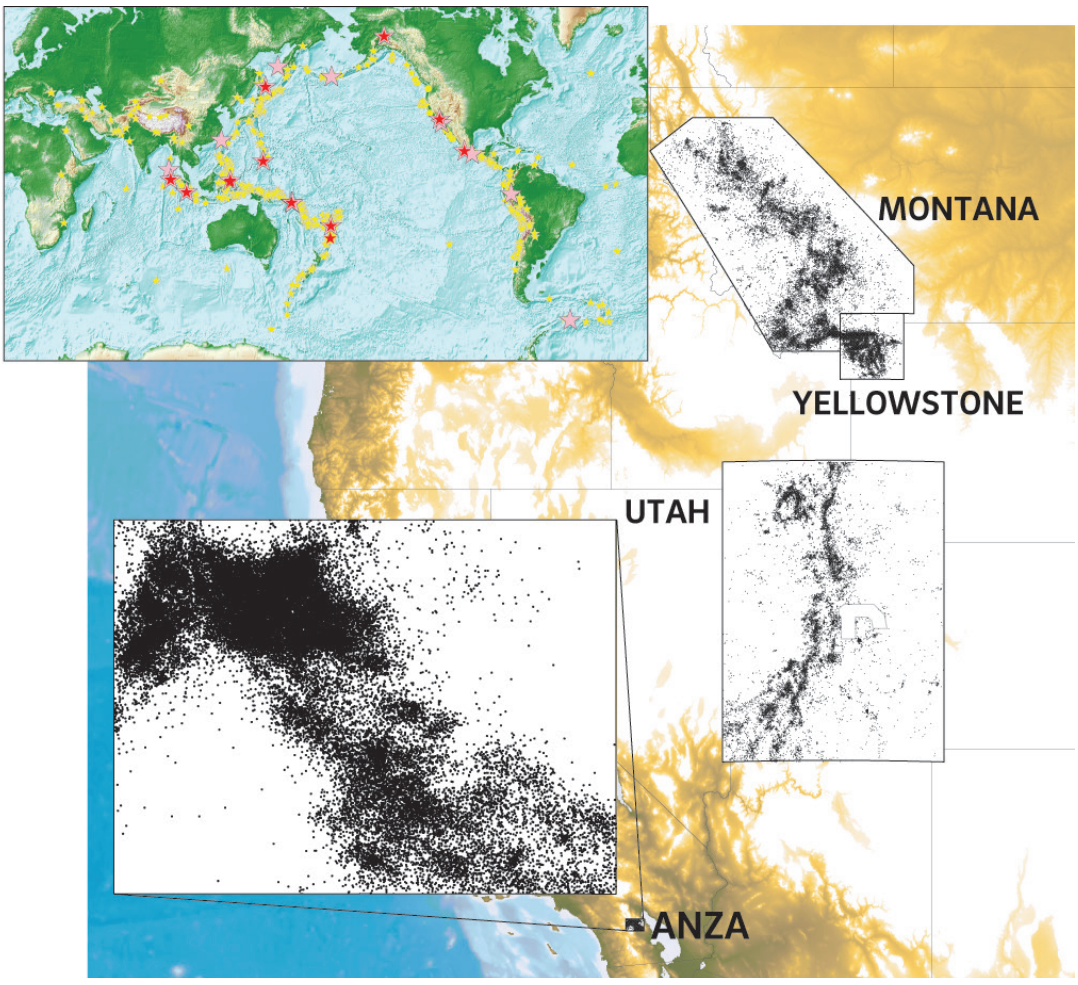

Figure 22. (top left inset) 500 mainshock earthquakes used in this study. Of these, 489 M ≥ 7.0 are teleseismic mainshocks (stars) and 11 are M ≥ 6.7 along the North American west coast (circles). Triggering mainshocks determined using the empirical method at the 95% significance level (pink, N = 19) and 99% (red, N = 12) are also shown. (basemap) Map of the four study regions (labeled).

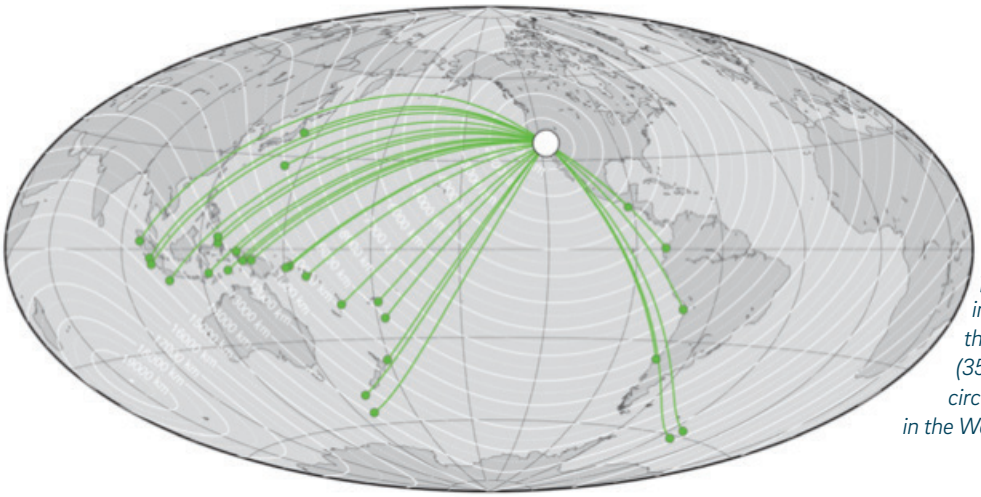

Figure 23. World map depicting great circle arc paths (green) from teleseismic earthquake that instantaneous triggered seismicity in the Coso Geothermal Field study area (35.5–36.5°N, 118.5–117°W) (white circle). Note that most events originate in the Western Pacific and South America.

RECENT PUBLICATIONS

Alfaro-Diaz, R.**, A.A. Velasco, K.L. Pankow and D. Kilb (2020). Optimally Oriented Remote Triggering in the Coso Geothermal Region. *Journal of Geophysical Research: Solid Earth*, **125**(8), e2019JB019131.

Cochran, E. S., J. Bunn, S.E. Minson, A.S. Baltay, D. Kilb, Y. Kodera and M. Hoshiba (2019). Event detection performance of the PLUM earthquake early warning algorithm in Southern California. *Bull. Seism. Soc. Am.*, doi: 10.1785/0120180326.

Garcia*, L., K. Luttrell, D. Kilb and F. Walter (2019). Joint geodetic and seismic analysis of surface crevassing near a seasonal glacier-dammed lake at Gornergletscher, Switzerland. *Annals of Glaciology,* 1-13. doi: 10.1017/aog.2018.32.

Johnson**, C. W., D. Kilb, A. Baltay and F. Vernon (2020). Peak ground velocity spatial variability revealed by dense seismic array in Southern California. *Journal of Geophysical Research: Solid Earth*, **125**(6), e2019JB019157. doi: 10.1029/2019jb019157.

Kilb, D. and F. Vernon (2020). Southern California jolted by moderate but intense quake. *Temblor.* doi: 10.32858/temblor.084.

Martynov, V. G., L. Astiz, D. Kilb and F.L. Vernon (2020). The M2 Tidal Tilt Results from USArray Seismic Data from the Western United States. *Bulletin of the Seismological Society of America.* doi: 10.1785/0120190314.

Minson, S. E., J.K. Saunders**, J.J. Bunn, E.S. Cochran, A.S. Baltay, D. Kilb, M. Hoshiba and Kodera, Y. (2020). Real-Time Performance of the PLUM Earthquake Early Warning Method during the 2019 M 6.4 and 7.1 Ridgecrest, California, Earthquakes. *Bulletin of the Seismological Society of America,* **110(**4), 1887-1903. doi: 10.1785/0120200021.

Pankow, K. L. and D. Kilb (2020). Going beyond rate changes as the sole indicator for dynamic triggering of earthquakes. *Scientific Reports*, **10**(1), 4120. doi: 10.1038/s41598-020-60988-2.

Rollins, C., R. S. Stein, G. Lin and D. Kilb (2019). The Ridgecrest earthquakes: Torn ground, nested foreshocks, Garlock shocks, and Temblor's forecast. *Temblor*, http://doi.org/10.32858/temblor.039.

Sahakian**, V. J., A. Baltay, T.C. Hanks, J. Buehler**, F.L. Vernon, D. Kilb and N.A. Abrahamson (2019). Ground motion residuals, path effects, and crustal properties: A pilot study in Southern California. *Journal of Geophysical Research: Solid Earth,* **124**(6), 5738-5753. doi: 10.1029/2018jb016796.

* graduate student ** post-doc

GABI LASKE

Professor in Residence

glaske@ucsd.edu, 858-534-8774

Regional and global seismology; surface waves and free oscillations; seismology on the ocean floor; observation and causes of seismic noise; natural disasters and the environment

Gabi Laske's main research area is the analysis of seismic surface waves and free oscillations, and the assembly of global and regional seismic models. She has gone to sea to collect seismic data on the ocean floor. Laske's global surface wave database has provided key upper mantle information in the quest to define whole mantle structure. Graduate students Christine Houser and Zhitu Ma as well as students from other universities have used her data to assemble improved mantle models. Most recently, she collaborated with postdoc Surya Pachhai to analyze inner-core sensitive modes and provided an improved model of inner-core anelastic structure.

Global reference models: Laske continues to compile and distribute global crustal models. CRUST1.0, A 1-degree crustal model, was released in 2013. Applications relying on CRUST1.0 are found across multiple disciplines in academia and industry. Laske maintains the distribution website and provides guidance to users. Laske continues collaborations with Walter Mooney from the USGS and others to update databases and ultimately provide a refined crustal model.

The AnICEotropy project: Laske has been collaborating with Fabian Walter and his graduate student Fabian Lindner at ETH, Switzerland to study ice quakes on the Glacier de la Plaine Morte, Switzerland. This plateau glacier that separates Cantons Berne and Valais develops a glacier lake, Lac des Faverges, during snow melt that frequently drains and floods the Simme valley to the north. Recent floods have become more frequent and larger, approaching the capacity of the flood control system. In 2016, Laske, her student Adrian Doran, and collaborators conducted a field experiment to identify precursory ice quake activity that helps improve early flood warning. This deployment also allowed a 'sandbox' azimuthal anisotropy analysis to test the hypothesis that seismic anisotropy is aligned with the crevasses on the glacier. This research is documented in two publications.

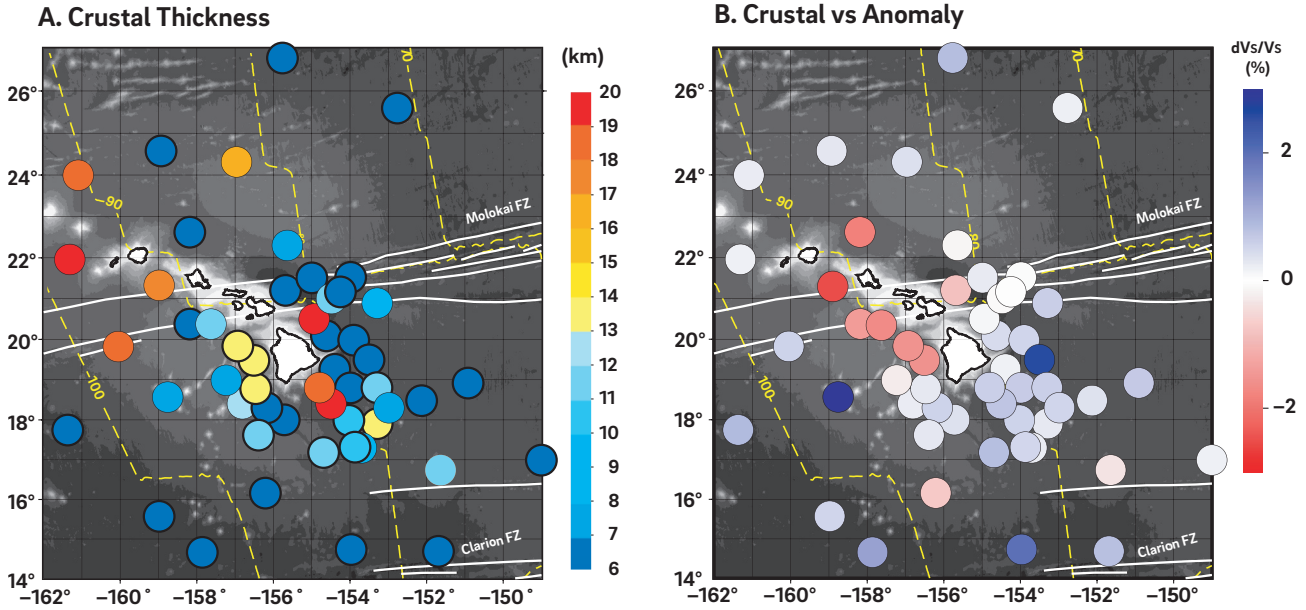

Figure 24. Model of the oceanic crystalline crust around Hawaii. The model resulted from a first-ever joint inversion of sea floor compliance and ambient noise dispersion curves. Sea floor compliance is the ground motion in response to pressure changes by passing ocean waves. Ambient-noise dispersion was modeled as Rayleigh wave dispersion.

The PLUME project: For the past decade or so, Laske and her team have analyzed records from ocean bottom seismometers (OBSs). She was the lead-PI of the Hawaiian PLUME project (Plume-Lithosphere-Undersea-Mantle Experiment) to study the plumbing system of the Hawaiian hotspot. Using a variety of seismic techniques including body wave, surface wave and receiver function analyses her team has published numerous results. Most recently, PhD student Adrian Doran conducted a first ever joint analysis of sea-floor compliance and ambient-noise Green's functions. His most recent paper describes a Monte-Carlo search for sediment and uppermost crustal structure. The team demonstrated that previous crustal thickness estimates may have been underestimated in areas of thick sediments and provided an updated model of the crust around Hawaii (Figure 24).

In the meantime, Laske secured funding to conduct a similar OBS experiment in 2021 halfway between Hawaii and North America to investigate 40-50 Myr old northeast Pacific lithosphere.

The CABOOSE project: The CAlifornia BOrderland Ocean SEismicity project (CA-BOOSE) is a collection of small OBS deployments, past and on-going, to assess seismicity offshore Southern California. In 2014, a 3-month deployment about 300 km west of La Jolla revealed never-before seen seismic activity in the Outer Borderland. Doran and Laske returned in the summers of 2015, 2017 and 2018 on UC ship fund cruises to continue investigation of the inner Borderland seismicity. For a recent deployment, development engineer Martin Rapa designed an in-situ calibration frame for the pressure sensor to help better understand the still poorly known instrument response of that sensor. Doran and Laske modeled the time series of three sensors. Benchmarking their results also against traditional post-processing techniques, they found significant, previously undocumented variance between the sensors.

The rich dataset of this deployment reveals numerous repeat events along the San Clemente Fault that have not been detected by the Southern California Seismic Network. The Laske team currently assemble a comprehensive event catalog. Related to this project, undergraduate student Spencer Okamoto currently analyzes recent earthquake swarms in the greater Salton Sea area for his SIO199 independent studies project. Okamoto majors in a field outside of Earth sciences. Nevertheless, during Laske's intro class SIO15 Natural Disaster, Okamoto developed great interest in the Earth sciences. His proficiency in Python programming and LaTex typesetting allows effective mentoring via Zoom during a COVID-19-restricted, remote-working environment.

RECENT PUBLICATIONS

Doran, A.K. and Laske, G., Melt-aected ocean crust and uppermost mantle near Hawaii - clues from ambient-noise phase velocity and sea floor compliance. *Geophys. J. Int.,* in press, doi:10.1093/gji/ggaa470, 2020.

Pachhai, S., Masters, G. and Laske, G., Probabilistic estimation of structure coefficients and their uncertainties, for inner-core sensitive modes, using matrix autoregression. *Geophys. J. Int.,* **221**, 2366{1383, doi:110.1093/gji/ggaa077, 2020.

Lindner, F., Walter, F., Laske, G., and Gimbert, F. Glaciohydraulic seismic tremors on an Alpine glacier. *The Cryosphere,* **14**, 2870398, doi:10.5194/tc-14-287-2020, 2020.

Doran, A.K., Rapa, M., Laske, G., Babcock, J. and McPeak, S., Calibration of differential pressure gauges through in situ testing. *Earth Space Sci.*, **6**, doi:10.1029/2019EA000783, 2019.

ROBERT J. MELLORS

Research Scientist

rmellors@ucsd.edu, 858-395-0170

Seismic sensors, optical fiber-based sensing, subsurface imaging of geothermal reservoirs, interferometric synthetic aperture radar.

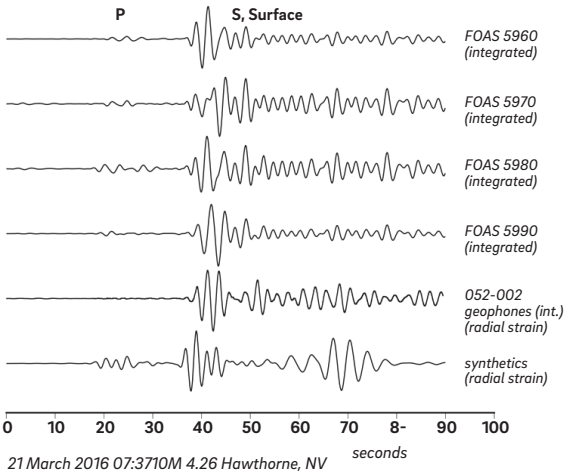

Figure 25. Comparison of fiber-optic acoustic data (FOAS) (upper four traces) with co-located geophone and synthetic. The event is a magnitude 4.4 earthquake located at a distance of 150 km. Al data is in strain as a function of time.

Recent technological advances in seismic sensors provide new capabilities for seismic monitoring and subsurface imaging. Photonic-based sensors, such as distributed acoustic sensing (DAS), offer exceptional potential for high-spatial density seismic measurements with a high dynamic range and wide frequency bandwidth. These sensors measure the strain (or strain-rate) at all points along a fiber and are capable of monitoring kilometers of fiber. The optical fiber sensors appear to be especially useful for boreholes, seafloor, ice sheets, and other challenging environments. The challenges lie in interpreting the response and of the photonic sensor, optimizing signal-to-noise, and effectively working with the large datasets, which often are 10's of TB in size. My research is focused on how to effectively use these sensors and includes both signal analysis and forward modeling of the signals (Sherman et al., 2019). We have shown that with filtering and stacking, the signal-to-noise of these sensors is comparable to standard geophones but with a wider frequency response (Figure 25) and the DAS sensors appear suitable for regional monitoring. The signals can be successfully matched using standard 2D wavenumber seismic propagation codes. The fiber sensors also possess exceptional dynamic range and remained on scale at a distance of less than 100 m from a subsurface chemical explosion consisting of 50 tons of high explosive (HE) (Figure 26). This work was done in collaboration with Rob Abbott of Sandia National Laboratories.

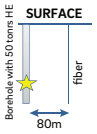

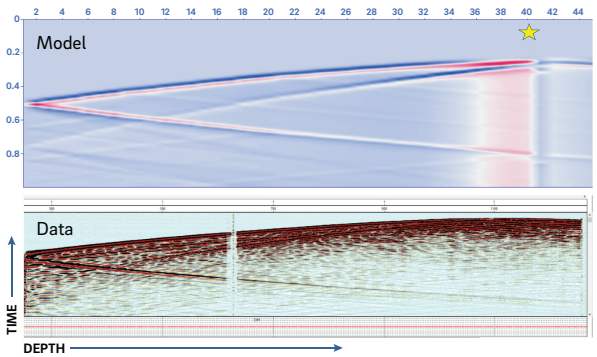

Figure 26. Comparison of fiber-optic acoustic data (bottom) with 3D finite difference synthetic (top). The fiber was installed in a borehole 80 m from a buried explosion (~50 tons of HE). Data collected by Rob Abbott of Sandia National Laboratories.

Research continued on geophysical methods applied to geothermal exploration. Geothermal energy is an attractive source of low-carbon energy, but finding new geothermal reservoirs is a challenging problem. We conducted a wide-scale survey of Western Saudi Arabia using data from a regional seismic network in collaboration with King Saud University (Al-Amri et al., 2020). Ambient noise interferometry was used to identify zones of low velocity. The low velocity zones matched known volcanic areas and may be useful for prioritizing geothermal exploration targets.

RECENT PUBLICATIONS

Al-Amri, A. M., K. Abdelrahman, R. Mellors, and D. Harris (2020). "Seismic identification of geothermal prospecting in Harrat Rahat, Northern Arabian Shield." *Arabian Journal of Geosciences*, DOI: 10.1007/S12517-020-05300-2

Chen, T., C. M. Snelson, and R. Mellors (2020). "Velocity Structure at the Source Physics Experiment Phase I Site Obtained with the Large-N Array Data", *Seismological Research Letters,* DOI: 10.1785/0220190104

Bonneville, A., Kouzes, R., Yamaoka, J., Lintereur, J. Flygare, G. S. Varner, I. Mostafanexhad., E. Guardincerri, C. Rowe, and R. Mellors (2019), Borehole muography of subsurface reservoirs, *Phil. Trans. of the Royal Soc. A-mathematical Phys. & Eng. Sci.*, DOI: 10.1098/RSTA.2018.0060

Sherman, C., R. Mellors, J. Morris, and F. Ryerson (2019), "Geomechanical modeling of distributed fiber-optic sensor measurements", *Interpretation*, DOI: 10.1190/INT-2018-0063.1

MATTHIAS MORZFELD

Associate Professor

matti@ucsd.edu, igppweb.ucsd.edu/~mmorzfeld

Computational and stochastic modeling, sampling methods for inverse problems, numerical analysis, reduced order modeling

I am an applied mathematician who works on computational tools that are useful in Earth science. The common theme that ties my work together is merging computational models with data via a Bayesian approach. This is easy to explain with the example of a weather forecast. Suppose you use a mathematical model for the weather to make a forecast. If the model calls for rain but you wake up to sunshine, then you should calibrate your model to this observation before you make a forecast for the next day. This is an example of Bayesian inference. My research focuses on the design, analysis and application of numerical methods for Bayesian inference problems in geophysics. Bayesian inference problems in geophysics are characterized by three important properties, which make finding a solution very difficult, both conceptually and computationally.

(i) The problems are "high-dimensional," which means that the computational model has many components, typically millions or hundreds of millions. Each component of the model needs to be updated in view of the data, which make computations difficult and, without clever mathematics, impossible to perform.

(ii) The models are "nonlinear," which means they are complicated and many standard tools and methods do not directly apply.

(iii) There are often many models that t the data equally well, and it is usually not clear which model one should ultimately choose.

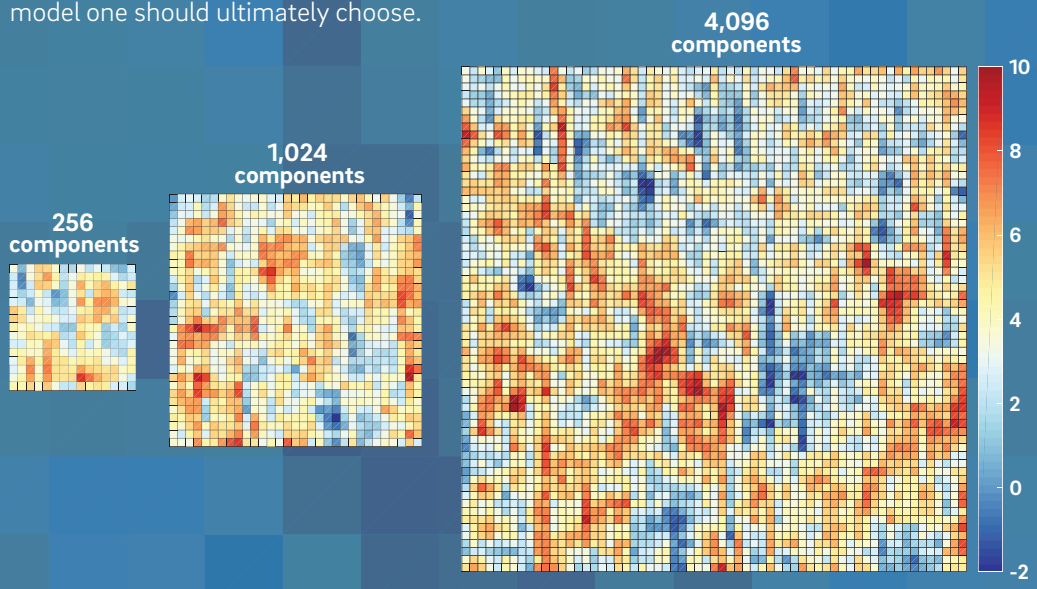

Figure 26. Illustration of how a problem becomes more complicated due to an increase in its dimension. The number of components that need to be updated in view of data can grow quickly and be very large (not thousands, as in this illustration, but rather millions or hundreds of millions). I create new algorithms that work equally well on "small" and "large" problems.

My research group continuously works an all three of these issues and brings new algorithms for Bayesian inference to bear in important geophysical problems. One recent mathematical success is connected to the nonlinearity and the huge dimension of geophysical inference problems. Together with collaborators at the National University of Singapore and the Massachusetts Institute of Technology, I could show, for the firrst time, how to construct algorithms for the solution of nonlinear Bayesian inference problems whose efficiency is entirely independent of the (huge) dimension of the problem.

In more practical project, we studied Earth's magnetic field, which is generated and sustained by the turbulent flow of liquid metal alloys in Earth's core. The dipole component of Earth's magnetic field, which is the reason why you can use a compass to navigate, is known to reverse. When a reversal occurs, the magnetic south pole becomes the north pole and vice versa. We know when reversals occurred (by studying the sea floor), but not much is known about why reversals occur. It is also unclear when the next reversal will happen. In fact, given the sequence of occurrences of reversals, one is tempted to think that we are overdue for a reversal: the last reversal occurred about 780,000 years ago and we typically see about four reversals per million year.

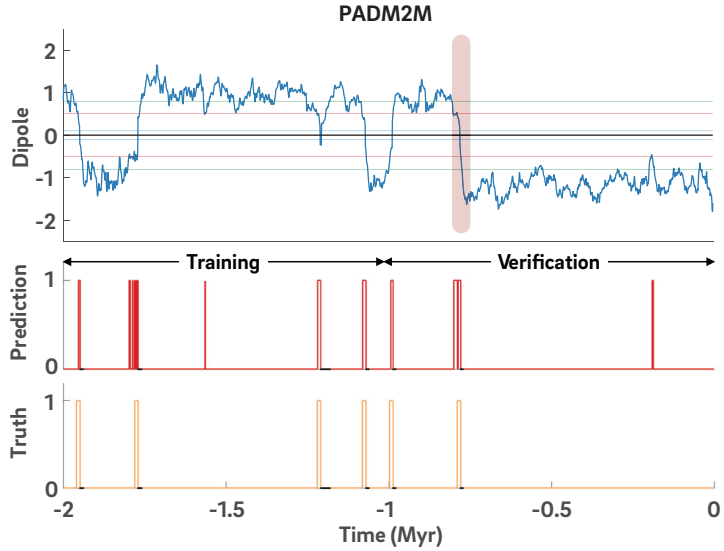

Figure 28. Top: Paleomagnetic reconstruction of the Earth's dipole strength and its polarity (negative sign corresponds to today's polarity). The paleomagnetic reconstruction, created at IGPP, spans the past 2 Myr. The most recent reversal (Brunhes-Matuyama), is highlighted in red. Bottom: Our "predictions" of past events and a comparison to what actually happened. Here, a "1" corresponds to the event \a reversal will occur soon," a "0" corresponds to \no reversal in sight." We used "predictions of the past" to study the reliability of our predictions of the future.

We thus set out to study the question: *Can we predict when a reversal of Earth's axial dipole will occur?* To answer this question, we borrowed some techniques from the machine learning community, started a collaboration across the Atlantic with researchers at IPGP (Institute de Physique du Globe de Paris), and combined a large collection of numerical models of Earth's magnetic field with paleomagnetic reconstructions, created at IGPP and at IPGP. This IGPP-IPGP collaboration is lead by IGPP graduate student Kyle Gwirtz, supported by a NASA Earth and Space Science Fellowship, and ultimately and unequivocally answers the question if, and if so how well, we can predict reversals of Earth's magnetic eld. Rest assured, our calculations show no signs of an upcoming reversal for the next few thousand years, but we could also discover and clearly describe the limitations of our ability to predict reversals.

Due to the pandemic, I spent lots of time at home with my two year old daughter Mia, and many of the solutions to the problems I study were discovered, this year, during long walks in Tecolote Canyon, or along the beach near Scripps pier. Mia also made a surprise appearance while I presented my work at UC Berkeley's Earth and Planetary Science Department during a colloquium. She did not explain reversals of Earth's magnetic field all so well, but she definitely caught the attention of everybody in attendance.

RECENT PUBLICATIONS

X.T. Tong, M. Morzfeld and Y.M. Marzouk, MALA-within-Gibbs samplers for high-dimensional distributions with sparse conditional structure, *SIAM Journal of Scientific Computing*, **42**(3), A1765{A1788 (2020), DOI https://doi.org/10.1137/19M1284014.

K. Gwirtz, M. Morzfeld, A. Fournier and G. Hulot, Can one use Earth's magnetic axial dipole field intensity to predict reversals? *Geophysical Journal International,* accepted with minor revisions.

JOHN ORCUTT

Distinguished Professor of Geophysics/RTAD

jorcutt@ucsd.edu; 858-210-8001

My interests include both continental and ocean seismology and new technologies to enhance the quality of seismic data, especially in the oceans. I continue to work on new autonomous ocean vehicles. Nearly 30 years ago Jon Berger and I installed the first satellite communications antenna on a Scripps ship that linked the ship with a commercial geosynchronous satellite. This project, HiSeasNet, later placed antennae on most UNOLS ships. HiSeasNet is now operated by Scripps' MARFAC facility and, during COVED-19, Scripps enhanced the available bandwidth to Mbps network speeds. The bandwidth is comparable to modern networks on continents and will revolutionize seagoing oceanography in coming years.

Seafloor noise levels, in quiet seas, are comparable to observations on the best continental and island installations. The quality of data can be substantially enhanced by autonomous seafloor burial and the use of new broadband seismometers and DPGs. Coupled with autonomous surface vehicles (ASVs), near real-time seafloor data can be transferred via acoustics and Iridium satellite communications. Latency; that is, the time of receipt of a group of data at the shore side facility minus the time of the oldest datum in that group is dominated by the sum of the digitizer group delay, the time to gather a group of data to telemeter, the time to send the data through the water column and the time to send the data through the satellite network. Overall analysis of months of operation shows median total system latency of 260s. The largest contribution to this latency involves establishing a connection through Iridium. Telemetry can be enhanced significantly by the use of Low/Medium Earth Orbit (LDEO/MEO) Small Sats. We are now experimenting with new technologies that will significantly reduce ship costs while providing a means for interacting with the remote seafloor packages to ensure data quality and provide the means for remote maintenance. The technologies will support a truly global distribution of the Global Seismic Network (GSN) and passive/active arrays and networks for Earth structure, earthquake source studies as well as nuclear test and tsunami detection.

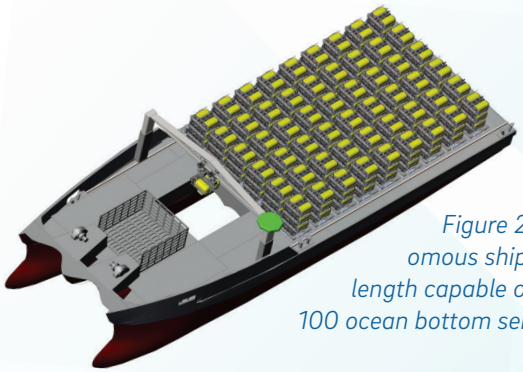

Figure 29. A conceptual autonomous ship approximately 40m in length capable of deploying and recovering 100 ocean bottom seismographs.

RECENT PUBLICATIONS

Orcutt, John A, (2020). "MEDEA and the Declassification of Navy GEOSAT Radar Altimetry Data," *Fall AGU Session.* ID# 676088

Orcutt, J., A. Berger, J. (2020). "Building and maintaining a global seismic network in the oceans" *Fall AGU Session* S059-02.

ROBERT L. PARKER

Professor of Geophysics, Emeritus

rlparker@ucsd.edu

Inverse theory, geomagnetism, spectral analysis, electromagnetic induction, numerical analysis

Recently Peter Molnar (former Green Scholar) asked me for assistance with a problem in gravity: How does one upward continue the geopotential of a Gaussian-shaped ridge, a simple model for what might be found across an uncompensated linear mountain chain. I did some calculations and showed

$$V(x, h) = V_0 \,\mathrm{Re}\{\exp \pi(h + ix)^2/a^2 \cdot [1 - \mathrm{erf}(\sqrt{\pi}(h + ix)/a)]\} \qquad (1)$$

where the potential at height $h = 0$ is the Gaussian

$$V(x, 0) = V_0 e^{-\pi x^2/a^2} \qquad (2)$$

Here erf *(x)* is the *error function*, well known in statistics and problems of heat flow. While this may seem to be the end of the story, there remains a nontrivial issue: the usual platforms for computation that I use, MATLAB and FORTRAN (even today!), provide erf for real but not complex variables as needed here. Obvious simple approximations will suffice for geophysics, but as a retiree, I decided to invest some time in developing an accurate and efficient algorithm for complex erf(*z*).

At first sight, the answer seems simple: use the power series

$$\mathrm{erf}(z) = \sum_{n=0}^{\infty} \frac{2}{\sqrt{\pi}} \frac{(-1)^n z^{2n+1}}{(2n+1)\, n!} \qquad (3)$$

Because erf is an entire function, this series is convergent for any finite *z*. If one needs a value with $|z| > 5$ the series requires far too many terms and suffers from loss of accuracy due to massive cancellation of large terms and accumulated round-off error of the computer arithmetic; my goal was to build an algorithm with an error less than 1 in 10^{15}, suitable for double-precision calculations, though admittedly ridiculous for Peter Molnar's original application.

Another way to calculate erf is via a continued fraction: one computes the function *w(z)* thus

$$w(z) = \frac{i/\sqrt{\pi}}{z -} \; \frac{\frac{1}{2}\cdot 1}{z -} \; \frac{\frac{1}{2}\cdot 2}{z -} \; \frac{\frac{1}{2}\cdot 3}{z -} \cdots \qquad (4)$$

and $\mathrm{erf}(z) = 1 - e^{-z^2} w(iz)$. This expansion is perfect for large $|z|$, where (3) performs so badly, but (4) is not convergent on the real axis which corresponds to the imaginary axis for erf. I found an algorithm for w involving Dawson's integral of a real variable due to Abrarov and Quine (2014), that covers the region. MATLAB does provide a real-variable function for Dawson's integral but it is unbelievably slow! So I wrote code for it based on yet another continued fraction.

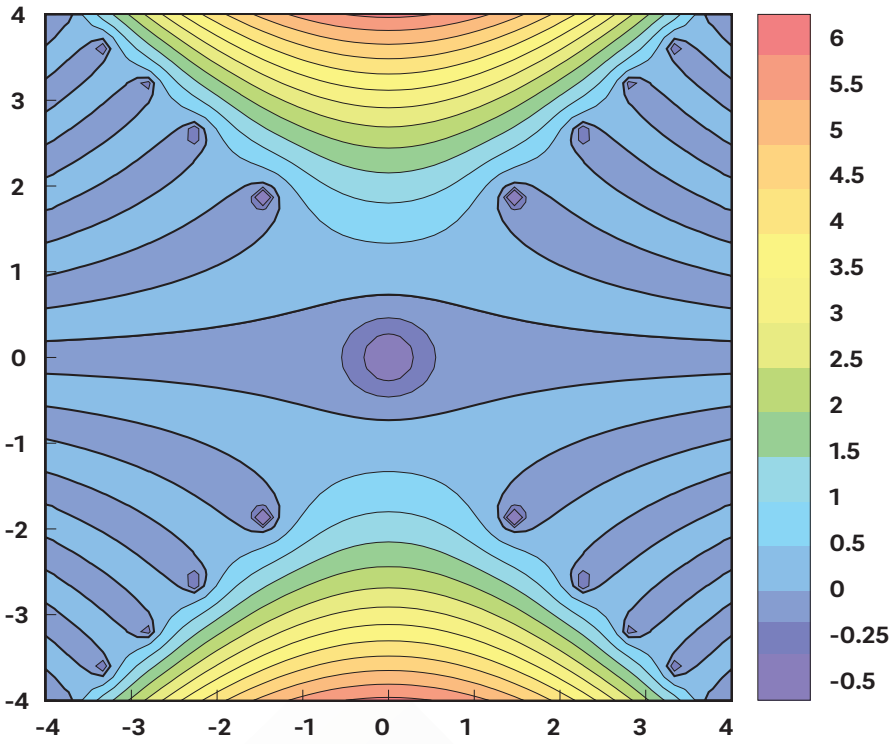

Figure 30. Altitude chart of erf, showing, $\log_{10} |erf(z)|$.

The function erf(*z*) has a pleasing appearance in the complex *z* plane, as is apparent in the contour plot above

Returning to Molnar's problem: no exotic functions arise if the potential on $z = h$ is modeled instead by the rational function

$$V(x, h) = \frac{aV_0}{h + a + x^2/(h + a)} \qquad (5)$$

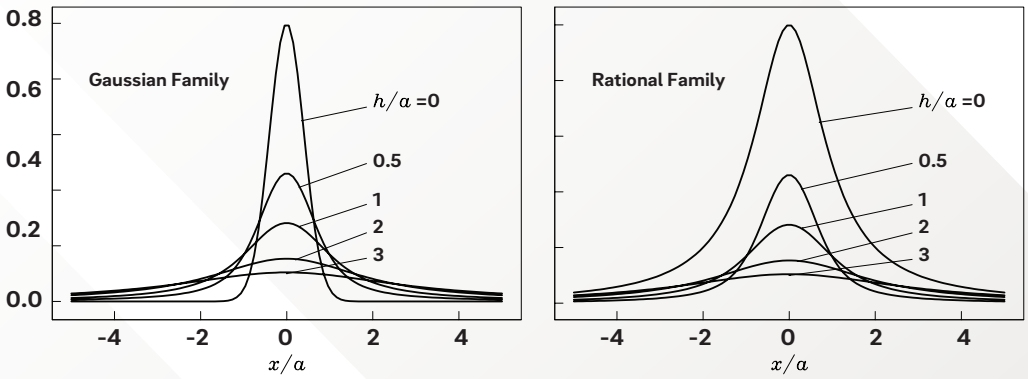

Figure 31. Potentials V/V_0 at various heights, as indicated.

For more about these functions see Chapter 7 of Abramowitz & Stegun (1965), and Section 7 of Olver et al. (2010).

REFERENCES

Abramowitz, M., and Stegun, I., Handbook of Mathematical Functions, Dover Publications, 1965.

Abrarov and Quine, arXiv:1411.1024v2, 2014.

Olver, F. W. J., and a cast of hundreds, NIST. Digital Library of Mathematical Functions, http;//dlmf.nist.gov.

ROSS PARNELL-TURNER

Assistant Professor

rparnellturner@ucsd.edu, 858-822-2975

Melting and deformation on mid-ocean ridges, mantle dynamics

I'm a marine geophysicist, and my group uses data that we collect at sea to learn about how oceanic crust is created and deformed, with a focus on slow-spreading ridges, and on plume-ridge dynamics. Although COVID-19 led to the postponement of a long-awaited ocean drilling expedition to the Reykjanes Ridge (Parnell-Turner et al., 2020), we are optimistic that our sea-going science will be able to resume next year, starting with a planned mission on RV Revelle in March 2021 to monitor vents at the East Pacific Rise.

We a broad range of observational methods to constrain how Earth's seafloor is being paved by new oceanic crust. Our objective is to develop a comprehensive understanding of the process of crustal formation, from convective upwelling deep within the mantle and melting beneath the crust, to earthquake seismicity, faulting, and hydrothermal venting. This work is underpinned by sea-going expeditions, where we take measurements with shipboard sonars, robots, and seafloor instruments, and collect data and samples using submersibles and drilling vessels.

We are investigating how new crust is formed at slowly-spreading mid-ocean ridges, in the presence of enigmatic and long-lived faults, called detachments. By recording

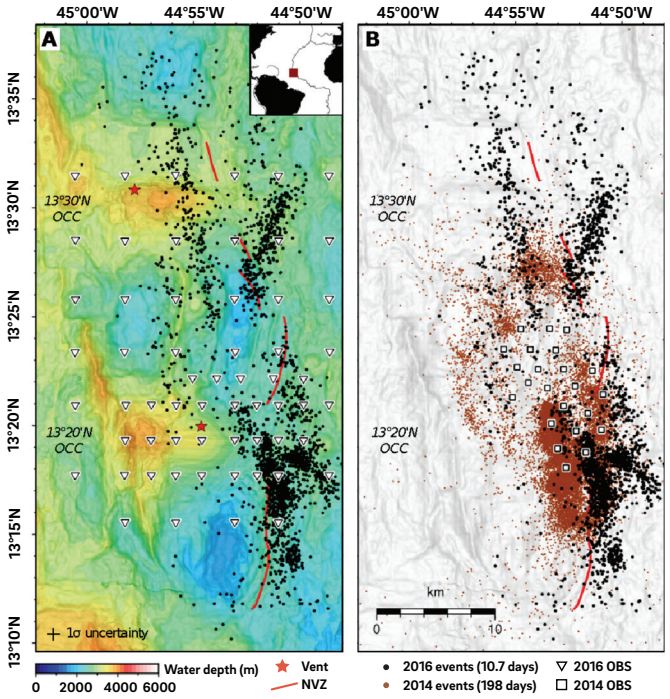

Figure 31. Seismicity at the Mid-Atlantic Ridge near 13°20'N (from Parnell-Turner et al., in press). (a) Inset shows study site (red box) and plate boundaries (black lines). Black dots are relocated microearthquakes recorded by OBSs (triangles) over ~11 days in 2016; red line is neovolcanic zone (NVZ); red stars are hydrothermal vents. Location of oceanic core complexes is shown by 13°20'N/13°30'N labels; cross size is average 68% confidence level in horizontal location uncertainty (0.9 km). (b) Brown dots are microearthquakes recorded over 198 days in 2014 (squares are OBSs).

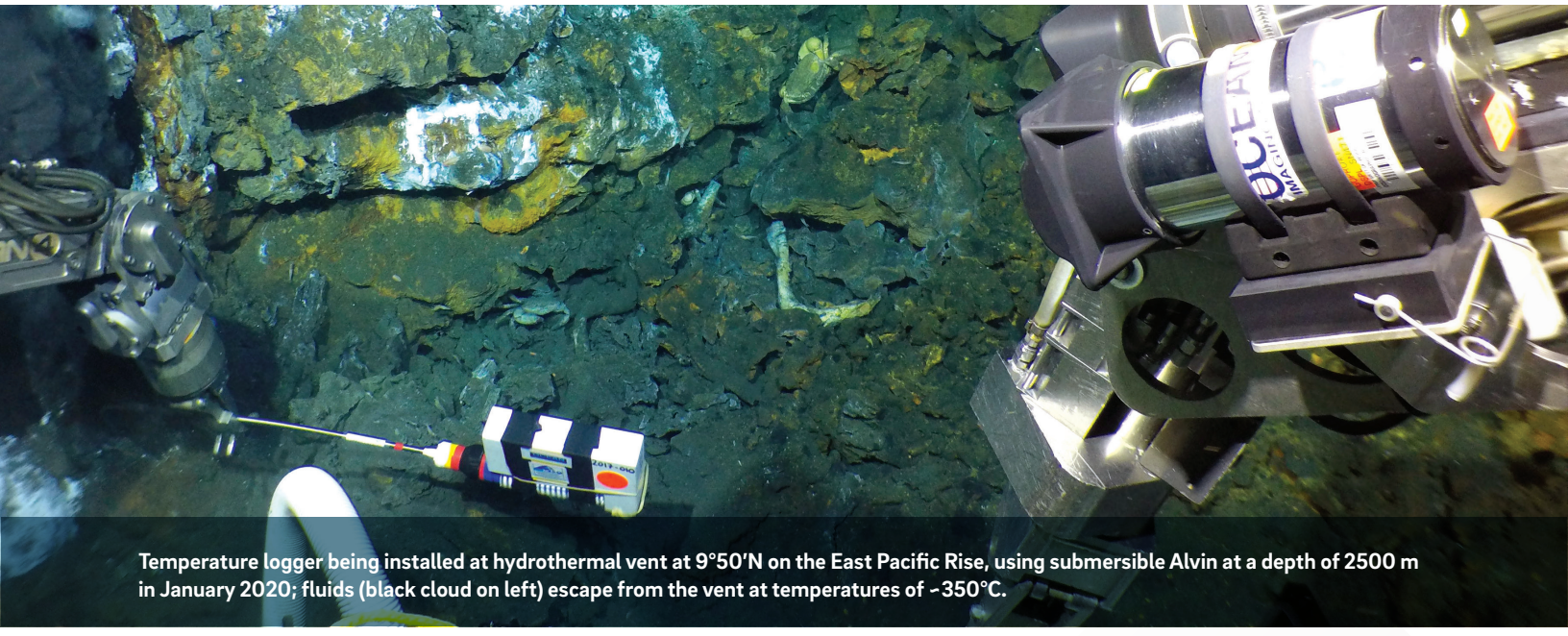

Temperature logger being installed at hydrothermal vent at 9°50'N on the East Pacific Rise, using submersible Alvin at a depth of 2500 m in January 2020; fluids (black cloud on left) escape from the vent at temperatures of ~350°C.

earthquakes using ocean bottom seismographs (OBSs), we have been able to show how this style of crustal accretion exhumes mantle rocks to the seafloor, and can cause intense earthquake activity. At 13°N on the Mid-Atlantic Ridge, we recently conducted the first repeat microearthquake experiment on a slow-spreading ridge, with OBS deployments two years apart (Figure 31). Changes in the patterns of seismicity shows that detachment fault systems vary on timescales as short as a few years, and also we found that adjacent detachment faults do not link-up in the subsurface along axis (Parnell-Turner et al., in press). Elsewhere on the Mid-Atlantic Ridge, we recently published our finding that rocks sampled from the detachment system at 16°N contain recycled subduction zone mantle peridotite. This composition could be explained by hydrous melting, and implies that arc mantle relicts may constitute up to 60% of the upper mantle by volume (Urann et al., 2020).

Another primary area of research has been how variations in melt supply influences the style of oceanic crust formed. In collaboration with IGPP alumnus Joyce Sim, we examined the 12 million-year-long record of crustal formation that is contained within the seafloor mapping data collected during the search for Malaysia Airlines Flight 370 (Figure 32). These bathymetric data have a resolution that is 15 times higher than previous maps, and illuminate the structure of a vast area of crust formed on the Southeast Indian Ridge. We found that crustal production, rather than being a constant process, has varied in cycles that last hundreds of thousands of years. This pattern can be explained by the varying amount of molten rock that rises from deep in Earth's mantle, arriving in episodic waves. This behavior could be a general feature of mid-ocean ridges spreading at similar rates, which has not been previously recognized due to a lack of available data (Parnell-Turner et al., 2020).

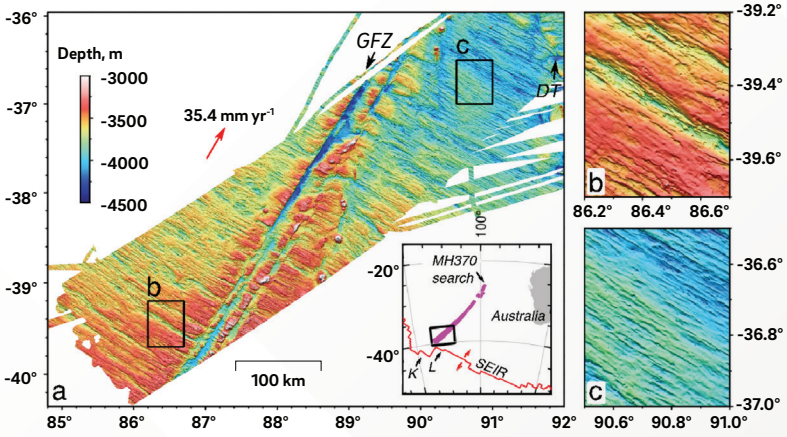

Figure 32. Multibeam bathymetric data collected during search for Malaysia Airlines Flight 370 (from Parnell-Turner et al., 2020). a) Inset: Southeast Indian Ridge (SEIR) and spreading vectors (red line/arrows); search area (magenta); study area (black box); spreading segments K and L. Main panel: southern portion of MH370 search area, bisected by Geelvinck FZ (GFZ); northern boundary is Diamantina trench (DT); red arrow is spreading vector, with half-spreading rate noted. (b) and (c) Zooms showing seafloor morphology from Segments K and L, respectively, highlighting examples of abyssal hills and longer-wavelength bathymetric ridges.

RECENT PUBLICATIONS

Hoggard, M. J., Parnell-Turner, R., & White, N. (2020). Hotspots and mantle plumes revisited: Towards reconciling the mantle heat transfer discrepancy. *Earth and Planetary Science Letters,* **542**, https://doi.org/10.1016/j.epsl.2020.116317

Parnell-Turner, R., Sohn, R. A., Peirce, C., Reston, T. J., Macleod, C. J., Searle, R. C., & Simão, N. (in press). Seismicity trends and detachment fault structure at 13°N, Mid-Atlantic Ridge. Geology.

Parnell-Turner, R., Briais, A., & LeVay, L. (2020). Expedition 395 Scientific Prospectus: Reykjanes Mantle Convection and Climate. International Ocean Discovery Program. https://doi.org/10.14379/iodp.sp.395.2020

Parnell-Turner, R., Sim, S. J., & Olive, J. A. (2020). Time-dependent crustal accretion on the Southeast Indian Ridge revealed by Malaysia Airlines flight MH370 search. *Geophysical Research Letters,* https://doi.org/10.1029/2020gl087349

Smith, D. K., Schouten, H., Parnell-Turner, R., Klein, E. M., Cann, J., Dunham, C., et al. (2020). The Evolution of Seafloor Spreading Behind the Tip of the Westward Propagating Cocos-Nazca Spreading Center. *Geochemistry, Geophysics, Geosystems.* https://doi.org/10.1029/2020gc008957

Urann, B. M., Dick, H. J. B., Parnell-Turner, R., & Casey, J. F. (2020). Recycled arc mantle recovered from the Mid-Atlantic Ridge. *Nature Communications*, **11**. https://doi.org/10.1038/s41467-020-17604-8

ANNE POMMIER

Associate Professor

pommier@ucsd.edu, 858-822-5025

Physics and chemistry of silicate melts and metal alloys; role of magma in planetary interiors, from the scale of volcanic magma reservoirs to planetary-scale magma oceans; evolution of planetary interiors from "deep time" (e.g., planet evolution) to the present.

Research projects over the past 12 months have mainly focused on the experimental investigation of the core of terrestrial planets (in particular, Mercury, Mars, Ganymede and the Moon). We also investigated the role of lawsonite in electromagnetic profiles of subduction zones. These studies were funded by NSF grants (NSF-NERC, NSF CAREER and NSF COMPRES).

Mercury's core (Pommier et al., 2019a): The weak intrinsic magnetic field of Mercury is intimately tied to the structure and cooling history of its metallic core. Recent constraints about the planet's internal structure suggest the presence of a FeS layer overlying a silicon-bearing core. Together with undergraduate student Tu Tran and ASU colleague Kurt Leinenweber, we performed 4-electrode resistivity experiments on core analogues up to 10 GPa and over wide temperature ranges in order to investigate the insulating properties of core materials. Our results show that the FeS layer is liquid and insulating, and that the electrical resistivity of a miscible Fe-Si(-S) core is comparable to the one of an immiscible Fe-S, Fe-Si core. The difference in electrical resistivity between the FeS-rich layer and the underlying Fe-Si(-S) core is at least 1 log unit at pressure and temperature conditions relevant to Mercury's interior. Estimates of the lower bound of thermal conductivity for FeS and Fe-Si(-S) materials are calculated using the Wiedemann-Franz law. A thick (> 40 km) FeS-rich shell is expected to maintain high temperatures across the core, and if temperature in this layer departs from an adiabat, then this might affect the core cooling rate. We observe that the presence of a liquid and insulating shell is not inconsistent with a thermally stratified core in Mercury and is likely to impact the generation and sustainability of a magnetic field.

Mars' core (Pommier et al., 2020): We performed a joint experimenta-modeling investigation of core cooling in small terrestrial bodies, in particular Mars. Significant amounts of light elements (S, O, Mg, Si) may compose the metallic cores of terrestrial planets and moons. However, the effect of multiple light elements on transport properties, in particular, electrical resistivity and thermal conductivity, is not well constrained. Electrical experiments were conducted at 10 GPa and up to 1850 K on high-purity powder mixtures in the Fe-S-O(±Mg, ±Si) systems using the multianvil apparatus and the four-electrode technique. The sample compositions contained 5 wt.% S, up to 3 wt.% O, up to 2 wt.% Mg, and up to 1 wt.% Si. We observe that above the eutectic temperature, electrical resistivity is significantly sensitive to the nature

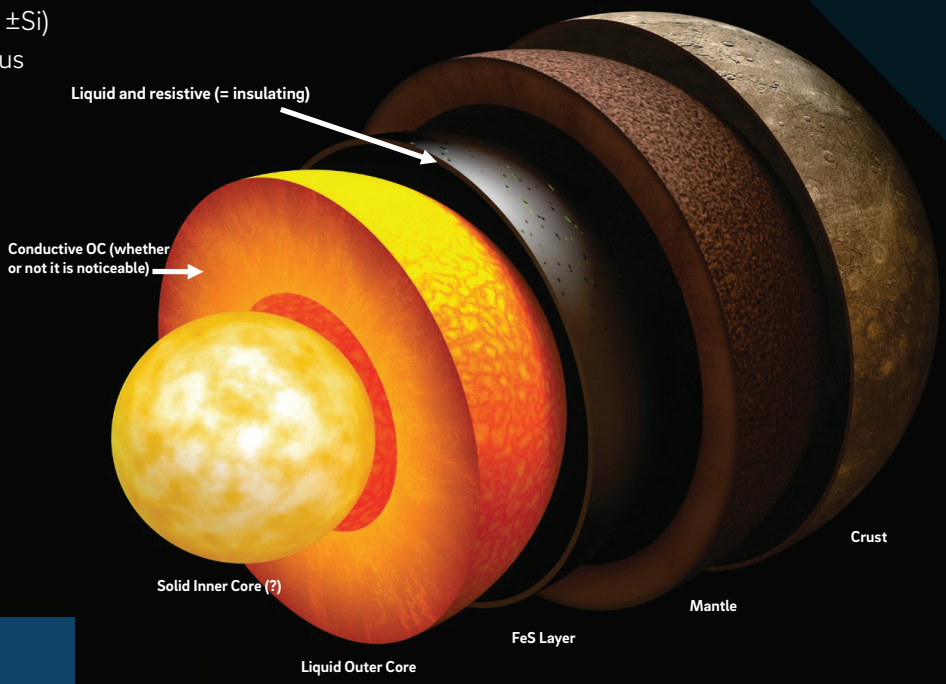

Image: After Charlier and Namur, 2019

and amount of light elements. For each composition, thermal conductivity-temperature equations were estimated using the experimental electrical results and a modified Wiedemann-Franz law. These equations were implemented in a thermochemical core cooling model to study the evolution of the dynamo. Modeling results suggest that bulk chemistry significantly affects the entropy available to power dynamo action during core cooling. In the case of Mars, the presence of oxygen would delay the dynamo cessation by up to 1 Gyr compared to an O-free, Fe-S core. Models with 3 wt% O can be reconciled with the inferred cessation time of the Martian dynamo if the core-mantle boundary heat flow falls from >2 TW to ~0.1 TW in the first 0.5 Gyr following core formation.

Ganymede's core and the Moon's core *(Pommier, 2020)*: Electrical resistivity experiments were conducted on three alloys in the iron-rich side of the Fe-Ni(-S) system (Fe-5 wt% Ni, Fe-10 wt% Ni, Fe-10 wt% Ni-5 wt% S) at 4.5 and 8 GPa and up to 1900 K using the multi-anvil apparatus and the 4-electrode technique. For all samples, increasing temperature increases resistivity. At a specified temperature, Fe-Ni(-S) alloys are more resistive than Fe by a factor of about 3. Fe-Ni alloys containing 5 and 10 wt% Ni present comparable electrical resistivity values. The resistivity of Fe-Ni(-S) alloys is comparable to the one of Fe = 5 wt% S at 4.5 GPa and is about three times higher than the resistivity of Fe = 5 wt% S at 8 GPa, due to a different pressure dependence of electrical resistivity between Fe-Ni and Fe-S alloys. Based on these electrical results and experimentally determined thermal conductivity values from the literature, lower and up- per bounds of thermal conductivity were calculated. For all Ni-bearing alloys, thermal conductivity estimates range between ~12 and 20 W/(m-K) over the considered pressure and temperature ranges. Adiabatic heat fluxes were computed for both Ganymede's core and the Lunar core, and heat flux values suggest a significant dependence to both core composition and the adiabatic temperature. Comparison with previous thermochemical models of the cores of Ganymede and the Moon suggests that some studies may have overestimated the thermal conductivity and hence, the heat flux along the adiabat in these planetary cores.

The role of lawsonite in electromagnetic profiles (Pommier et al., 2019b): Together with collaborators at other institutions (Quentin Williams, UCSC and Rob Evans, WHOI), we conducted an experimental investigation of the electrical properties of natural polycrystalline lawsonite from Reed Station, CA. Lawsonite represents a particularly efficient water reservoir in subduction contexts, as it can carry about 12 wt % water and is stable over a wide pressure range. Experiments were performed from 300 to about 1325 °C and under pressure from 1 to 10 GPa using a multianvil apparatus. We observe that temperature increases lawsonite conductivity until fluids escape the cell after dehydration occurs. At a fixed temperature of 500 °C, conductivity measurements during compression indicate electrical transitions at about 4.0 and 9.7 GPa that are consistent with crystallographic transitions from orthorhombic C to P and from orthorhombic to monoclinic systems, respectively. Comparison with lawsonite structure studies indicates an insignificant temperature dependence of these crystallographic transitions. We suggest that lawsonite dehydration could contribute to (but not solely explain) high conductivity anomalies observed in the Cascades by releasing aqueous fluid at a depth (~50 km) consistent with the basalt-eclogite transition. In subduction settings where the incoming plate is older and cooler (e.g., Japan), lawsonite remains stable to great depth. In these cooler settings, lawsonite could represent a vehicle for deep water transport and the subsequent triggering of melt that would appear electrically conductive, though it is difficult to uniquely identify the contributions from lawsonite on field electrical profiles in these more deepseated domains.

RECENT PUBLICATIONS

Pommier A., K. Leinenweber, T. Tran, Mercury's Thermal Evolution Controlled by an Insulating Liquid Outermost Core?, *Earth and Planetary Science Letters*, **517**, 125-134, 2019a.

Pommier A., Q. Williams, R. L. Evans, I. Pal, Z. Zhang, Electrical Investigation of Natural Lawsonite under Temperature in the Pressure Range 1-10 GPa and Application to Subduction Contexts, *J. Geophys. Res.,* 10.1029/2018JB016899, 2019b.

Pommier A., Experimental Investigation of the Effect of Nickel on the Electrical Resistivity of Fe-Ni and Fe-Ni-S Alloys under Pressure, *American Mineralogist,* **105** (7), 1069-1077, 2020.

Pommier A., C. Davies, R. Zhang, A Joint Experimental-Modeling Investigation of the Effect of Light Elements on Dynamos in Small Planets and Moons, *Journal of Geophysical Research-Planets,* doi: 10.1029/2020JE006492, 2020.

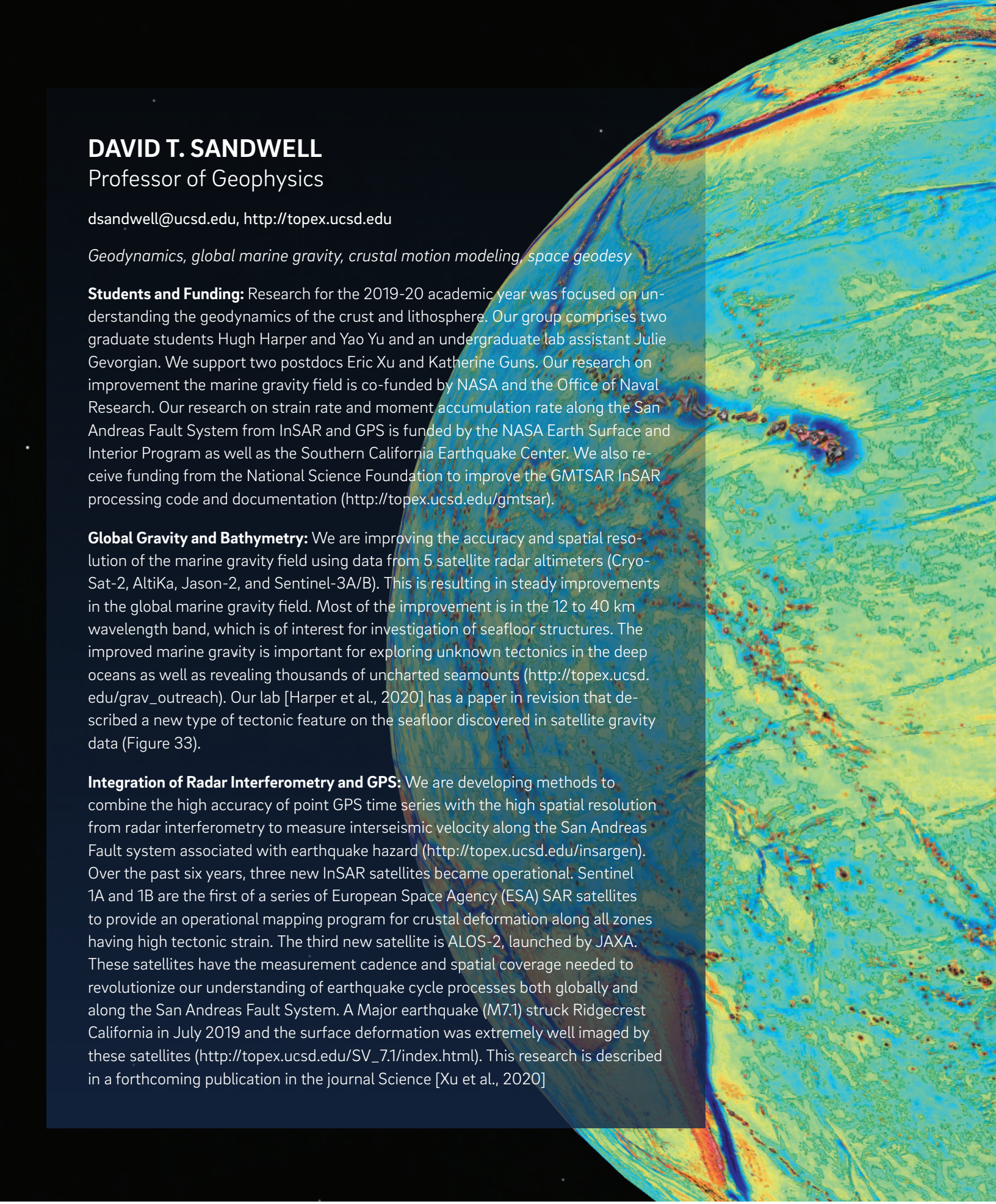

DAVID T. SANDWELL
Professor of Geophysics

dsandwell@ucsd.edu, http://topex.ucsd.edu

Geodynamics, global marine gravity, crustal motion modeling, space geodesy

Students and Funding: Research for the 2019-20 academic year was focused on understanding the geodynamics of the crust and lithosphere. Our group comprises two graduate students Hugh Harper and Yao Yu and an undergraduate lab assistant Julie Gevorgian. We support two postdocs Eric Xu and Katherine Guns. Our research on improvement the marine gravity field is co-funded by NASA and the Office of Naval Research. Our research on strain rate and moment accumulation rate along the San Andreas Fault System from InSAR and GPS is funded by the NASA Earth Surface and Interior Program as well as the Southern California Earthquake Center. We also receive funding from the National Science Foundation to improve the GMTSAR InSAR processing code and documentation (http://topex.ucsd.edu/gmtsar).

Global Gravity and Bathymetry: We are improving the accuracy and spatial resolution of the marine gravity field using data from 5 satellite radar altimeters (CryoSat-2, AltiKa, Jason-2, and Sentinel-3A/B). This is resulting in steady improvements in the global marine gravity field. Most of the improvement is in the 12 to 40 km wavelength band, which is of interest for investigation of seafloor structures. The improved marine gravity is important for exploring unknown tectonics in the deep oceans as well as revealing thousands of uncharted seamounts (http://topex.ucsd.edu/grav_outreach). Our lab [Harper et al., 2020] has a paper in revision that described a new type of tectonic feature on the seafloor discovered in satellite gravity data (Figure 33).

Integration of Radar Interferometry and GPS: We are developing methods to combine the high accuracy of point GPS time series with the high spatial resolution from radar interferometry to measure interseismic velocity along the San Andreas Fault system associated with earthquake hazard (http://topex.ucsd.edu/insargen). Over the past six years, three new InSAR satellites became operational. Sentinel 1A and 1B are the first of a series of European Space Agency (ESA) SAR satellites to provide an operational mapping program for crustal deformation along all zones having high tectonic strain. The third new satellite is ALOS-2, launched by JAXA. These satellites have the measurement cadence and spatial coverage needed to revolutionize our understanding of earthquake cycle processes both globally and along the San Andreas Fault System. A Major earthquake (M7.1) struck Ridgecrest California in July 2019 and the surface deformation was extremely well imaged by these satellites (http://topex.ucsd.edu/SV_7.1/index.html). This research is described in a forthcoming publication in the journal Science [Xu et al., 2020]

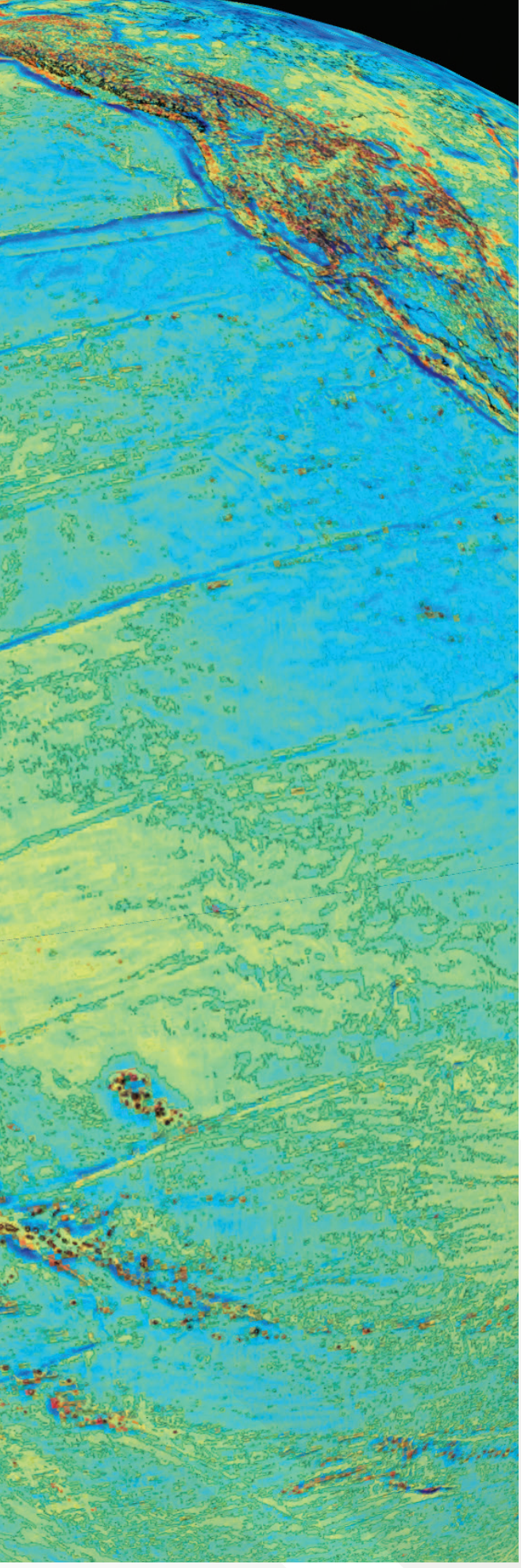

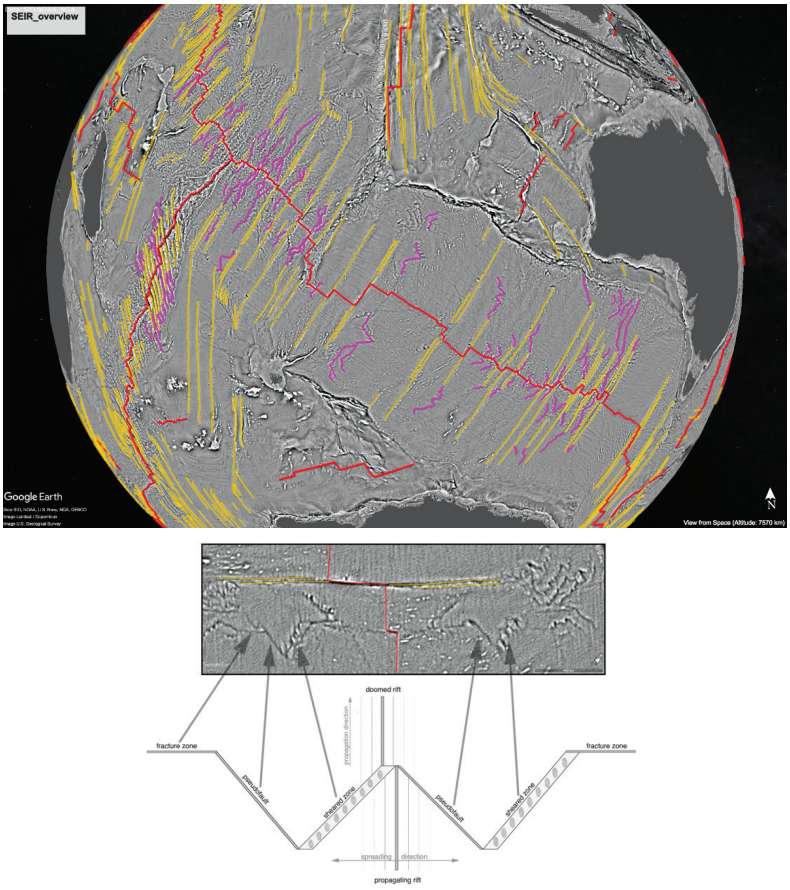

Figure 33. (upper) Gravity field of the Southeast Indian (https://topex.ucsd.edu/grav_outreach/files/global_grav_gradient.kmz). The active spreading boundary has orthogonal ridges and transform faults (red lines). The straight fracture zones (yellow) record the opening direction of southern Indian Ocean. The symmetrical magenta lines are newly-discovered seesaw propagators. (lower) Normal propagators create a V-shaped wake consisting of a sheared zone and pseudofault. Seesaw propagators reverse propagation direction leaving W-shaped scars in the seafloor.

RECENT PUBLICATIONS

Xu, X, D. T. Sandwell, Harper, L. A. Ward, C. W. D. Milliner, B. R. Smith-Konter, P. Fang, and Y. Bock, Surface deformation associated with fractures near the 2019 Ridgecrest earthquake sequence, *Science*, accepted, October 1, 2020.

Harper, H., B. Tozer, D. T. Sandwell, and R. N. Hey, Marine vertical gravity gradients reveal the global distribution and tectonic significance of "seesaw" ridge propagation, *J. Geophys. Res.*, revised, October 1, 2020.

Xu, X., D. T. Sandwell, and B. Smith-Konter (2020). Coseismic Displacements and Surface Fractures from Sentinel-1 InSAR: 2019 Ridgecrest Earthquakes, *Seismol. Res.* Lett. XX, 1–7, doi: 10.1785/ 0220190275.

Sandwell, D. T., Harper, H., Tozer, B., & Smith, W. H. (2019). Gravity Field Recovery from Geodetic Altimeter Missions. *Advances in Space Research*, https://doi.org/10.1016/j.asr.2019.09.011

Tozer, B., Sandwell, D. T., Smith, W. H. F., Olson, C., Beale, J. R., & Wessel, P. (2019). Global bathymetry and topography at 15 arc seconds: SRTM15+. *Earth and Space Science*, **6**(10), 1847-1864. https://doi.org/10.1029/2019EA000658.

PETER SHEARER

Distinguished Professor of Geophysics

pshearer@ucsd.edu, 858-534-2260

Seismology, Earth structure, earthquake physics

My research uses seismology to learn about Earth structure and earthquakes, using data from the global seismic networks and local networks in California, Nevada, Hawaii, and Japan. My work in crustal seismology has focused on improving earthquake locations using waveform cross-correlation, systematically estimating small-earthquake stress drops from P-wave spectra, and studying properties of earthquake clustering, especially swarms and foreshock sequences. At deeper depths, much of my research has involved resolving properties of the mantle transition-zone discontinuities.

I am currently collaborating with Rachel Abercrombie to compare and test methods for spectral analysis of local earthquakes. In particular we have investigated the origins of the large uncertainties and scatter in stress-drop estimates by comparing different empirical Green's function (EGF) approaches to analysis of P-wave spectra from small to moderate earthquakes in Southern California. We examined this issue by analyzing a compact cluster of over 3,000 aftershocks of the 1992 Landers earthquake (see Fig. 34). We applied and compared two different analysis and modeling methods: (1) the spectral decomposition and global EGF fitting approach and (2) a more traditional EGF method of modeling spectral ratios. The main source of differences comes from the modeling approach used to estimate the EGF. The global EGF-fitting approach suffers from parameter trade-offs among the absolute stress drop, the stress-drop scaling with moment, and the high-frequency falloff rate, but has the advantage that the relative spectral shapes and stress drops among the different events in the cluster are well resolved even if their absolute levels are not. The spectral ratio approach solves for a different EGF for each target event without imposing any constraint on the corner frequency, *fc*, of the smaller events, and so can produce biased results for target event *fc*. Placing constraints on the small-event *fc* improves the performance of the spectral ratio method and

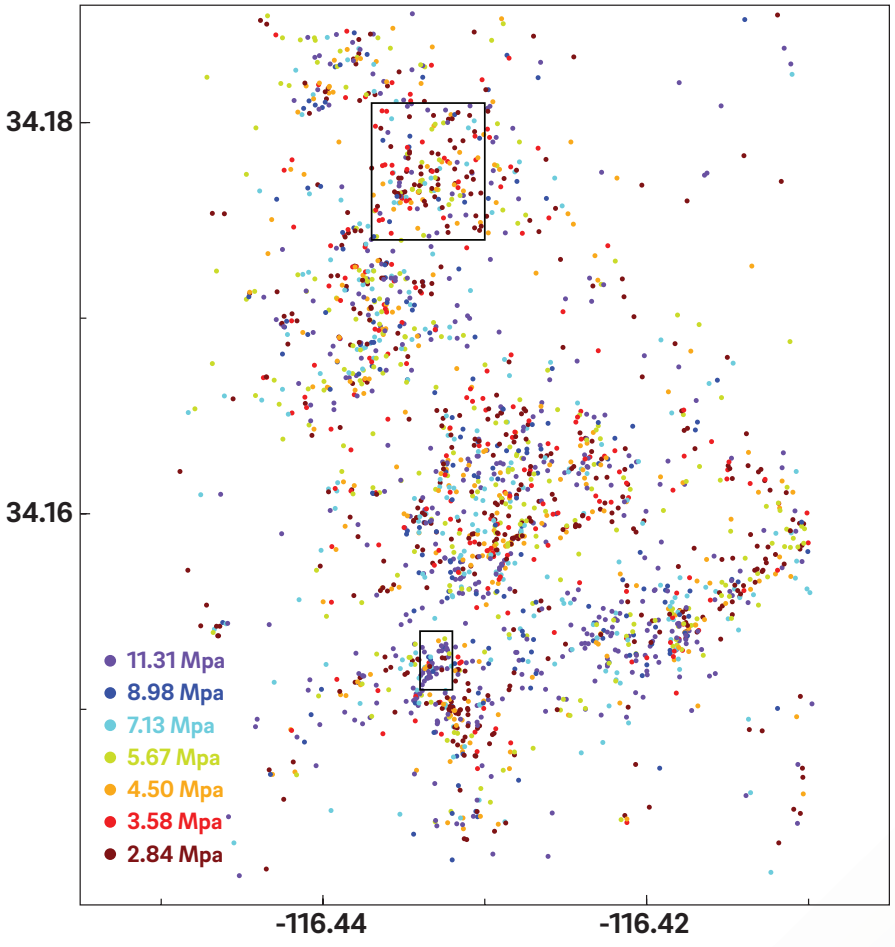

Figure 34. Individual event stress-drop estimates for over 3000 aftershocks of the 1992 Landers earthquake in southern California. Lower-stress drops are shown in red and describe earthquakes that radiate less high-frequency energy than other earthquakes of similar size. Higher stress drop events are plotted in blue and radiate relatively more high-frequency energy. Rectangles surround example regions with lower-than-average stress drop (northern box) and higher-than-average stress drop (southern box), see Shearer et al. (2019) for details.

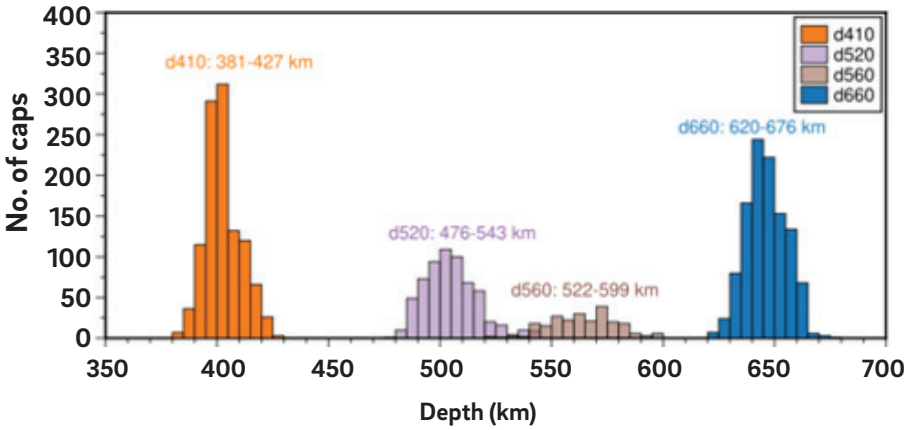

Figure 35. Histograms showing apparent depths of the 410-, 520-, 560- and 660-km discontinuities as measuring using a global study of SS precursors. From Tian et al. (2020).

enables the two methods to yield very similar results. These results will inform our efforts to compute reliable stress drop estimates for small earthquakes across southern California and other regions.

The 520-km seismic discontinuity in Earth's upper mantle is much more difficult to observe than the 410- and 660-km discontinuities, but is important for understanding the composition and dynamics of the mantle. Recent work with former IGPP Green Scholar postdoc Shawn Wei and his group at the University of Michigan has examined upper-mantle discontinuities by analyzing SS precursors at global seismic stations (see Fig. 35). Observed depth variations in the 520-km discontinuity imply both thermal and compositional heterogeneities in the mantle transition zone. A second discontinuity at ~560-km depth, previously interpreted as splitting of the 520-km discontinuity, is most commonly detected in cold subduction zones and hot mantle regions. The depth separation between the 520- and 560-km discontinuities varies from ~80 km in cold regions to ~40 km in hot areas. These results, combined with mineral physics results for the wadsleyite-ringwoodite phase change and exsolution of calcium-perovskite (Ca-pv) from majorite garnet impose constraints on mantle chemistry and possible recycling of oceanic crust (Tian et al., 2020).

RECENT PUBLICATIONS

Fan, W., J. J. McGuire, and P. M. Shearer, Abundant spontaneous and dynamically triggered submarine landslides in the Gulf of Mexico, *Geophys. Res. Lett.*, **47**, doi: 10.1029/2020GL087213, 2020.

Shearer, P. M., R. E. Abercrombie, D. T. Trugman, and W. Wang, Comparing EGF methods for estimating corner frequency and stress drop from P-wave spectra, *J. Geophys. Res.,* **124**, 3966-3986, doi: 10.1029/2018JB016957, 2019.

Tian, D., M. Lv, S. S. Wei, S. M. Dorman, and P. M. Shearer, Global variations of Earth's 520- and 560-km discontinuities, *Earth Planet. Sci. Lett.,* **552**, doi: 10.1016/j.epsl.2020.116600, 2020.

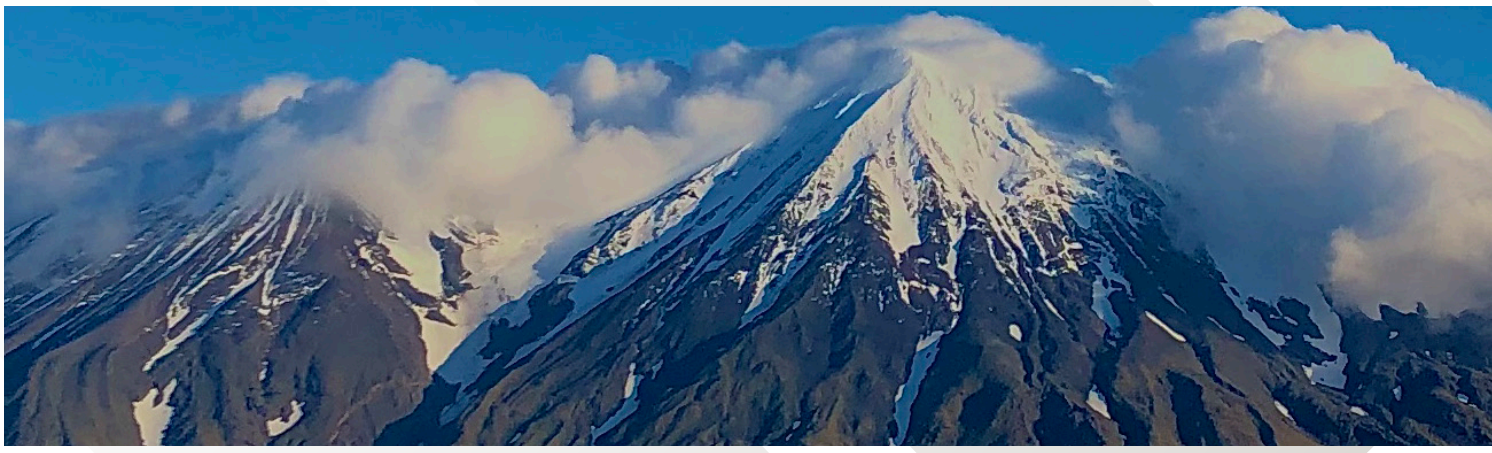

LEONARD J. SRNKA

Professor of Practice

lsrnka@ucsd.edu, 858-822-1510

Land and marine electromagnetic (EM) methods; integrated geophysical data analysis and interpretation; inverse theory; energy outlooks and global change

Research continued on developing theory and methods to quantify the spatial resolution and uncertainties in subsurface electrical conductivities derived using various electromagnetic (EM) methods. The central question is: what can be deduced from such results, and with what confidence? This is known within inverse theory as the inference problem. Current approaches include theoretical-analytical (Medin et al., 2007; Constable et al., 2015), deterministic (Gist et al., 2013), and statistical methods (Chen et al., 2012; Ray and Key, 2012; Ray et al., 2013, 2014; Houck et al., 2013). Bob Parker from Scripps (R.L. Parker, SEMC Workshop, La Jolla 2017 and private communication, 2019) has argued that the best theoretical-analytical results can determine only average values and uncertainties within a specified depth range. Medin et al. (2007) show a good example of this for the case of 1D (spherically symmetric) geomagnetic sounding.

After more than 70 years of research, technique development and applications, the lack of practical EM inference methods continues to be an obstacle to better acceptance and more uptake of geophysical EM methods. Approximate methods are sought in this research, even if these are ad hoc but still useful (e.g. not quite theoretically correct). Perhaps seismic techniques can be of assistance. However, current understanding is not encouraging – the physics of seismic propagation and EM diffusion are very different. But some researchers are undaunted. Leon Thomsen (2014) discussed seismic/EM differences and similarities in some detail and argues that EM data can be imaged in a manner analogous to very attenuative reflection seismic data and that an impulsive-type source is preferred over continuous waveforms. This latter conclusion is almost certainly incorrect; processing of continuous seismic vibrator data to derive equivalent impulses is a well-established technique. Neese and Thomsen (2014) use numerical model data to demonstrate the feasibility of seismic-like EM data processing and imaging.

Research in progress is investigating this and other approximate methods, starting with single-frequency model data and inversions. Since it is well known that different EM inversion methods often produce significantly different results using the same data (Constable et al., 2015), the question arises as to which domain contains the "true" native resolution - data, inversion, or even final image domain. Of course, data quality plays a key role. Numerous studies have shown that EM subsurface feature detection and resolution are directly (but not linearly) dependent on the accuracy of data phase and amplitude. Since such data are always noisy, the derived answers are always non-unique. Evaluating seismic vibrator reflection data processing modified for the strongly dissipative behavior of diffusive (anomalously dispersive) EM propagation, where there is no well-defined group velocity, is showing some success in the data domain. For pseudo-wavelet traveltime imaging, in the place of a well-defined group velocity the center-of-energy velocity discussed many years ago by Vainshtein (1957) and Brillouin (1960), and more recently by Mainardi (1983), may prove to be a useful (if not exactly correct) substitute.

REFERENCES

Vainshtein, L. A., 1957. Group velocity of damped waves. *Soviet Phys. Techn. Phys.*, **2**, 2420-2428.

Brillouin, L. A., 1960. Wave Propagation and Group Velocity, Academic Press, New York.

Mainardi, F., 1983. Signal velocity for transient waves in linear dissipative media. *Wave Motion* **5**, 33-41.

Medin, A. E., R. L. Parker and S. Constable, 2007. Making sound inferences from geomagnetic sounding. *Phys. Earth Planet. Int.,* **160**, 51–59.

Chen, J., G. Hoversten, K. Key, G. Nordquist, and W. Cumming, 2012. Stochastic inversion of magnetotelluric data using sharp boundary parameterization and application to a geothermal site. *Geophysics*, **77**, E265–E279, doi:10.1190/GEO2011-0430.1.

Ray, A. and K. Key, 2012. Bayesian inversion of marine CSEM data with a trans-dimensional self-parametrizing algorithm. *Geophysical Journal International,* **191**, 1135–1151.

Ray, A., D. Alumbaugh, G.M. Hoversten, and K. Key, 2013. Robust and accelerated Bayesian inversion of marine controlled-source electromagnetic data using parallel tempering. *Geophysics*, **78**, E271—E280.

Ray, A., K. Key, T. Bodin, D. Myer, and S. Constable, 2014. Bayesian inversion of marine CSEM data from the Scarborough gas field using a transdimensional 2-D parameterization. Geophysical Journal International, **199**, 1847–1860, doi: 10.1093/gji/ggu370.

Constable, S., A. Orange, and K. Key, 2015. And the geophysicist replied: "Which model do you want?". *Geophysics*, **80**, E197–E212.

Gist, G., A. Ciucivara, R. Houck, M. Rainwater, D. Willen, and J.-J. Zhou, 2013. Case Study of a CSEM False Positive - Orphan Basin, Canada. Technical Program Extended Abstracts, *SEG Annual Meeting,* 805-808.

Houck, R. T., A. Ciucivara, and S. Hornbostel, 2013. Probabilistic Interpretation of CSEM Resistivity. SEG Annual Meeting, 718-721.

Thomsen, L. 2014. Electromagnetics and seismics: the deep connections. Technical Program Extended Abstracts, SEG Annual Meeting, Denver, 855-859, doi: 10.1190/segam2014-0798.1.

Neese, J. W. and Thomsen, L. 2014. Seismic processing of numerical EM data. Technical Program Extended Abstracts, SEG Annual Meeting, Denver, 869-874, doi: 10.1190/segam2014-0798.1.

DAVE STEGMAN

Associate Professor

dstegman@ucsd.edu, 858-822-0767

Global tectonics, planetary geophysics, computational geodynamics

The past year I've had the pleasure to work with my three PhD students (Joyce Sim, Andrea Adams, and Nic Blanc), my post-doc Adina Pusok, and my former SURF student, Madeleine Kerr. We used both numerical models and theoretical models to work on a wide range of topics from how magnetic elds are generated in the molten silicate mantle of the early Earth (Blanc et al., EPSL 2020), to how melt is generated and focused at mid-ocean ridges (Sim et al., PEPI 2020), to how mantle plumes and rollback subduction might operate on Venus. For this report I'll just focus on a single research highlight.

For many years, I've been working on this puzzle of how the Indian plate moved towards Asia since 70 Ma (Million years ago). The reason this problem is so fascinating is because during the Cretaceous, the Indian plate moved at some of the fastest speeds ever recorded. It actually broke the "plate tectonic speed limit" by moving more than twice as fast as typical subducting tectonic plates move. The onset of this episode is coincident with the arrival of the Reunion Plume which caused the massive volcanic eruption of the Deccan flood basalts. My previous work with Scripps colleague, Steve Cande, showed that this plumehead generated tectonic forces large enough to alter plate motions, what we termed the "Plume-push Force" (Cande and Stegman, *Nature* 2011). But there are further details of the Indian plate's journey preserved in the Indian Ocean sea floor that remain quite enigmatic. The high resolution ship track date clearly document that there are two distinct pulses of fast motion: a rapid acceleration, followed by an equally rapidbslowdown and then a second speed-up with a longer duration (black line in Figure 36, left panel). In recent work with IGPP Post-doc, Adina Pusok, we use an extensive dataset to confirm these observations and then employed numerical models of subduction to show that the arrival of the Deccan mantle plume-head at 6367Ma started a sequence of events that can explain this history of plate motion (Pusok and Stegman, Science Advances 2020). We successfully demonstrated that very high plate speeds recorded during 65-60 Ma directly resulted from when a mantle plume forced a subduction system into compression, leading to initiation of a double subduction system. This brief, yet intense, period of forced convergence allows for superfast plate motions of the rst peak (Figure 1, top right panel), and later evolves into a self-sustaining double subduction zone that is able to drive the system at the anomalously fast speeds seen in the second peak (Figure 36, bottom right panel). Our models support a two-stage India-Eurasia collision sequence starting with the 'soft' collision at 50 Ma between the purported intra-oceanic arc above the middle plate accreting onto the Eurasian

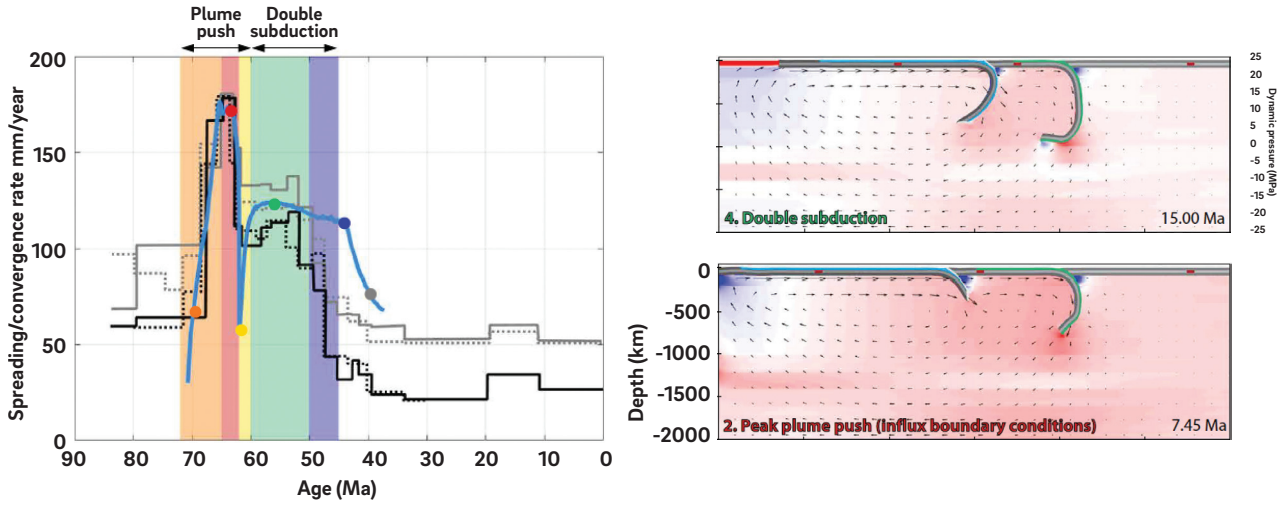

Figure 36. India-Eurasia convergence data and results of numerical models from (Pusok and Stegman, 2020). Left panel: Observed spreading rates versus age for the Central Indian Ridge (black lines) and SouthEast Indian Ridge (gray lines). Blue line shows computed convergence rate between the left plate and overriding plate in our numerical model. Distinct periods of time are color coded to reflect stages in the tectonic system's evolution from single subduction (orange), to subduction initiation (red), then transitioning (yellow) to equilibrium double subduction (green), and finally single subduction again (purple). The time periods define two regimes when the system is dominated by the plume (forced convergence) and when the system is dominated by the slabs (double subduction). Right panels: Snapshots of the time evolution of a subduction system that is composed of three plates, representing India (left plate), an intraoceanic plate (middle plate), and Eurasia (overriding plate). Movie of full-time evolution available in online publication. During the double subduction regime, the mantle flow and plate convergence are dominated by interaction between the two slabs, as indicated by high pressure within the region conned between them. Top: Peak intensity of the plume push force driving the peak convergence of the system at the level that has been observed corresponding to the red-colored marker and time window of left panel. Bottom: Having transitioned into double subduction-driven system, the pull from both slabs drives fast convergence and the magnitude is sustained for the duration of time observed in the sea floor record.).

margin, followed by the 'hard' collision between continental India and Eurasia as early as 43 Ma or as late as 6425-20 Ma. Our hypothesis supports recent interpretations that Greater India was not an extension of the Indian continent, but instead was a micro-continent separated from northern cratonic India by an ocean basin.

We had previously investigated how double subduction systems operate more generally and identified under what circumstances two subducting slabs could reinforce each other and enhance the overall convergence rate of the system (Pusok and Stegman, G-Cubed, 2019). We investigated a wide range of conditions and developed a new metric, called the Double Subduction Factor (DSF), that is able to quantify the magnitude of how the slabs and plate motions are coupled together and how this coupling evolves over time. We also re-examined some fundamental assumptions about how to model this system, in general, and we demonstrate that 1) including a free-surface boundary condition plays an essential role for these dynamics, and 2) that allowing for the larger domain of the Earth's mantle by including a lower mantle dramatically changes the model outcomes compared to a more geometrically conned space.

RECENT PUBLICATIONS

Pusok, A. E. and D. R. Stegman, "The convergence history of India-Eurasia records multiple subduction dynamics processes" *Science Advances,* **6** no.19, eaaz8681 (2020)

Pusok, A. E. and D. R. Stegman,"Formation and stability of same-dip double subduction systems" *J. Geophys. Res. (Solid Earth)*, **124** no. 7, 7387-7412 (2019)

Blanc, N. A., D. R. Stegman, and L. B. Ziegler, "Thermal and magnetic evolution of a crystallizing basal magma ocean in Earth's mantle." *Earth and Planetary Science Letters,* **534** 116085 (2020)

Sim, S. J., M. Spiegelman, D. R. Stegman, and C. Wilson, "The in uence of spreading rate and permeability on melt focusing beneath mid-ocean ridges." *Physics of the Earth and Planetary Interiors,* 106486 (2020)

PETER WORCESTER

Researcher Emeritus, RTAD

pworcester@ucsd.edu 858-534-4688

Acoustical oceanography, ocean acoustic tomography, underwater acoustics.

My research is focused on the application of acoustic remote sensing techniques to the study of large-scale ocean structure and on improving our understanding of the propagation of sound in the ocean, including the effects of scattering from small-scale oceanographic variability. My recent research has been focused in the Arctic Ocean, which is undergoing dramatic changes in both the ice cover and ocean structure. Changes in sea ice and the water column affect both acoustic propagation and ambient sound. This implies that what was learned about Arctic acoustics in the past is now largely obsolete. I have most recently been involved in the analysis of data collected during the 2015–2017 Canada Basin Acoustic Propagation Experiment (CANAPE) and in the conduct of the 2019–2020 U.S.-Norwegian Coordinated Arctic Acoustic Thermometry Experiment (CAATEX). Here I report on the CANAPE experiment. My colleague, Dr. Matthew Dzieciuch, reports on the status of the CAATEX experiment in his annual report.

CANAPE was designed to determine the fundamental limits to the use of acoustic methods and signal processing imposed by ice and ocean processes in the new Arctic. To achieve this goal, the CANAPE project conducted two experiments: (1) the short term 2015 CANAPE Pilot Study and (2) the yearlong 2016–2017 CANAPE experiment (Fig. 1). The hope is that these first steps will lead to a permanent acoustic monitoring, navigation, and communications network in the Arctic Ocean. The specific goals of the CANAPE project include (1) understanding the impacts of changing sea ice and oceanographic conditions on acoustic propagation and fluctuations; (2) characterizing the depth dependence and temporal variability of the ambient sound field; and (3) measuring the spatial and temporal variability in the upper ocean throughout the annual cycle by combining acoustic and other data with ocean models.

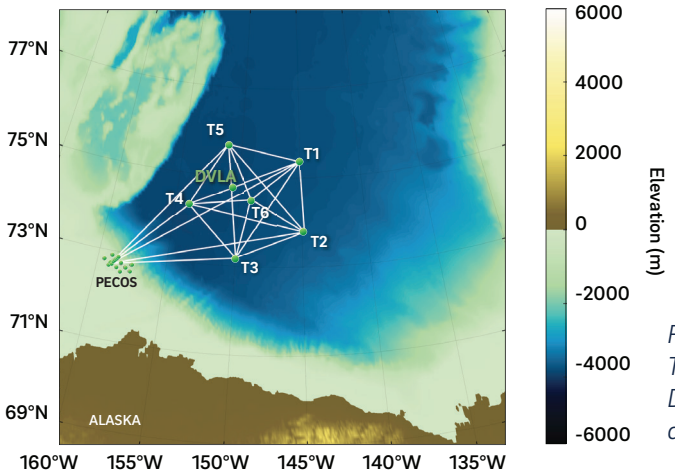

Figure 37. The 2016–2017 CANAPE experiment consisted of six Teledyne Webb Research acoustic transceivers (T1–T6) and a DVLA receiver (DVLA). The array radius is 150 km. There was additional instrumentation on the continental shelf (PECOS).

The 2016–2017 CANAPE experiment included components in both the deep Canada Basin and on the continental shelf and slope north of Alaska. Dr. Dzieciuch and I had primary responsibility for the deep-water CANAPE experiment, for which six acoustic transceiver moorings and a Distributed Vertical Line Array (DVLA) receiver mooring were deployed north of Alaska during August-September 2016 and recovered during September-October 2017 (Fig. 1). The sources transmitted linear frequency-modulated signals with bandwidths of 100 Hz and center frequencies of approximately 250 Hz. The experiment combined measurements of acoustic propagation and ambient sound with the use of an ocean acoustic tomography array to help characterize the oceanographic variability throughout the year in the central Canada Basin. The one-year deployment in a fixed geometry provides measurements in open water during summer, in the marginal ice zone (MIZ) as it transitions across the array during the spring and autumn, and under complete ice cover during winter. All of the ice covering the array during 2016–2017 was first-year ice that reached a maximum thickness of about 1.5 m in late winter and early spring, even though the Canada Basin has historically been a region with extensive multi-year ice that survived over one or more summers.

The measured travel times were remarkably stable, with peak-to-peak variability of only about 20 milliseconds over the entire year. In comparison, travel times in mid-latitudes at similar ranges vary by something like an order of magnitude more (~200 milliseconds peak-to-peak) due to the effects of ocean mesoscale variability with spatial scales of roughly 100 km and time scales of about one month. The high-frequency travel-time fluctuations at periods shorter than a day caused by small-scale oceanographic variability were also much smaller than in mid-latitudes. This was not unexpected, because the ocean internal wave field that scatters sound is much weaker in the Arctic Ocean than in mid-latitudes. In addition, the transmission loss increased significantly in winter, likely in part because of scattering when the signals reflect from the ice cover and in part due to changes in the ocean stratification. Finally, ambient sound also varied over the year, with minimum levels in May-June 2017 when the ice was thickest.

RECENT PUBLICATIONS

Ballard, M. S., et al. (2020), Temporal and spatial dependence of a yearlong record of sound propagation from the Canada Basin to the Chukchi Shelf, J. Acoust. Soc. Am., 148(3), 1663–1680, doi:10.1121/10.0001970.

Howe, B. M., J. Miksis-Olds, E. Rehm, H. Sagen, P. F. Worcester, and G. Haralabus (2019), Observing the oceans acoustically, Frontiers in Marine Science, 6:426, doi:10.3389/fmars.2019.00426.

Mikhalevsky, P. N., B. J. Sperry, K. F. Woolfe, M. A. Dzieciuch, and P. F. Worcester (2020), Deep ocean long range underwater navigation, J. Acoust. Soc. Am., 147(4), 2365–2382, doi:10.1121/10.0001081.

Worcester, P. F. (2019), Tomography, in Encyclopedia of Ocean Sciences, Third Edition, edited by J. K. Cochran, H. J. Bokuniewicz and P. L. Yager, pp. 328–346, Elsevier, Oxford, doi:10.1016/B978-0-12-409548-9.11591-X.

Worcester, P. F., M. A. Dzieciuch, and H. Sagen (2020), Ocean acoustics in the rapidly changing Arctic, Acoustics Today, 55–64, doi:10.1121/AT.2020.16.1.55.

MARK ZUMBERGE

Research Geophysicist

mzumberge@ucsd.edu, 858-534-3533

Measurements of crustal deformation on land and on the seafloor. We use laser interferometry through optical fibers to measure strain in boreholes and trenches on land, and through optical fibers pressed into the sediment on the seafloor. We are using new cold-atom interferometry technology to make precise absolute measurements of gravity on land and planning to further the development for its application on the seafloor. We make continuous, calibrated pressure measurements on the seafloor to detect vertical deformation. We also are developing opto-mechanical borehole sensors for geodetic and seismic research on land. Finally, we are participating in a community effort to expand seafloor geodesy with the GPS-A method (described below). Many individuals are collaborators in these projects, including Jon Berger, Adrian Borsa, David Chadwell, Fanghui Deng, Donald Elliott, William Hatfield, David Price, Dennis Rimington, Glenn Sasagawa, Frank Wyatt, and Surui Xie.

A long, ongoing, collaborative effort to expand our knowledge of crustal deformation occurring on the seafloor finally gained a foothold through a $5M grant from the National Science Foundation to establish a pool of equipment for seafloor geodesy. A multi-institutional group of PIs (David Chadwell, Scripps; Noel Bartlow, Univ. of Kansas; Andrew Newman, Georgia Tech.; David Schmidt, Univ. of Washington; and Spahr Webb, Columbia Univ.) advocated through several proposal cycles that we cross the coastline boundary and establish offshore geodetic sites to enhance models of subduction zone tectonics constrained so far mostly by onshore GPS stations. These efforts culminated in a grant to Scripps to purchase 51 Sonardyne seafloor transponders and three Liquid Robotics SV3 wavegliders enabling us to establish a network of 16 seafloor stations whose positions can be determined with cm resolution using a combination of GPS and acoustic ranging. Our current effort is to commission this equipment, readying it for a community-defined deployment in 2021 or 2022.

Figure 38. On the left is a Sonardyne seafloor transponder. It listens for coded acoustic pulses and replies with a unique pulse of its own. Measuring the round-trip time-of-flight of the pulses gives a measure of the distance between the transponder and the waveglider on the surface that initiated the connection. On the right is a Liquid Robotics SV3 waveglider, the latest generation vehivle available. It has been fitted with additional GPS antenna, an acoustic transducer, and inertial navigation sensors to equip it with GPS-A capability. Scripps has purchased 51 transponders, each with a 10-year battery pack, and three of the GPS-A wavegliders.

The method of GPS-A (more precisely now GNSS-A) or Global Positioning System Acoustics was developed over several decades by Fred Spiess and David Chadwell of the Marine Physical Lab at Scripps. In this technique, the position of a sea surface platform is tracked with GPS antennas while it ranges to seafloor transponders acoustically. The horizontal position of the center of an array of transponders can be determined to within about a cm. This can be accomplished even though the sound velocity profile of the ocean is imperfectly known; the fact that its variation is primarily in the vertical dimension when averaged over time enables the method to obtain such high precision. In the latest embodiment of the method, the sea surface platform is an autonomous vehicle: a Liquid Robotics waveglider. This vehicle uses wave power to propel itself and solar power to drive sensors, controllers, and satellite communication. In the GPS-A mode it navigates in a small circle centered amid three seafloor acoustic transponders, timing the round-trip propagation of coded sound pulses to each. Inertial sensors on the vehicle enable the precise tracking of the coordinates of its acoustic transducer relative to two GPS antennas. Combining the GPS, inertial, and acoustic data series yields the seafloor coordinates in a global reference frame. Repeated month-long visits of a waveglider to each site over many years will reveal horizontal velocity vectors of the seafloor crust as it is subducted beneath the continent. The long-term goal is to establish which parts of a subducting plate are locked and which parts are creeping along. Doing so will enable the determination of the level of hazard presented by earthquakes and tsunamis along the coastline.

In addition to gaining horizontal information from the sites, one third of the transponders contain a continuous pressure recorder whose measurements can reveal vertical movement of the seafloor. Because ambient sweater pressure is determined by depth (primarily), change in pressure accompanies change in depth – this is detectable at the cm level also. While oceanographic and gauge drift complicate the interpretation of the data, it has been shown that an interesting and important component of the subduction process known as slow-slip (sometimes called slow-earthquake or also episodic tremor and slip) is evident in pressure records, further illuminating the process under study.

A community workshop is being planned in the Spring of 2021 in which marine geodesists and other stakeholders will collaborate to design an experiment to deploy the equipment in an as-yet-to-be-named region. The Cascadia subduction zone and the Aleutian Trench are front-running candidates.

REFERENCES

Sasagawa, G. S., Zumberge, M. A., & Cook, M. J. (2018). Laboratory simulation and measurement of instrument drift in quartz-resonant pressure gauges. *IEEE Access,* **6**, 57334-57340. doi: 10.1109/access.2018.2873479

Zumberge, M. A., Hatfield, W., & Wyatt, F. K. (2018). Measuring seafloor strain with an optical fiber interferometer. *Earth and Space Science,* **5**(8), 371-379. doi: 10.1029/2018ea000418

Cecil H. and Ida M. Green
Institute of Geophysics and Planetary Physics
Scripps Institution of Oceanography, UC San Diego
9500 Gilman Drive, La Jolla, CA 92093-0225, USA
igpp.ucsd.edu